Muscular dystrophy and the gene for speed

Author:
Chan, Stephen Ming Kit

Publication Date:
2009

DOI:
https://doi.org/10.26190/unsworks/23042

License:
https://creativecommons.org/licenses/by-nc-nd/3.0/au/
Link to license to see what you are allowed to do with this resource.

Downloaded from http://hdl.handle.net/1959.4/44997 in https://unsworks.unsw.edu.au on 2024-05-05

Muscular dystrophy and the gene for speed

PhD Thesis

submitted December 2009

Stephen Chan
Department of Physiology
School of Medical Sciences
University of New South Wales

COPYRIGHT STATEMENT

'I hereby grant the University of New South Wales or its agents the right to archive and to make available my thesis or dissertation in whole or part in the University libraries in all forms of media, now or here after known, subject to the provisions of the Copyright Act 1968. I retain all proprietary rights, such as patent rights. I also retain the right to use in future works (such as articles or books) all or part of this thesis or dissertation.
I also authorise University Microfilms to use the 350 word abstract of my thesis in Dissertation Abstract International (this is applicable to doctoral theses only).
I have either used no substantial portions of copyright material in my thesis or I have obtained permission to use copyright material; where permission has not been granted I have applied/will apply for a partial restriction of the digital copy of my thesis or dissertation.'

Signed …….....

Date …….....

AUTHENTICITY STATEMENT

'I certify that the Library deposit digital copy is a direct equivalent of the final officially approved version of my thesis. No emendation of content has occurred and if there are any minor variations in formatting, they are the result of the conversion to digital format.'

Signed …….....

Date …….....

ORIGINALITY STATEMENT

'I hereby declare that this submission is my own work and to the best of my knowledge it contains no materials previously published or written by another person, or substantial proportions of material which have been accepted for the award of any other degree or diploma at UNSW or any other educational institution, except where due acknowledgement is made in the thesis. Any contribution made to the research by others, with whom I have worked at UNSW or elsewhere, is explicitly acknowledged in the thesis. I also declare that the intellectual content of this thesis is the product of my own work, except to the extent that assistance from others in the project's design and conception or in style, presentation and linguistic expression is acknowledged.'

Signed …….....

Date …….....

Supervisor

Dr Stewart Head

Department of Physiology
School of Medical Sciences
University of New South Wales

Co-supervisor

Professor Kathryn North

Institute for Neuroscience
and Muscle Research
The Children's Hospital at Westmead

Discipline of Paediatrics and Child Health
Faculty of Medicine, University of Sydney

Acknowledgement

I would like to thank my supervisor, Dr Stewart Head, and my co-supervisor, Professor Kathryn North, for their wonderful guidance and support. I would also like to thank all the members of their laboratories for their help throughout this project.

ABSTRACT

Dystrophin and α-actinin-3 are two proteins found within, or in close association with, the Z-disc of skeletal muscle. Dystrophin deficiency results in the condition of Duchenne muscular dystrophy, while α-actinin-3 deficiency impairs athletic performance in sprint and power activities. Because of their location and protein interactions, and the observed effects of their deficiency in humans, they are most commonly perceived as having structural roles within muscle. This thesis attempts to gain insight into whether their roles are purely structural, or whether they may have more complex functions. Using dystrophin-deficient *mdx* mice, this thesis found that muscles with a greater degree of morphological deformity (fibre branching) showed a greater loss of force following eccentric (lengthening) contractions. This result indicates that evidence previously used to argue in favour of a structural role for dystrophin may have been confounded by the presence of deformed fibres. This thesis also characterised the phenotype of the *Actn3* knockout mouse, a newly generated model of α-actinin-3 deficiency. The phenotype was examined at whole muscle and skinned fibre levels. *Actn3* knockout muscles showed changes indicative of a shift from fast fibre-type properties towards slower fibre-type properties in the absence of α-actinin-3. These results suggest a possible role for α-actinin-3 in promoting the differentiation of fast-twitch, glycolytic properties in muscle fibres.

TABLE OF CONTENTS

Introduction **1**

Overview of skeletal muscle structure in relation to dystrophin and α-actinin-3 ..... **2**

Phenotypes of dystrophin deficiency and α-actinin-3 deficiency **6**

Duchenne muscular dystrophy 6

Consequences of α-actinin-3 deficiency 7

Hypothesised functions of dystrophin and α-actinin-3 ..... **9**

The structural hypothesis of dystrophin function **10**

Critique of the structural hypothesis 11

The ion channel hypothesis of dystrophin function 13

Proposed functions of α-actinin-3 ..... **14**

The rate of force response in fast-twitch and slow-twitch fibres 16

Metabolism in fast-twitch and slow-twitch fibres 18

Aims of thesis **21**

Presentation of results **23**

Paper A **24**

Declaration **25**

Abstract **26**

Introduction **27**

Methods **29**

Animals used 29

Muscle preparation 29

Lengthening contraction protocol 30

Force measurement 31

Muscle stiffness 32

Statistical analyses 32

Muscle fibre morphology 33

Results **34**

Length, mass and cross-sectional area 34

Contractile properties before lengthening contractions 34

Damage following lengthening contractions 36
Muscle fibre morphology 37
Muscle stiffness 40
Discussion 41
Acknowledgements 43

Paper B 44
Declaration 45
Abstract 46
Introduction 47
Methods 49
Animals used 49
Muscle preparation 49
Force-frequency curve 49
Eccentric contractions 50
Muscle mass 50
Muscle stiffness 50
Fatigue 50
Muscle fibre morphology 51
Statistical analyses 51
Results 52
Sample sizes and ages 52
General physical properties 52
Maximum forces generated by muscles 52
Force-frequency characteristics 52
Eccentric contractions 54
Muscle stiffness 56
Fibre morphology 56
Fatigue 57
Discussion 62
Grants 65
Appendix to Paper B 66
Method 66
Result 66

Paper C **67**

Declaration **68**

Abstract **69**

Introduction **70**

Methods **72**

Animals used 72

Fibre preparation – skinned fibre experiments 72

Ca^{2+} loading of sarcoplasmic reticulum 72

Contractile apparatus 73

Muscle preparation – whole muscle experiments 74

Twitch relaxation 74

Force-frequency curve 74

Tetanus relaxation 75

Mass and cross-sectional area 75

Statistical analyses 75

Results **76**

Ca^{2+} loading of the sarcoplasmic reticulum 76

Ca^{2+} and Sr^{2+} activation characteristics of individual skinned fibres 78

Frequency of myofibrillar oscillations 80

Mass and cross-sectional area 81

Twitch relaxation 82

Tetanus relaxation 82

Force-frequency characteristics 83

Discussion **87**

Author contributions **92**

Acknowledgements **92**

Appendix to Paper C **93**

Methods 93

Results – maximum forces 93

Results – fatigue 94

Conclusion **96**

References 106

Publications 115

LIST OF TABLES AND FIGURES

Tables

Paper A

Table 2.1 Force deficits of normal and *mdx* fast-twitch muscles following lengthening contractions 28

Paper B

Table 3.1 Properties of wild-type and α-actinin-3 knockout muscles 53

Table 3.2 Twitch half-relaxation time 66

Conclusion

Table 5.1 Main differences between Actn3 knockout EDL muscles and wild-type muscles 104

Figures

Introduction

Figure 1.1 Hierarchy of skeletal muscle structure 3

Figure 1.2 Location of dystrophin and α-actinin within the muscle fibre 5

Figure 1.3 Histological and immunofluorescence features of DMD 7

Figure 1.4 *ACTN3* genotype frequencies in athletes and controls 8

Figure 1.5 Expression of α-actinin-2 and α-actinin-3 in the *Actn3* knockout mouse 9

Figure 1.6 Force deficits following eccentric contractions in fast-twitch *mdx* muscles 10

Figure 1.7 Abnormal morphology of mdx muscle fibres 11

Figure 1.8 The ion channel hypothesis 13

Figure 1.9 Protein interactions of α-actinin 15

Figure 1.10 Major events of the excitation-contraction-relaxation process in a muscle fibre 16

Figure 1.11 Main metabolic pathways in skeletal muscle 19

Paper A

Figure 2.1. The lengthening contraction protocol 30

Figure 2.2. A representative force-frequency curve 31

Figure 2.3. Length, mass and cross-sectional area 34

Figure 2.4. Contractile properties before lengthening contractions 35

Figure 2.5. Damage following lengthening contractions 36

Figure 2.6. Fibre branching in younger and older *mdx* muscles 38

Figure 2.7. Low power images of enzymatically dispersed single muscle fibres from younger *mdx* mice 39

Figure 2.8. Low power images of enzymatically dispersed single muscle fibres from older *mdx* mice 39

Figure 2.9. Muscle stiffness 40

Paper B

Figure 3.1. Aggregated force-frequency curves 53

Figure 3.2. Eccentric contractions 55

Figure 3.3. Measures of damage from eccentric contractions 55

Figure 3.4. Muscle stiffness 56

Figure 3.5. Fibre morphology 57

Figure 3.6. Changes in 100-Hz force during fatigue and recovery 59

Figure 3.7. Force-frequency characteristics at various stages of fatigue experiments 60

Figure 3.8. Post-recovery force as a percentage of pre-fatigue force 61

Paper C

Figure 4.1. Ca^{2+} loading of the sarcoplasmic reticulum 77

Figure 4.2. Ca^{2+} and Sr^{2+} activation characteristics of individual skinned fibres 79

Figure 4.3. Myofibrillar oscillations in Ca^{2+} and Sr^{2+} solutions 80

Figure 4.4. Mass and cross-sectional area 81

Figure 4.5. Twitch relaxation 84

Figure 4.6. Tetanus relaxation 85

Figure 4.7. Force-frequency characteristics 86

Figure 4.8 Maximum force generation 93

Figure 4.9 Fatigue 95

Conclusion

Figure 5.1 Importance of distinguishing between primary and secondary factors in the pathogenesis of DMD 99

Introduction

This thesis focusses on two proteins found in skeletal muscle: dystrophin, the protein absent in Duchenne muscular dystrophy; and α-actinin-3, the product of the gene known colloquially as the "gene for speed". Both of these proteins are located within, or are closely associated with, the Z-disc of skeletal muscle fibres. By virtue of their location and protein interactions, they are often considered to be structural proteins, conferring mechanical stability to the muscle fibre during contraction. The aim of this thesis will be to examine the roles of these two proteins, to gain insight into whether their roles are purely structural, or whether they may have additional functions within skeletal muscle.

In the case of dystrophin, this will involve studying *mdx* mouse muscle to address the question: is contraction-induced damage to dystrophin-deficient muscle purely a consequence of dystrophin's absence, or is it also partly due to the morphological abnormalities that dystrophin-deficient fibres develop over time?

In the case of α-actinin-3, *Actn3* knockout mouse muscle will be studied to address the questions: does α-actinin-3 deficiency lead to greater muscle damage during contraction, and do the properties of α-actinin-3-deficient muscle suggest possible non-structural roles for this protein?

Overview of skeletal muscle structure in relation to dystrophin and α-actinin-3

Figure 1.1 illustrates the structure of skeletal muscle. A single muscle, such as the biceps muscle, is composed of fasciculi, or bundles, of muscle fibres **(A)**. Each fibre is an elongated, multinucleated cell **(B)**. The contractile filaments within a fibre are bundled into cylindrical units known as myofibrils **(C)**. Each myofibril is divided along its length into sarcomeres **(D)** (Brooks, 2003). A sarcomere is the basic contractile unit of muscle. The sarcomere is bounded at each end by a Z-disc (or Z-line), and the filaments responsible for muscle contraction span the space between the Z-discs. The thin actin filaments are anchored to the Z-disc and extend towards the centre of the sarcomere. The thick myosin filaments extend from the centre of the sarcomere towards the Z-discs and are connected to the Z-discs via the protein titin (Frank *et al.*, 2006). Interaction between the actin filaments and the "heads" of the myosin filaments produces muscle contraction.

Figure 1.2 shows the locations of α-actinin-3 and dystrophin within the muscle fibre. Panel **(A)** is a representation of the peripheral part of a muscle fibre, showing a couple of myofibrils just inside the sarcolemma, or plasma membrane, of the fibre. The Z-discs of the

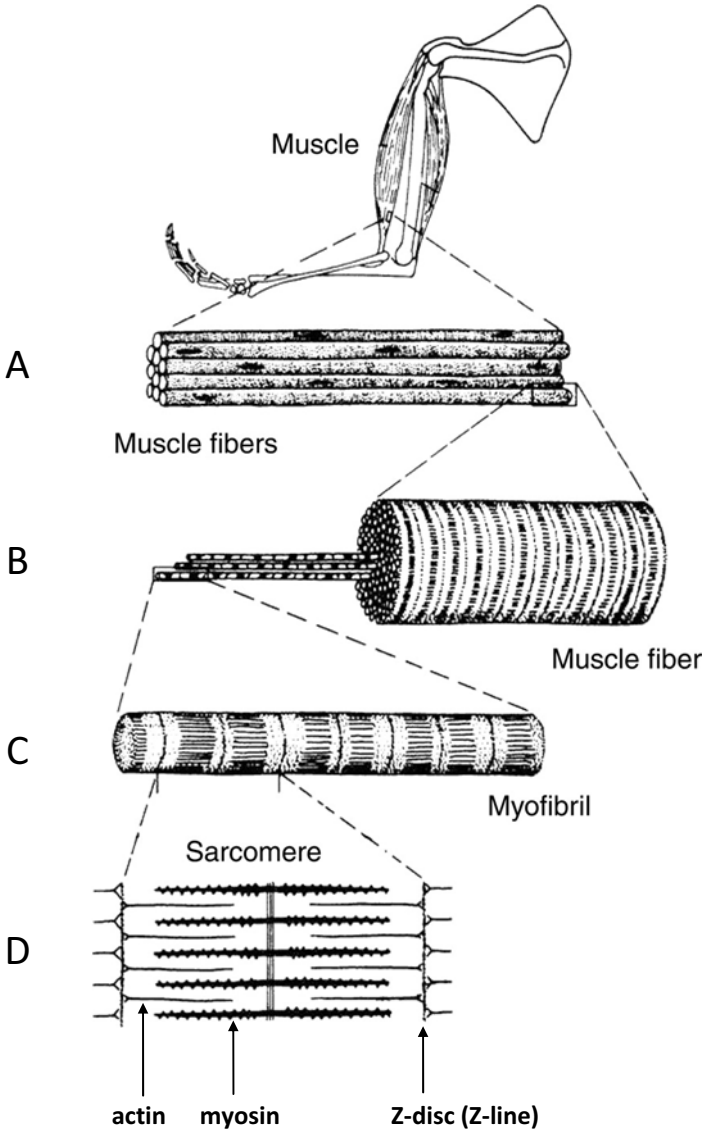

Figure 1.1 Hierarchy of skeletal muscle structure. The diagram shows the functional units within skeletal muscle, from the fasciculus **(A)**, to the muscle fibre **(B)**, to the myofibril **(C)**, to the sarcomere **(D)**. *Reproduced from Brooks (2003).*

myofibrils are composed mainly of α-actinin, of which α-actinin-3 is one isoform. The Z-discs of adjacent myofibrils are linked together by desmin filaments. The Z-discs of the myofibrils adjacent to the sarcolemma are connected to the sarcolemma by a structure known as a costamere, a collection of filaments and proteins which includes dystrophin. Hence α-actinin-3 and dystrophin are important components of a protein network that connects the interior of the muscle fibre to the sarcolemma. It is not surprising, then, that these two proteins are often thought of as structural proteins involved in the lateral transmission of contractile forces from sarcomeres through to the sarcolemma, extracellular matrix and neighbouring muscle fibres (Ervasti, 2003).

Dystrophin is a 427kDa rod-shaped protein that forms part of the dystrophin-associated protein complex (DAPC), a membrane-spanning structure that links the peripheral myofibrils to the extracellular matrix. Panel **(B)** is a diagrammatic representation of the DAPC and is an expanded view of the upper boxed region in panel (A). At its amino terminal, dystrophin binds to actin filaments which, in turn, connect to the Z-discs of the peripheral myofibrils. Near its carboxyl terminal, dystrophin binds to an integral membrane protein which, through further links, connects to the basal lamina. Gene mutations in certain components of the complex lead to various forms of muscular dystrophy. Mutations in the sarcoglycans underlie various types of limb girdle muscular dystrophy, and mutations in laminin lead to a form of congenital muscular dystrophy. Mutations in dystrophin that result in a complete absence of the protein give rise to the Duchenne form of muscular dystrophy, while mutations resulting in partly functional dystrophin give rise to a milder condition known as Becker muscular dystrophy (O'Brien & Kunkel, 2001).

α-Actinin-3 is one of two isoforms of α-actinin found in skeletal muscle, the other being α-actinin-2. The α-actinins are the main protein component of the Z-disc. Panel **(C)** is a diagram showing how α-actinin is arranged within the Z-disc, and is an expanded view of the lower boxed region in panel (A). α-Actinin exists as an antiparallel homodimer that binds to actin filaments through its actin-binding domain. It thus cross-links the actin filaments of adjacent sarcomeres and anchors them to the Z-disc. α-Actinin-2 is found in all types of muscle fibres, while α-actinin-3 is mainly restricted to fast glycolytic fibres (MacArthur & North, 2004).

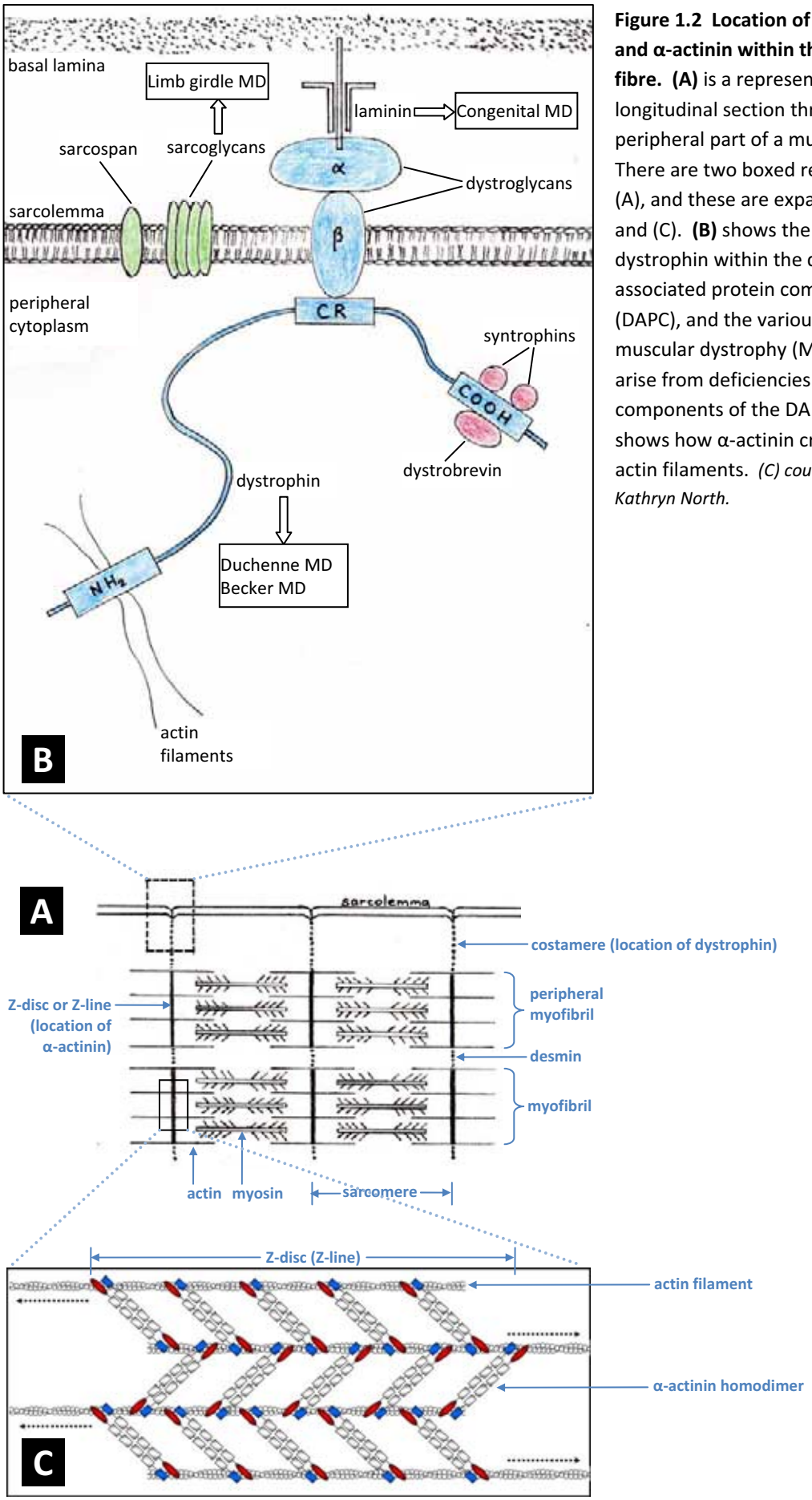

Figure 1.2 Location of dystrophin and α-actinin within the muscle fibre. (A) is a representation of a longitudinal section through the peripheral part of a muscle fibre. There are two boxed regions in (A), and these are expanded in (B) and (C). **(B)** shows the location of dystrophin within the dystrophin-associated protein complex (DAPC), and the various forms of muscular dystrophy (MD) that arise from deficiencies in components of the DAPC. **(C)** shows how α-actinin cross-links actin filaments. *(C) courtesy of Prof Kathryn North.*

Phenotypes of dystrophin deficiency and α-actinin-3 deficiency

Although dystrophin and α-actinin-3 are both components of the protein network that links the sarcomeres to the sarcolemma and extracellular matrix, deficiencies in these proteins give rise to vastly differing consequences. Dystrophin deficiency leads to the debilitating condition of Duchenne muscular dystrophy, while α-actinin-3 deficiency has effects that are largely noticed only when muscles are exerted to extreme levels, as in elite sporting activities.

Duchenne muscular dystrophy

Duchenne muscular dystrophy (DMD) is an X-linked recessive condition of skeletal muscle affecting 1 in 3,500 live male births (Mueller & Young, 1998). It is caused by mutations in the dystrophin gene that result in a complete absence of this protein. DMD is the most common of the muscular dystrophies, defined as "a group of inherited disorders which are characterised by a progressive muscle wasting and weakness" (Emery, 1993). Their unifying feature is their muscle histology, while they are distinguished from one another by the underlying genetic defect and the severity and distribution of muscle involvement (Emery, 2002).

In the Duchenne form of muscular dystrophy, onset is around 3 to 5 years of age, when parents notice abnormalities in the boy's motor development. He may show a delay in learning to walk, a waddling gait, a tendency to fall easily, and difficulty in climbing stairs. In almost all cases, the child has never been able to run properly (Emery, 1993). Initially, proximal muscles are affected, but eventually the whole musculature is involved. A typical feature of the disease is calf pseudohypertrophy, an enlargement of the calves due to replacement of muscle by adipose and connective tissue (Mueller & Young, 1998). As the muscle wasting progresses, joint contractures and lumbar lordosis develop and boys are generally wheelchair-bound by age 12. In later stages, there is pronounced deformity of the thoracic spine, a weakening of the intercostal muscles and a gradual decline in pulmonary function. The mean age at death is 18 years, with the usual cause being pneumonia compounded by cardiac involvement. Although primarily a disease of the skeletal musculature, DMD may also be accompanied by cardiomyopathy or mental impairment, with about 20% of boys having an IQ below 70 (Emery, 2002).

Laboratory investigations show grossly elevated serum levels of creatine kinase, an intracellular muscle enzyme, which decline to normal values only in the late stages of the disease when muscle bulk is greatly diminished (Emery, 1993). The histological features of

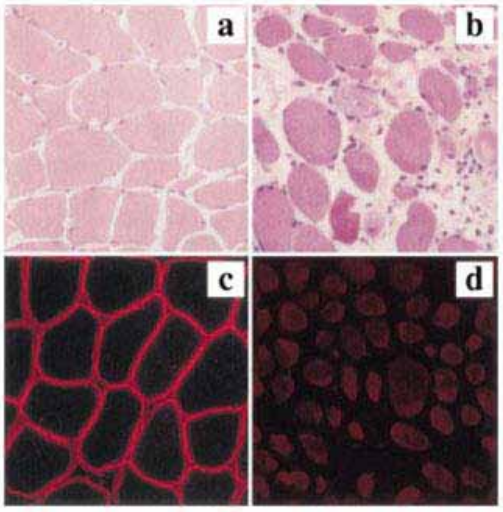

Figure 1.3 Histological and immunofluorescence features of DMD. The top two panels show the differences in histology between normal muscle **(a)** and the muscle of a patient with DMD **(b)**. The fibres of normal muscle are uniform in size and densely packed. The fibres of DMD muscle are variable in size and separated by large amounts of connective tissue. The bottom two panels show the differences between normal muscle **(c)** and DMD muscle **(d)** when they are stained for dystrophin. In normal muscle, dystrophin is localised to the plasma membrane of muscle fibres; in DMD muscle, it is virtually absent. *Reproduced from O'Brien & Kunkel (2001).*

DMD (**Figure 1.3**) are typical of the muscular dystrophies: variation in fibre diameters; proliferation of connective tissue; degeneration, necrosis and phagocytosis of muscle fibres; and the presence of regenerating fibres possessing basophilic cytoplasm and large, centrally located nuclei with prominent nucleoli (Girolami *et al.*, 1999). In the electron miscroscope, discontinuities known as delta lesions can be detected in the plasma membrane (Engel *et al.*, 1994).

The most widely studied animal model of DMD is the *mdx* mouse. As in humans, this mouse has a dystrophin mutation resulting in complete absence of the protein. The *mdx* mouse is not a perfect model of the human disease, displaying a milder phenotype and a greater capacity for muscle regeneration (Khurana & Davies, 2003). However, as almost all past studies use this animal model, and a major objective of this thesis is to offer an alternative interpretation of these studies, the *mdx* mouse model will be the one used in the experiments described in this thesis.

Consequences of α-actinin-3 deficiency

About 1 billion people worldwide are completely deficient in α-actinin-3, due to a common polymorphism in the *ACTN3* gene (North *et al.*, 1999). In contrast to dystrophin deficiency, α-actinin-3 deficiency is not associated with any disease phenotype. This may be because upregulation of α-actinin-2 is able to compensate for a loss of α-actinin-3 (Mills *et al.*, 2001). However, studies on elite athletes suggest that α-actinin-3 may have unique functions in skeletal muscle for which α-actinin-2 cannot compensate.

Figure 1.4 shows the results of a study of elite athletes at the Australian Institute of Sport (Yang *et al.*, 2003). The athletes were classified as either power athletes (engaged in sports such as sprinting and short-distance swimming), or endurance athletes (engaged in

sports such as long-distance cycling and running). A group of controls was drawn from the general population for comparison. Each column shows the percentage of people who: (i) do not have the polymorphism in their *ACTN3* gene (RR genotype, *blue*); (ii) are heterozygous for the polymorphism (RX genotype, *yellow*); and (iii) are homozygous for the polymorphism (XX genotype, *red*) and hence completely lack α-actinin-3.

The frequency of the XX genotype was significantly lower among power athletes than among the general population. In fact, no power athlete who had competed at Olympic level was completely deficient in α-actinin-3. On the other hand, there was a trend towards a higher frequency of the XX genotype among endurance athletes compared to controls. These results suggest that α-actinin-3 deficiency is detrimental to sprint and power performance at the elite level, but beneficial to endurance performance.

Other independent studies have since reported lower frequencies of the XX genotype in elite sprint and strength athletes (Niemi & Majamaa, 2005; Roth *et al.*, 2008); higher frequencies of the RR genotype in elite sprinters (Papadimitriou *et al.*, 2008); and higher frequencies of the XX genotype in elite endurance athletes (Eynon *et al.*, 2009). Among non-athletes, α-actinin-3 deficiency has also been associated with reduced muscle strength (Clarkson *et al.*, 2005) and poorer sprinting performance (Moran *et al.*, 2007). Such observations have led to the *ACTN3* gene acquiring the name "the gene for speed".

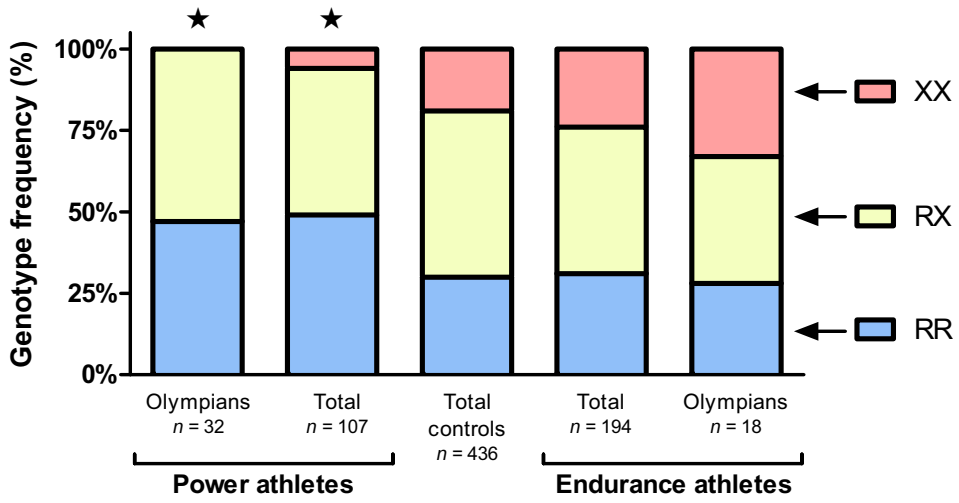

Figure 1.4 *ACTN3* genotype frequencies in athletes and controls. RR individuals do not have the polymorphism in their *ACTN3* gene and hence have two functioning copies of this gene. RX individuals are heterozygous for the polymorphism. XX individuals are homozygous for the polymorphism and hence completely lack α-actinin-3. A star above a column indicates that the frequency of the XX genotype in that cohort was significantly different from controls. The frequency of the XX genotype is significantly lower among power athletes than controls, while there is a tendency towards a higher frequency of the XX genotype among endurance athletes than controls. *Based on data presented in Yang et al. (2003).*

The recently generated *Actn3* knockout mouse (MacArthur *et al.*, 2007) is an animal model of α-actinin-3 deficiency. This knockout mouse is completely deficient in α-actinin-3 and displays upregulation of α-actinin-2 (**Figure 1.5**). It also has reduced grip strength compared with wild-type controls (MacArthur *et al.*, 2008) and can run 33% further than wild-types on a motorised treadmill endurance test (MacArthur *et al.*, 2007). Hence the phenotype of the *Actn3* knockout mouse resembles that of humans with the XX genotype, and is thus a useful model of α-actinin-3 deficiency.

Hypothesised functions of dystrophin and α-actinin-3

As mentioned, dystrophin and α-actinin-3 are commonly perceived to have structural roles due to their location within the protein network linking the Z-discs, sarcolemma and extracellular matrix (Ervasti, 2003). While there is experimental evidence to support this perception, there is also evidence to suggest that their roles are more complex than merely providing stability to the muscle fibre and sarcolemma during contractile activity. Here an evaluation will be provided of the main hypotheses regarding the functions of these two proteins. The main

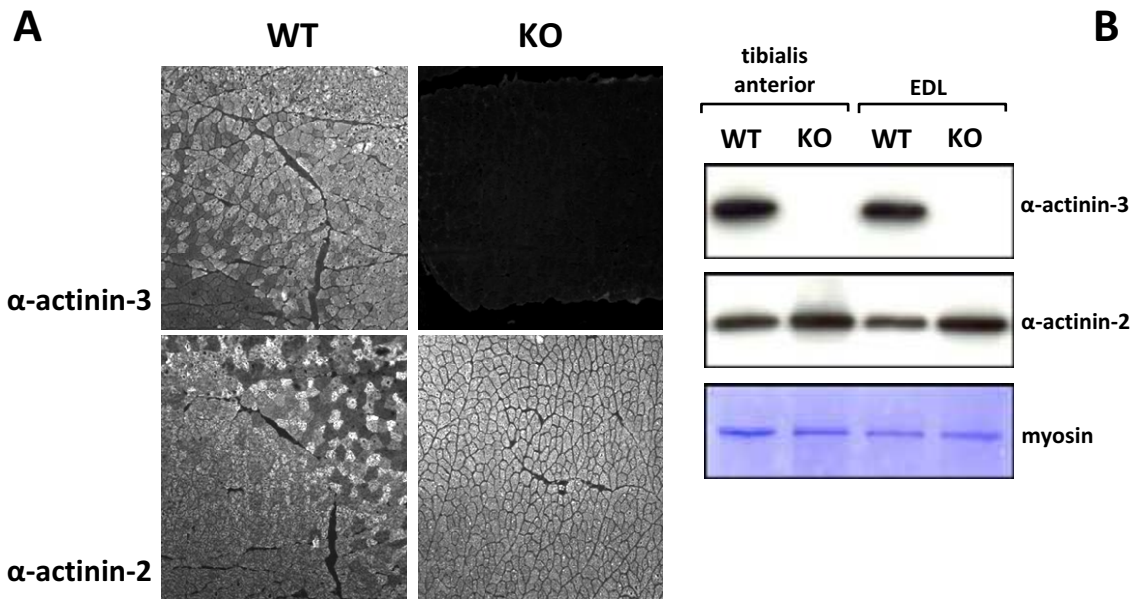

Figure 1.5 Expression of α-actinin-2 and α-actinin-3 in the *Actn3* knockout mouse. (A) shows immunohistochemical staining for α-actinin-3 and α-actinin-2 in cross-sections of quadriceps muscle from wild-type (WT) and knockout (KO) mice. There is a complete absence of α-actinin-3 staining in the KO cross-section, and staining for α-actinin-2 is more homogeneous in KO than in WT. **(B)** is an immunoblot analysis of tibialis anterior and extensor digitorum longus (EDL) muscles showing absence of α-actinin-3 and upregulation of α-actinin-2 in KO compared with WT mice. Total myosin is shown as a loading control. *Courtesy of Prof Kathryn North.*

theories of dystrophin's function can be grouped for simplicity under two headings: (i) the structural hypothesis; and (ii) the ion channel hypothesis. In the case of α-actinin-3, the proposed functions can be classified for simplicity as (i) structural; and (ii) fibre type differentiation and metabolism.

The structural hypothesis of dystrophin function

How the absence of dystrophin can result in the muscle degeneration seen in DMD is still debated. One theory, the structural hypothesis, proposes that dystrophin's role is to mechanically stabilise the sarcolemma, protecting it from stresses developed during contractile activity. In the absence of dystrophin, the membrane is damaged during muscle contraction, resulting in muscle degeneration (Petrof, 2002). This is a highly plausible hypothesis, given the structure of the DAPC (Figure 1.2), the occurrence of delta lesions in the sarcolemma and the presence in serum of enzymes normally located inside muscle fibres (Ervasti, 2003).

Strong experimental support for this theory has come from studies involving eccentric (lengthening) contractions in fast-twitch muscles from the *mdx* mouse (**Figure 1.6**). An eccentric contraction is one in which the muscle is stretched while activated, such as occurs in the quadriceps muscle when running downhill. Eccentric contractions place more strain on muscles than any other type of contraction.

In these *in vitro* studies, fast-twitch muscles were subjected to eccentric contractions

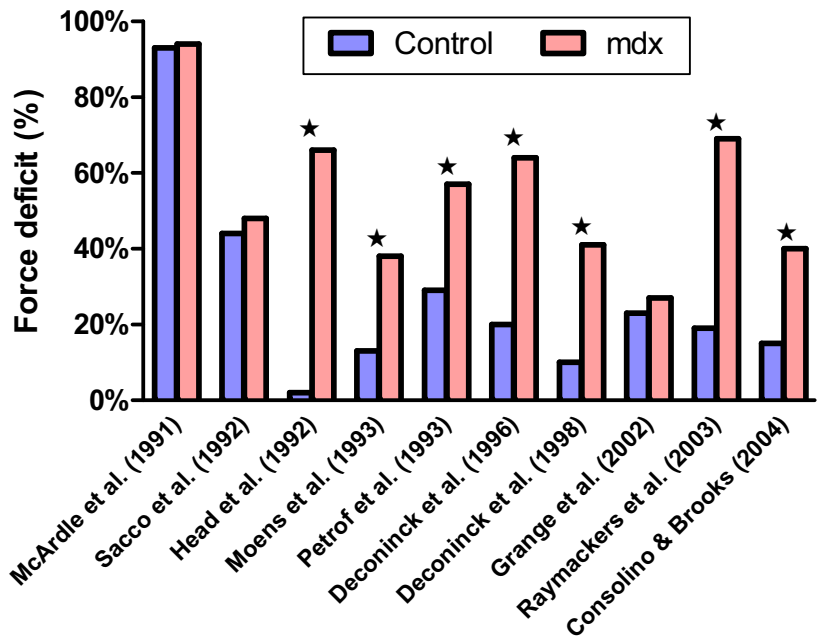

Figure 1.6 Force deficits following eccentric contractions in fast-twitch *mdx* muscles. A higher force deficit is indicative of greater muscle damage. A star indicates a significant difference ($p<0.05$) between *mdx* and control muscle. Note: this figure is a graphical representation of Table 2.1, page 28.

and the damage in *mdx* muscles compared with controls. The extent of damage was measured by the force deficit, which is the decrease in muscle force after undergoing eccentric contractions, expressed as a percentage of the force produced before the contractions. The higher the force deficit, the greater the damage. The results of these studies are shown in **Figure 1.6**. Almost all the studies found higher force deficits in fast-twitch *mdx* muscles than in controls. These higher force deficits were also associated with greater membrane damage in *mdx* muscle fibres as assessed by uptake of a membrane-permeant dye (Petrof *et al.*, 1993; Moens *et al.*, 1993). Taken together, these results suggest that muscles lacking dystrophin are more easily damaged by contractile stresses than muscles possessing dystrophin, and appear to argue strongly for a mechanical role of dystrophin in physically supporting the sarcolemma during contractile activity.

Critique of the structural hypothesis

Despite the strength of the evidence from these studies, it may be criticised on several grounds. Firstly, to attribute the greater force deficits of *mdx* muscle to its lack of dystrophin is to assume that absence of dystrophin is the only feature distinguishing *mdx* muscle from normal muscle. There could be other differences which are contributing to the increased susceptibility to contraction-induced injury. One of the most striking differences between *mdx* muscle fibres and normal muscle fibres is in their morphology. Fibres from *mdx* muscle are often branched or split and the prevalence of these deformed fibres increases with age (Head

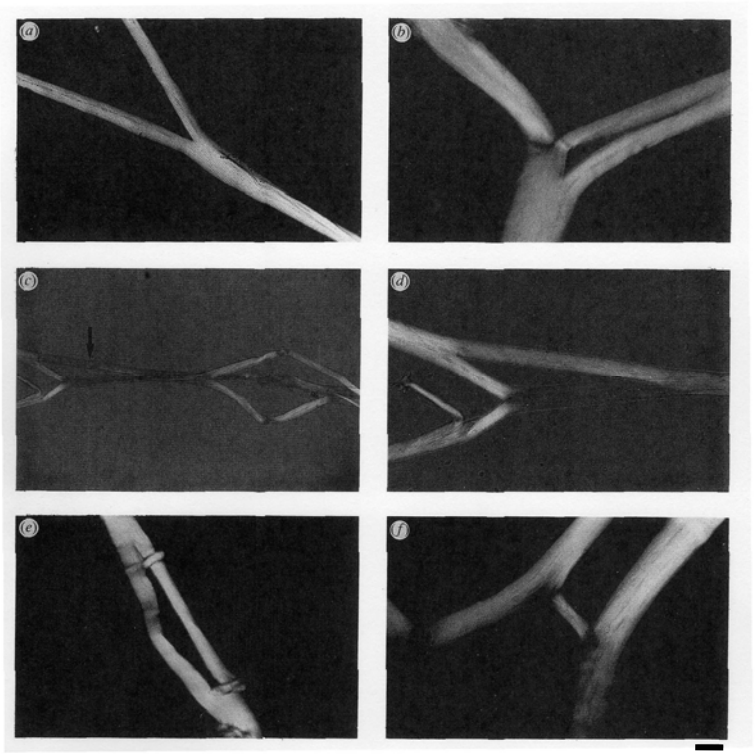

Figure 1.7 Abnormal morphology of *mdx* muscle fibres. Low-power images of deformed fibres from the extensor digitorum longus (EDL), soleus (SOL) and flexor digitorum brevis (FDB) muscles of *mdx* mice aged 26-84 weeks. Many abnormal branching patterns can be observed. Scale bar units (in microns): (a) 30 (b) 10 (c) 60 (d) 30 (e) 20 (f) 30. *Reproduced from Head et al. (1992).*

et al., 1992). Examples of branched fibres from *mdx* muscle are shown in **Figure 1.7**. Branched fibres are thought to result from incomplete lateral fusion of regenerating myoblasts and myotubes as they attempt to reconstitute a damaged segment of a muscle fibre (Schmalbruch, 1984). In rodent models, they have been found in muscles undergoing repetitive degeneration and regeneration, as in muscular dystrophy (Head *et al.*, 1990; Head et al., 1992), whole muscle transplants (Bourke & Ontell, 1984) and muscles injected with bupivacaine (Tamaki & Akatsuka, 1994). They have also been demonstrated in muscle biopsies from patients with DMD (Schmalbruch, 1984).

Intuitively, these branched fibres could be structurally weak. High shear stresses might occur at branch points during intense contractile activity, leading to fibre rupture (Head *et al.*, 2004). Action potentials would be propagated more slowly along narrow branches than along the main fibre, leading to asynchronous contractile activity with more active regions pulling on less active ones, resulting in fibre damage (Head *et al.*, 1990). Indeed, experiments in another mouse model of muscular dystrophy showed that when individual fibres were stimulated, fibre segments which contained branch points were more liable to rupture than fibre segments without branch points, and when whole muscles were stimulated, branched fibres were preferentially damaged over unbranched fibres (Head *et al.*, 1990).

It is highly possible then, that the susceptibility of *mdx* muscle to contraction-induced damage is more a consequence of structurally weak, branched fibres than an absence of dystrophin. One would need to be cautious in using the above studies as evidence for the structural hypothesis, when there is the possibility that a significant proportion of the fibres in the *mdx* muscles are branched.

A second qualification concerning the structural hypothesis is that some studies failed to find that muscles deficient in dystrophin or other DAPC components were any more susceptible to mechanical damage than controls. In experiments on mice lacking laminin, the protein that connects the DAPC to the basal lamina, Head *et al.* (2004) found similar force deficits between laminin-deficient mice and controls. Law *et al.* (1995) found that it took the same stress, strain and energy to stretch *mdx* muscles to the point of rupture as it took for control muscles.

A third criticism of the structural hypothesis is that it fails to provide a role for dystrophin in non-contractile tissues. Dystrophin is found, in various isoforms, in many different tissues in the body, most notably in the central nervous system (CNS), where it is expressed in cortical neurons, cerebellar Purkinje cells and the retina (Muntoni *et al.*, 2003). The importance of dystrophin in the CNS is suggested by the frequency of cognitive impairment among boys with DMD (Emery, 2002), and by the finding that inhibitory input is

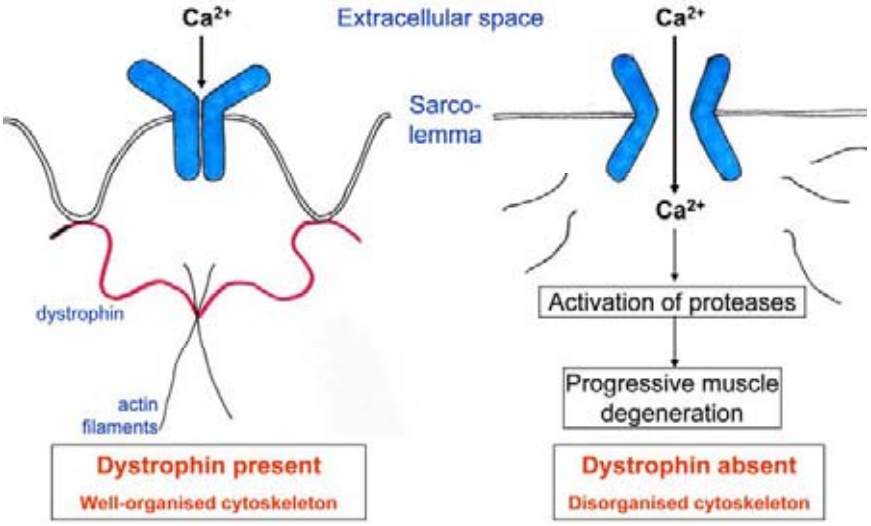

Figure 1.8 The ion channel hypothesis. Dystrophin helps to organise the sub-sarcolemmal cytoskeleton. When dystrophin is absent, the cytoskeleton becomes disorganised, allowing Ca^{2+} to enter. *Based on Carlson (1998).*

reduced in the Purkinje cells of *mdx* mice (Anderson *et al.*, 2003). There is a very high degree of structural similarity between the dystrophin isoforms that are expressed in skeletal muscle and the CNS (Muntoni *et al.*, 2003), so it is possible that dystrophin has a similar role in all these tissues. The tissues of the CNS are not subject to significant mechanical stress, so dystrophin's role in these cells may be different from that suggested by the structural hypothesis.

The ion channel hypothesis of dystrophin function

In light of these criticisms, various alternative theories of dystrophin's function have been proposed. The main alternative theory is the ion channel hypothesis, which arose from the observation that intracellular Ca^{2+} concentrations were increased in dystrophin-deficient muscle (Gillis, 1999). One advantage of the ion channel hypothesis is that it provides a universal function for dystrophin, as all tissues possess ion channels.

A simplified statement of this theory is depicted in **Figure 1.8**. According to this theory, dystrophin helps to organise the subsarcolemmal cytoskeleton, ensuring proper function of ion channels in the plasma membrane. When dystrophin is present, the cytoskeleton is well-organised, resulting in ion channels having a normal conformation which prevents entry of Ca^{2+}. When dystrophin is absent, the cytoskeleton is poorly organised, leading to a conformational change in ion channels which allows entry of Ca^{2+}. As the intracellular Ca^{2+} concentration rises, proteases are activated and muscle degeneration ensues (Carlson, 1998).

Hence, under the ion channel hypothesis, the absence of dystrophin does not mechanically weaken the sarcolemma; rather it results in the abnormal functioning of sarcolemmal ion channels. Studies on the *mdx* mouse have reported abnormal distribution and functioning of several classes of sarcolemmal ion channel. These include: (i) non-selective cation channels that are open at rest (Franco & Lansman, 1990; Fong *et. al.*, 1990; Turner *et. al.*, 1991; Tutdibi *et. al.*, 1999); (ii) stretch-activated non-selective cation channels that open during contractile activity (Yeung *et. al.*, 2003; Millay *et. al.*, 2009); (iii) acetylcholine receptors (Carlson, 1996; Carlson & Officer, 1996); (iv) store-operated Ca^{2+} channels (Boittin *et. al.*, 2006); and (v) L-type voltage-gated Ca^{2+} channels (Friedrich *et. al.*, 2008).

The abnormal functioning of stretch-activated cation channels in *mdx* muscle appears to be an important factor contributing to the greater susceptibility of *mdx* muscle to damage from eccentric contractions. Yeung *et al.* (2003) subjected single non-branched *mdx* muscle fibres to eccentric contractions and found greater force deficits in the *mdx* muscle fibres than in controls. However, this difference in force deficit was eliminated by the addition of gadolinium, an established blocker of mechanosensitive channels. This showed that the greater force deficit in *mdx* fibres was attributable to increased Ca^{2+} entry through mechanosensitive channels, rather than a direct result of membrane damage.

The stretch-sensitive TRPC family of ion channels has been proposed as the mechanosensitive channels which function abnormally in the absence of dystrophin (Whitehead *et. al.*, 2006; Millay *et. al.*, 2009). In addition, Zanou *et al.* (2009) identified TRPV2 as a mechanosensitive channel responsible for an increased force deficit in *mdx* EDL muscle following eccentric contractions.

Proposed functions of α-actinin-3

As in the case of dystrophin, α-actinin is commonly considered to have a structural role. The fact that it cross-links actin filaments and is the major component of the Z-disc suggests that it functions to maintain stability of the sarcomeres during contraction and transmit forces through the Z-discs to the sarcolemma. Given the association of α-actinin-3 with enhanced sprint and power performance, it is plausible that this particular isoform is required to maintain the structural integrity of muscle fibres during intense contractile activity. Furthermore, the expression of α-actinin-3 is restricted largely to fast-twitch glycolytic fibres, the fibre type that generates the largest contractile forces.

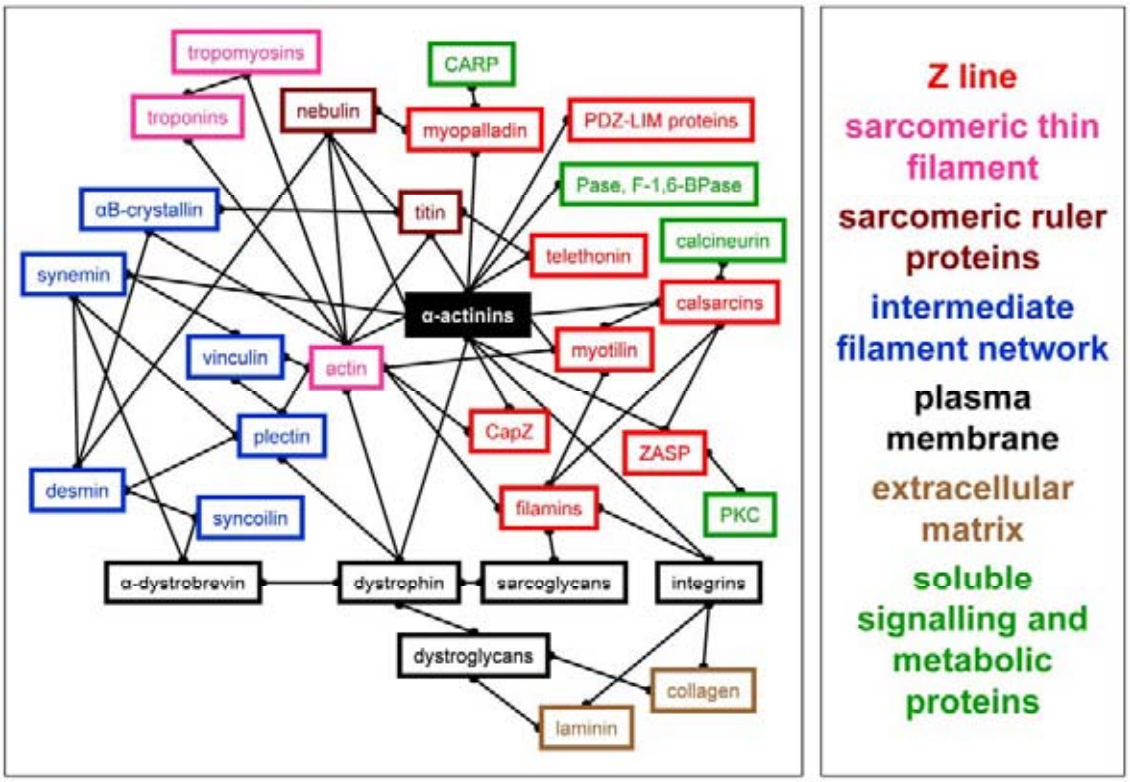

Figure 1.9 Protein interactions of α-actinin. α-Actinin forms a hub at the intersection of pathways involved in cellular signalling and metabolism, as well as pathways involved in maintaining cell structure and integrity. Pase – glycogen phosphorylase; F-1,6-Bpase – fructose-1,6-bisphosphatase. *Courtesy of Prof Kathryn North.*

However, α-actinin does not interact only with actin. It also interacts with a vast array of non-structural proteins, suggesting that its role may be far more complex than a purely structural one (MacArthur & North, 2004). **Figure 1.9** is a summary of the direct and indirect protein interactions of α-actinin. It can be seen that α-actinin forms a hub at the intersection of pathways involved in cellular signalling and metabolism, as well as pathways involved in maintaining cell structure and integrity.

As shown in the diagram, α-actinin interacts with glycogen phosphorylase and fructose-1,6-bisphosphatase, enzymes involved in the regulation of metabolism (MacArthur & North, 2004). It also interacts with calsarcin, which in turn interacts with calcineurin. Calcineurin is a signalling molecule which promotes the formation of slow-twitch, oxidative fibres (Frey *et al.*, 2008). Hence, in addition to any structural function it may perform, α-actinin is highly likely to be involved in fibre type differentiation as well. The fact that α-actinin-3 is specifically expressed in fast-twitch glycolytic fibres raises the possibility that this particular isoform may promote the development of fast-twitch, glycolytic characteristics in muscle fibres, and in its absence slower-twitch, more oxidative characteristics may develop. This role is plausible in light of the observations in elite athletes; a rapid twitch response in the

presence of α-actinin-3 would be beneficial for activities such as sprinting which require rapid contractions, while a greater use of oxidative metabolism in the absence of α-actinin-3 would be beneficial for endurance activities.

Given the possible role of α-actinin-3 in fibre type differentiation, it will be useful to provide an overview of the main distinguishing features between fibre types. Fibres are functionally classified into two main types: fast-twitch and slow-twitch. They differ from one another in two main respects. The first is the speed of the force response to a single action potential. The second is the degree of reliance on oxygen in metabolism (Brooks, 2003).

The rate of force response in fast-twitch and slow-twitch fibres

As the names suggest, fast-twitch fibres have a faster rate of contraction and, importantly, a faster rate of relaxation than slow-twitch fibres (Bottinelli & Reggiani, 2000; Burke *et al.*, 1973). The factors affecting the rate of contraction and relaxation are best understood in terms of the excitation-contraction-relaxation process in muscle fibres. This process is illustrated in **Figure 1.10**.

An action potential travels along the sarcolemma **(1)** and down the transverse tubule **(2)**. The depolarisation signal is detected at the sarcoplasmic reticulum (SR) membrane **(3)**, causing the release of Ca^{2+} **(4)** from the SR into the cytoplasm **(5)**. The Ca^{2+} binds to troponin C **(6)**, leading to a conformational change in tropomyosin that exposes the myosin-binding sites on the actin filament. This allows the myosin heads **(7)** to interact with actin and produce

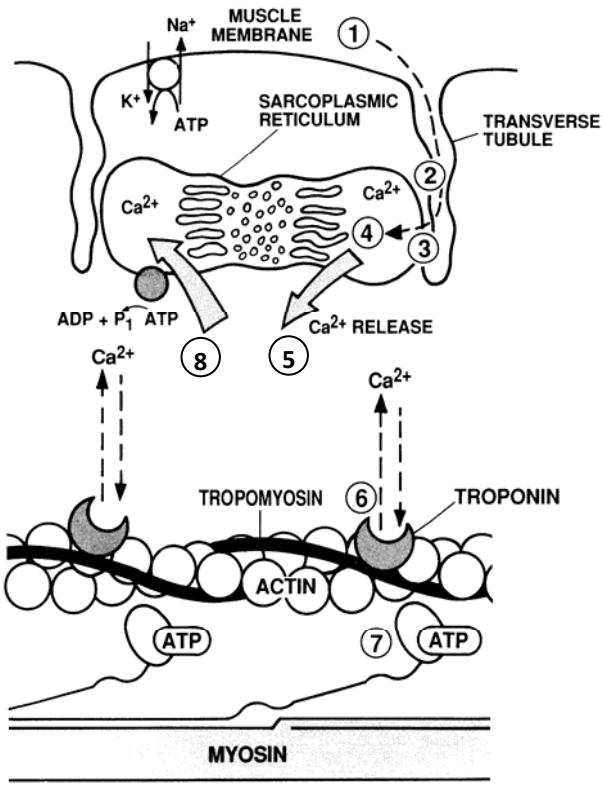

Figure 1.10 Major events of the excitation-contraction-relaxation process in a muscle fibre. *Reproduced from Fitts (1994).*

contraction through repeated hydrolysis of ATP by myosin ATPase. Relaxation is due to the re-uptake of Ca^{2+} into the SR by a Ca^{2+}-ATPase pump **(8)**. As Ca^{2+} dissociates from troponin C, the myosin-binding sites on actin are again covered by tropomyosin, preventing interaction with the myosin heads.

The differences in rate of force response between fast-twitch and slow-twitch fibres are mainly due to: (i) the sensitivity of the myofibrillar apparatus to Ca^{2+} (Steps 6 and 7); (ii) the rate of tension development when myosin and actin interact in steady-state conditions (Step 7); and (iii) the rate of Ca^{2+} release and re-uptake by the SR (Steps 4 and 8) (Bottinelli & Reggiani, 2000).

The sensitivity of the myofibrillar apparatus to Ca^{2+} is usually described by the force-pCa relationship, that is, the amount of force produced by the contractile filaments at different concentrations of Ca^{2+} (Bottinelli & Reggiani, 2000). Fast-twitch fibres generally have a steeper force-pCa relationship than slow-twitch fibres (Fink *et al.*, 1986; Williams *et al.*, 1993), so that a given change in $[Ca^{2+}]$ leads to a greater change in force in fast-twitch fibres than in slow-twitch fibres. Another feature of the force-pCa relationship that distinguishes fast-twitch from slow-twitch fibres is the threshold Ca^{2+} concentration for activation. Slow-twitch fibres activate at lower Ca^{2+} concentrations than fast-twitch fibres (Bortolotto *et al.*, 2000).

The rate of tension development when myosin and actin interact in steady-state conditions is largely determined by the isoforms of myosin heavy chain (MHC) that are expressed by the fibre. Fast-twitch fibres express the type II isoforms of MHC. These isoforms have a high ATPase activity, allowing rapid interaction between actin and myosin, leading to a high shortening velocity and rapid twitch response. The type II isoforms are IIa, IIx and IIb (in order of increasing shortening velocity) (Trinh & Lamb, 2006). Slow-twitch fibres express the type I isoform of MHC, which has a low ATPase activity, leading to a low shortening velocity and slow twitch response (Brooks, 2003).

The rate of Ca^{2+} release and re-uptake by the SR are both considerably slower in slow-twitch than in fast-twitch fibres (Bottinelli & Reggiani, 2000). One reason is that slow-twitch fibres have a smaller surface area of SR membrane. Additionally, in regards to Ca^{2+} re-uptake, slow-twitch fibres have a two- to threefold lower density of Ca^{2+}-ATPase pumps in the SR membrane than fast-twitch fibres (Pette & Staron, 1990). Also, the maximum Ca^{2+} capacity of the SR in slow-twitch fibres is only about one-third of that in fast-twitch fibres, due to smaller amounts of calsequestrin being available to buffer rises in $[Ca^{2+}]$ (Fryer & Stephenson, 1996). This inhibits the ability of the Ca^{2+}-ATPase to pump Ca^{2+} back into the SR lumen. The slower rate of Ca^{2+} re-uptake contributes to the slower rate of relaxation in slow-twitch fibres compared with fast-twitch fibres (Fryer & Stephenson, 1996).

If α-actinin-3 plays a role in the differentiation of fast-twitch properties as hypothesised, then α-actinin-3 deficiency would be associated with a shift towards slower-twitch characteristics, and we would expect to see a reduced steepness of the force-pCa relationship, a shift towards slower MHC isoforms and a slower rate of SR Ca^{2+} uptake in *Actn3* knockout mouse muscle fibres. Immunohistochemical analysis of *Actn3* knockout mouse muscle suggests that there is no shift in MHC isoform expression (MacArthur *et al.*, 2008), but it is still possible that there are changes in the Ca^{2+} sensitivity of the contractile proteins and the rate of SR Ca^{2+} uptake.

Metabolism in fast-twitch and slow-twitch fibres

Another distinguishing feature between fibre types is their form of metabolism; specifically, whether they rely predominantly on oxidative metabolism or on anaerobic glycolysis to generate ATP. **Figure 1.11** is an overview of the main pathways used by muscle cells to generate ATP. The process of metabolism essentially involves transferring the energy from the C—C and C—H bonds in metabolic fuels to the phosphate bond in ATP. The energy transfer is achieved by passing electrons to electron-acceptors such as NAD^+, which thus becomes reduced to NADH. The electrons from NADH are ultimately passed to oxygen, and the energy released is used to form the phosphate bond of ATP (Marks *et al.*, 1996).

The main metabolic fuels used in muscle cells are internal stores of glycogen, and circulating glucose and fatty acids. All these fuels are eventually oxidised to acetyl CoA, which enters the tricarboxylic acid cycle (TCA cycle) in mitochondria. Here acetyl CoA is completely oxidised to CO_2, and its electrons passed to NAD^+, which becomes reduced to NADH. NADH then gives its electrons to the electron transport chain, a series of proteins located in the inner mitochondrial membrane. These proteins pass the electrons to O_2, and the energy released is used to form the phosphate bond of ATP.

Because this process relies on O_2 to form ATP, it is termed oxidative metabolism. However, as the diagram shows, some ATP is also formed during glycolysis, the process whereby glycogen and glucose are oxidised to pyruvate. The NADH can be reoxidised to NAD^+ by the reduction of pyruvate to lactate, without needing to use the electron transport chain. Because this method of ATP generation does not require O_2, it is termed anaerobic glycolysis. It produces ATP more quickly than oxidative metabolism, but does not produce as much ATP. Muscle fibres that rely mainly on oxidative metabolism are called “oxidative”, while those that rely mainly on anaerobic glycolysis are called “glycolytic”.

Fast-twitch fibres have MHC isoforms that consume ATP rapidly and hence they rely mainly on anaerobic glycolysis, which can regenerate ATP quickly (Bottinelli & Reggiani, 2000).

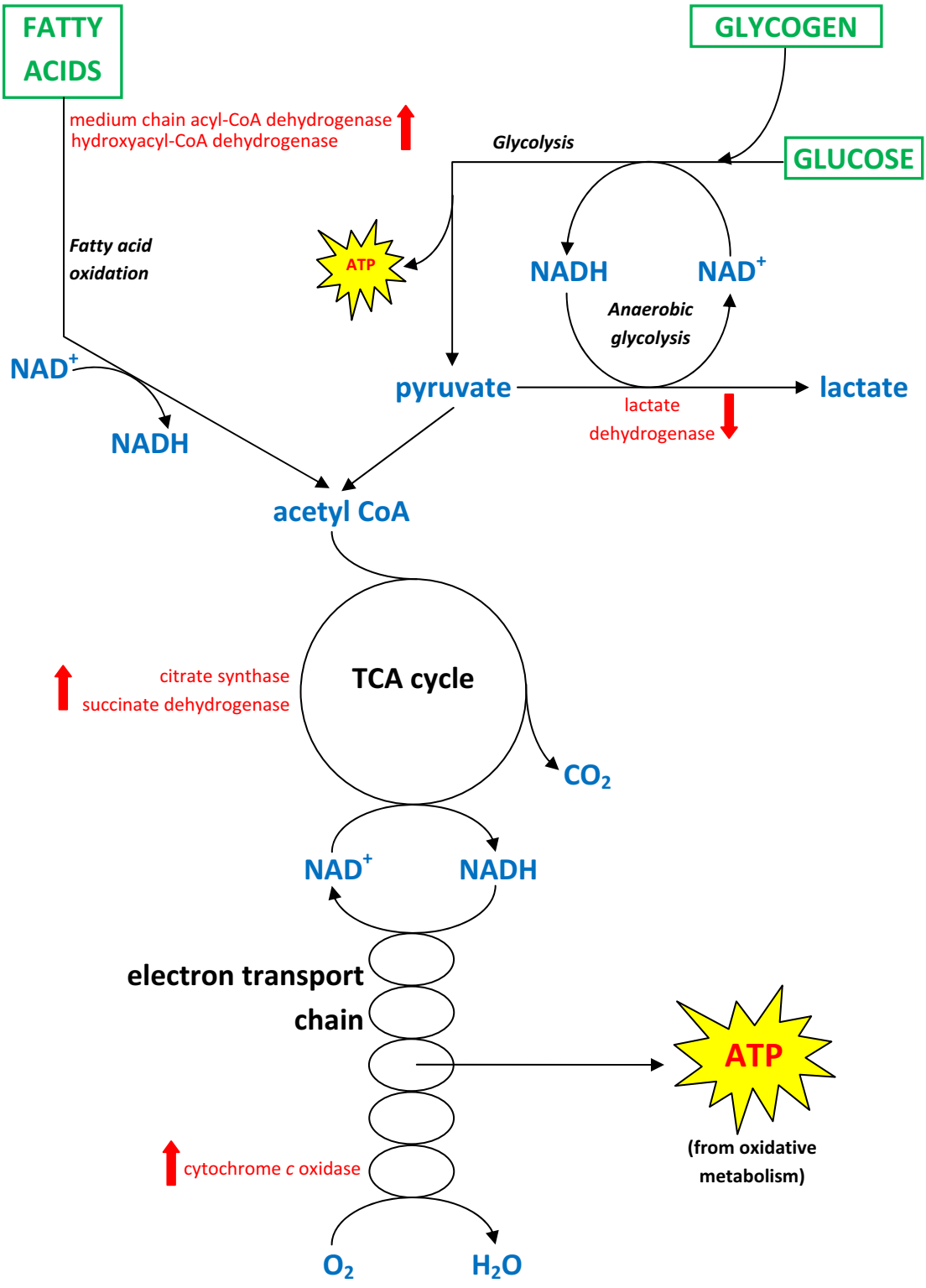

Figure 1.11 Main metabolic pathways in skeletal muscle. Metabolism essentially involves the transfer of energy from the chemical bonds in metabolic fuels (shown in *green*) to the phosphate bond in ATP. Shown in *red* are the names of enzymes found to have altered activity in *Actn3* knockout mouse muscles. *Red up arrows* indicate increased activity; *red down arrows* indicate reduced activity. *Based on Marks et al. (1996).*

Slow-twitch fibres have MHC isoforms that consume ATP more slowly and hence they rely mainly on oxidative metabolism, which can produce large amounts of ATP for long, sustained contractions (Brooks, 2003). A class of fast-twitch fibres that expresses predominantly type IIa myosin relies on both oxidative metabolism and anaerobic glycolysis to produce ATP. These fibres are generally called "fast-twitch oxidative/glycolytic" to distinguish them from "fast-twitch glycolytic" fibres, which predominantly express the other type II isoforms of MHC (Pette & Staron, 1990). α-Actinin-3 expression is restricted mainly to fast-twitch glycolytic fibres (MacArthur & North, 2004).

If α-actinin-3 plays a role in the differentiation of fast-twitch fibres as hypothesised, we would expect to see fast-twitch glycolytic fibres shift towards oxidative metabolic pathways in the absence of α-actinin-3. Enzyme assays performed on muscles from *Actn3* knockout mice suggest that this is indeed the case (MacArthur *et al.*, 2007; MacArthur *et al.*, 2008).

Shown in red in Figure 1.11 are the names of enzymes found to have altered activity in *Actn3* knockout mouse muscle. They are listed next to the parts of the metabolic process that they catalyse. Lactate dehydrogenase, which catalyses the reduction of pyruvate to lactate in anaerobic glycolysis, was found to have a lower activity in *Actn3* knockouts than in controls (MacArthur *et al.*, 2007; MacArthur *et al.*, 2008). As the figure shows, this would mean less pyruvate was converted into lactate, leaving more to be converted to acetyl CoA, which enters the pathway towards generation of ATP by oxidative metabolism. On the other hand, increased activity was found in various enzymes involved in fatty acid oxidation, the TCA cycle and the electron transport chain, all components of the pathway that produces ATP using oxygen (MacArthur *et al.*, 2008). Hence, all these alterations to enzyme activity in *Actn3* knockout mouse muscle serve to reduce the use of anaerobic glycolysis and promote the use of oxidative metabolism.

Aims of thesis

The main aim of this thesis is to re-assess the common perception of dystrophin and α-actinin-3 as structural proteins. While they may play a role in maintaining the structural integrity of a muscle fibre during contractile activity, they may also have additional functions. This thesis aims to offer alternative interpretations of data previously taken to suggest a structural role, or to offer evidence of additional non-structural functions. The main questions this thesis attempts to address are as follows.

1. Are dystrophin-deficient fibres more susceptible to contraction-induced injury because dystrophin is absent, or is it also because these fibres have an abnormal branched morphology?

To address this question, extensor digitorum longus (EDL) muscles from *mdx* mice will be subjected to eccentric (lengthening) contractions. Mice will be divided into two age groups: a "younger" group (about 1 to 2 months old) in which fibre branching was expected to be minimal, and an "older" group (about 6 to 7 months old) in which fibre branching was expected to be more extensive. Muscle damage from the eccentric (lengthening) contractions will be assessed by the force deficit. The extent of fibre branching will be assessed by examining individual fibres obtained from enzymatic muscle digests. If an association is found between the degree of damage and the degree of fibre branching, this would suggest that morphological abnormalities contribute to a dystrophic muscle's increased vulnerability to injury. If this were true, the greater force deficits in *mdx* muscle reported in previous studies may not be a consequence of dystrophin's absence, but a consequence of fibre branching, and one would need to reconsider the use of these findings as evidence for the structural hypothesis of dystrophin's function.

2. Does α-actinin-3 deficiency result in a greater susceptibility to contraction-induced injury?

This question will be addressed by subjecting EDL muscles from *Actn3* knockout mice to eccentric (lengthening) contractions. Greater force deficits in *Actn3* knockout muscles compared with controls would be evidence of a structural role for α-actinin-3. However, if damage in knockouts was no different from controls, this would suggest that the role of α-actinin-3 is not a structural one, or that this particular function can be largely performed by α-actinin-2 when α-actinin-3 is absent.

3. What is the phenotype of α-actinin-3 deficient muscle, and do any aspects of this phenotype suggest a shift from fast-twitch towards slower-twitch characteristics?

The *Actn3* knockout mouse is a newly generated model of α-actinin-3 deficiency, so it would be useful to characterise the phenotype of muscles from this mouse. Various physical and contractile properties of whole EDL muscle will be measured, including: mass and cross-sectional area, maximum force, twitch and tetanus relaxation rates, and force-frequency characteristics. The fatiguability of α-actinin-3-deficient muscles will also be examined. These properties will be measured in male and female mice of various ages, to see if the phenotype of α-actinin-3 deficiency varies by age and gender. The EDL muscle will be used in these studies because this muscle contains a very high proportion of fast glycolytic fibres (at least 80% in this mouse strain (MacArthur *et al.*, 2008)). This is the fibre type in which α-actinin-3 is found, so any consequences of α-actinin-3 deficiency should be readily apparent in this muscle.

As mentioned, one hypothesised function of α-actinin-3 is that it promotes differentiation of fast-twitch, glycolytic characteristics in muscle fibres, and slower-twitch, more oxidative characteristics would develop in its absence. Hence we also wished to see if any aspects of the whole muscle phenotype indicate a shift towards a slower-twitch, more oxidative profile in the absence of α-actinin-3. If such a shift occurred, we would expect to see changes such as smaller mass and cross-sectional area, smaller forces, slower relaxation of twitch and tetanus, better fatigue resistance, and faster recovery from fatigue in *Actn3* knockout muscles compared with controls.

4. What changes occur at the level of the contractile proteins and sarcoplasmic reticulum in α-actinin-3-deficient fibres?

Question 3 addressed the changes that occur at a whole muscle level in the absence of α-actinin-3. This question addresses the changes that occur at a subcellular level. As mentioned, two of the features that characterise a muscle fibre as fast-twitch or slow-twitch are the rate of Ca^{2+} re-uptake by the SR, and the sensitivity of the contractile proteins to Ca^{2+}. The rate of Ca^{2+} uptake by the SR will be examined by loading the SR of mechanically skinned fibres with Ca^{2+} for predetermined periods of time and then emptying the SR of Ca^{2+} using caffeine. The Ca^{2+} sensitivity of the contractile proteins will be examined by activating chemically skinned fibres with Ca^{2+} and Sr^{2+} solutions of varying concentrations. If, as hypothesised, the loss of α-actinin-3 leads to a shift towards slower-twitch characteristics, one would expect changes such as a reduced rate of Ca^{2+} uptake by the SR and a reduced steepness of the force-pCa relationship in fibres from *Actn3* knockout mouse muscle.

Presentation of results

The results of these investigations will be presented as three papers. The first two have been published while the third has been submitted and was under review as at December 2009.

Paper A

Chan S, Head SI & Morley JW (2007). Branched fibers in dystrophic *mdx* muscle are associated with a loss of force following lengthening contractions. *American Journal of Physiology Cell Physiology* 293: C985-C992.

This paper addresses Question 1 under "Aims of thesis" above.

Paper B

Chan S, Seto JT, MacArthur DG, Yang N, North KN & Head SI (2008). A gene for speed: contractile properties of isolated whole EDL muscle from an α-actinin-3 knockout mouse. *American Journal of Physiology Cell Physiology* 295: C897-C904.

This paper addresses Questions 2 and 3 under "Aims of thesis" above. This is an initial study of contractile properties of whole muscle from the *Actn3* knockout mouse, using adult male mice aged 8 to 10 weeks.

Paper C

Chan S, Seto JT, Houweling PJ, Yang N, North KN & Head SI. Contractile properties of EDL muscle and skinned fibres from α-actinin-3 KO mice of various ages. Submitted to *Experimental Physiology*.

This paper addresses Question 4 under "Aims of thesis" above. It also addresses Question 3 in a fuller manner than *Paper B*, using both male and female mice from a range of age groups.

Paper A

Declaration

This chapter is a reproduction of the published paper:

> Chan S, Head SI & Morley JW (2007). Branched fibers in dystrophic *mdx* muscle are associated with a loss of force following lengthening contractions. *Am J Physiol Cell Physiol* 293: C985-C992.

Current status

Published.

Author contribution

The contribution of S.C. to this paper was 70%, and consisted of designing and performing the experiments, analysing the data, and writing the paper.

Note on format

The paper as presented in this chapter is a reproduction of the final manuscript submitted to the publisher on 18th May 2007. This was the manuscript that was accepted for publication. In reproducing this manuscript here, only the spelling, referencing style, and the numbering style of figures and tables have been modified. This has been done to achieve consistency with the rest of the thesis. Some figures have also been reproduced in colour where appropriate. References are listed with all other references at the end of the thesis.

The paper is reprinted in its published format in the "Publications" section at the end of the thesis.

Abstract

We demonstrated that the susceptibility of skeletal muscle to injury from lengthening contractions in the dystrophin-deficient *mdx* mouse is directly linked with the extent of fibre branching within the muscles and that both parameters increase as the *mdx* animal ages. We subjected isolated extensor digitorum longus (EDL) muscles to a lengthening contraction protocol of 15% strain and measured the resulting drop in force production (force deficit). We also examined the morphology of individual muscle fibres. In *mdx* mice 1 to 2 months of age, 17% of muscle fibres were branched, and the force deficit of 7% was not significantly different from that of age-matched littermate controls. In *mdx* mice 6 to 7 months of age, 89% of muscle fibres were branched, and the force deficit of 58% was significantly higher than the 25% force deficit of age-matched littermate controls. These data demonstrated an association between the extent of branching and the greater vulnerability to contraction-induced injury in the older fast-twitch dystrophic muscle. Our findings demonstrate that fibre branching may play a role in the pathogenesis of muscular dystrophy in *mdx* mice, and this could affect the interpretation of previous studies involving lengthening contractions in this animal.

Introduction

Duchenne muscular dystrophy (DMD) is an X-linked recessive disorder characterised by progressive wasting of skeletal muscle, affecting 1 in 3,500 live male births. It is caused by the absence of dystrophin, a 427 kDa protein which in normal muscle fibres is found just internal to the sarcolemma. Controversy still surrounds the function of dystrophin and the mechanisms by which its absence leads to the skeletal muscle degeneration seen in DMD (Brown & Lucy, 1997; Emery, 2002). There are several hypotheses as to the role played by dystrophin in skeletal muscle. For simplicity we will group them under 2 headings: 1) The structural hypothesis (Petrof *et al.*, 1993) and 2) The ion channel hypothesis (Carlson, 1998).

1) In the structural hypothesis the absence of dystrophin leaves the membrane weakened and susceptible to tearing during muscle contraction, leading to irreversible fibre damage followed by necrosis. Support for this theory comes from well-established evidence that the fast-twitch muscles of the dystrophin-deficient *mdx* mouse are more easily damaged by lengthening contractions (contractions with stretch) than are normal muscles (see **Table 2.1**).

2) In the ion channel hypothesis the absence of dystrophin is suggested to lead to the pathological function of a sarcolemmal ion channel, and several ion channels have been singled out as promising candidates for the primary cause of the pathology in dystrophin deficient dystrophies (for review see (Allard, 2006)). The majority of these studies hypothesise that the end consequence of the proposed channelopathy is an increased intracellular flux of Ca^{2+}, and this increase in $[Ca^{2+}]_i$ results in fibre damage through mediators such as proteases and reactive oxygen species (ROS) (Whitehead *et al.*, 2006). It is important to note that in the ion channel hypothesis the absence of dystrophin does not chronically weaken the sarcolemma; rather it disrupts ion channel function.

The etiology of the muscle degeneration in *mdx* mice is complicated by the fact that as *mdx* muscle ages the architecture of the dystrophic muscle fibres becomes grossly abnormal (Head *et al.*, 1992). These abnormal fibres, termed branched or split fibres, are more prone to damage during contraction, as high shear stresses occur at branch points during intense contractile activity, leading to fibre rupture at these points. Direct evidence demonstrating the increased fragility of branched fibres was presented in Head *et al.* (1990) where it was demonstrated that when individual fibres were stimulated, fibre segments which contained branch points were more liable to rupture than fibre segments without branch points, and when whole muscles were stimulated, branched fibres were preferentially damaged over

unbranched fibres within the muscle. The question arises, then, as to whether the increased susceptibility of *mdx* muscles to injury during lengthening contractions is due directly to the absence of dystrophin, or whether the morphological changes (branching) of fibres leads to weakened regions (branch points) that are the site of damage during contraction.

The aim of our study was to address this question by examining *mdx* mice in two age groups: a "younger" group about 1 to 2 months old, in which fibre branching was moderate (<20%), and an "older" group about 6 to 7 months old, in which fibre branching was more extensive (>80%). We hypothesised that the "older" group would experience a greater loss of force than the "younger" group following a mild protocol of lengthening contractions. By examining the association between the extent of fibre branching and the susceptibility to injury, we attempted to gain some insight into the role of branched fibres in the pathogenesis of muscular dystrophy in the *mdx* mouse.

Study	**Age of mice (weeks)**	**Strain†**	**Muscle**	**Force deficits**	
				normal	***mdx***
McArdle *et al.* (1991)	5 - 6	30%	EDL	93%	94%
Sacco *et al.* (1992)	16 - 26	*in situ* ‡	tibialis anterior	44%	48%
Head *et al.* (1992)	> 45	12%	EDL	2%	66%*
Moens *et al.* (1993)	~ 3 - 70	~ 8%	EDL	13%	38%*
Petrof *et al.* (1993)	12 - 15	10%	EDL, diaphragm	29%	57%*
Deconinck *et al.* (1996)	16	7%	gastrocnemius	20%	64%*
Deconinck *et al.* (1998)	10	8%	EDL	10%	41%*
Grange *et al.* (2002)	1-2	10%	EDL	23%	27%
Raymackers *et al.* (2003)	12	7%	EDL	19%	69%*
Consolino & Brooks (2004)	20	18%§	EDL	15%	40%*

Table 2.1 Force deficits of normal and *mdx* fast-twitch muscles following lengthening contractions. A "*" indicates a significant difference in force deficit between *mdx* and normal. Higher force deficits are taken as indicators of a greater degree of muscle damage. †The "strain" is the length by which the muscle is stretched, as a percentage of its original length. ‡The length of stretch could not be measured in this study as the muscle was not dissected out. Instead the muscle was stretched by moving the foot. §A variety of strains was used in this study. Only the results for the middle strain are shown.

Methods

Animals used

mdx mice with littermate controls were obtained from the Animal Resources Centre (Perth, Australia). Female C57BL/10ScSn-DMD (*mdx*) mice were mated with male C57BL/10ScSn mice. The offspring of this first mating were then mated together. The male offspring of this second mating comprise a colony of *mdx* mice and littermate controls sharing a common genetic background, and it is this colony which was used in this study. Littermate control mice were distinguished from *mdx* mice on the basis of serum creatine kinase (CK) levels. Mice with CK < 1,000 IU were classified as controls, while mice with CK > 1,000 IU were classified as *mdx*. Western blotting for the presence of dystrophin has shown this to be an ultra-reliable method for phenotyping the mice in this colony (Kueh *et al.*, 2004). Phenotype was further confirmed when muscle fibres were examined with confocal microscopy; *mdx* fibres have many centrally located nuclei, while almost all nuclei in control fibres are peripherally located.

In all, 13 mice were used for the experiments assessing contractile properties, contraction-induced damage and fibre morphology. These consisted of 6 "younger" mice aged 6 to 8 weeks and 7 "older" mice aged 27 to 31 weeks. Immediately before experimentation, animals were anaesthetised with halothane and sacrificed by cervical dislocation. Use of animals was approved by the University of New South Wales Animal Care and Ethics Committee.

Muscle preparation

The extensor digitorum longus (EDL) muscle was dissected from the hindlimb and tied by its tendons to a force transducer (World Precision Instruments, Fort 10) at one end and a linear tissue puller (University of New South Wales) at the other, using silk suture (Deknatel 6.0). The muscle was placed in a bath continuously superfused with Krebs solution, with composition (mM): 4.75 KCl, 118 NaCl, 1.18 KH_2PO_4, 1.18 $MgSO_4$, 24.8 $NaHCO_3$, 2.5 $CaCl_2$ and 10 glucose, with 0.1% fetal calf serum and continuously bubbled with 95% O_2-5% CO_2 to maintain pH at 7.4. The muscle was stimulated by delivering an electrical current between two parallel platinum electrodes, using an electrical stimulator (A-M Systems). At the start of the experiment, the muscle was set to its optimum length L_0 by finding the length that produced maximum twitch force. All experiments were conducted at room temperature (~ 22°C to 24°C).

In total, 23 muscles were used, 11 in the "younger" group (5 controls and 6 *mdx*) and 12 in the "older" group (4 controls and 8 *mdx*).

Lengthening contraction protocol

The lengthening contraction protocol is illustrated in **Figure 2.1**. At time = 0 ms, the muscle was stimulated by supramaximal pulses of 1 ms duration and 100 Hz frequency. At time = 750 ms, after it had attained its maximum isometric force, the muscle was stretched at a speed of 1 mm/s until it was 15% longer than its optimum length, held at this length for 2 seconds, then returned at the same speed to its original position. The electrical stimulus was stopped at time = 5000 ms. This lengthening contraction was performed 3 times, at intervals of 5 minutes. The strain of 15% of muscle length was equivalent to a strain of 33% of fibre length, assuming that fibre length is 45% of muscle length (Brooks & Faulkner, 1988).

A mild strain of 15% was chosen because preliminary experiments indicated that this strain did not damage control muscles of younger mice (unpublished data). This would allow us to determine if muscles from *mdx* mice were more susceptible to damage. An excessively severe strain would substantially damage all muscles, thus obscuring differences in fragility between *mdx* and control muscles. The lengthening contraction protocol was initiated at a similar isometric force plateau in all groups tested to ensure a similar absolute force was experienced by all the muscles.

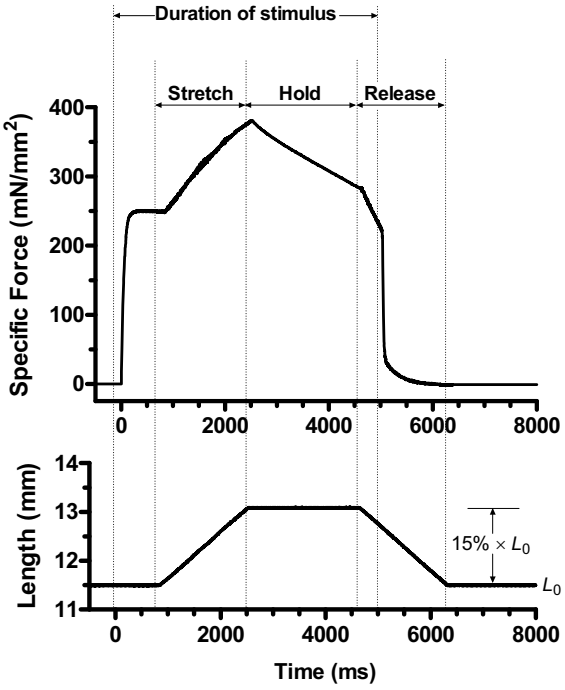

Figure 2.1. The lengthening contraction protocol. The diagrams show recordings of (top panel) force and (bottom panel) muscle length, obtained during one lengthening contraction in a muscle from an 8 week-old *mdx* mouse. Electrical stimulation starts at time = 0 ms. At time = 750 ms, the muscle is stretched at 1 mm/s until it is 15% longer than its optimum length L_0, held at this length for 2 s, then returned at the same rate to its original length. Stimulation is stopped at time = 5000 ms. 3 such contractions were performed, at intervals of 5 minutes. A strain of 15% was used.

Force measurement

Muscle force was measured using a force-frequency curve, an example of which is shown in **Figure 2.2**. The muscle was stimulated for 500 ms at different frequencies (5, 15, 25, 37.5, 50, 62.5, 75, 87.5 and 100 Hz), and maximum force recorded at each frequency of stimulation. A curve relating the muscle force *P* to the stimulation frequency *f* was then fitted to these data. The curve had the following equation (Motulsky & Christopoulos, 2003):

$$P = P_{\min} + \frac{P_{\max} - P_{\min}}{1 + \left(\frac{K_f}{f}\right)^h}$$

The values of the parameters P_{min}, P_{max}, K_f and h were outputs of the fitting procedure, and their meaning in relation to the force-frequency curve is illustrated in Figure 2.2. P_{min} is the force developed at minimum stimulation frequency; P_{max} is the force developed at maximum stimulation frequency; K_f is the frequency at which the force developed is halfway between P_{min} and P_{max}; h is known as the Hill coefficient. In this study, the values of r^2 for the fitting procedure were not lower than 99.6%.

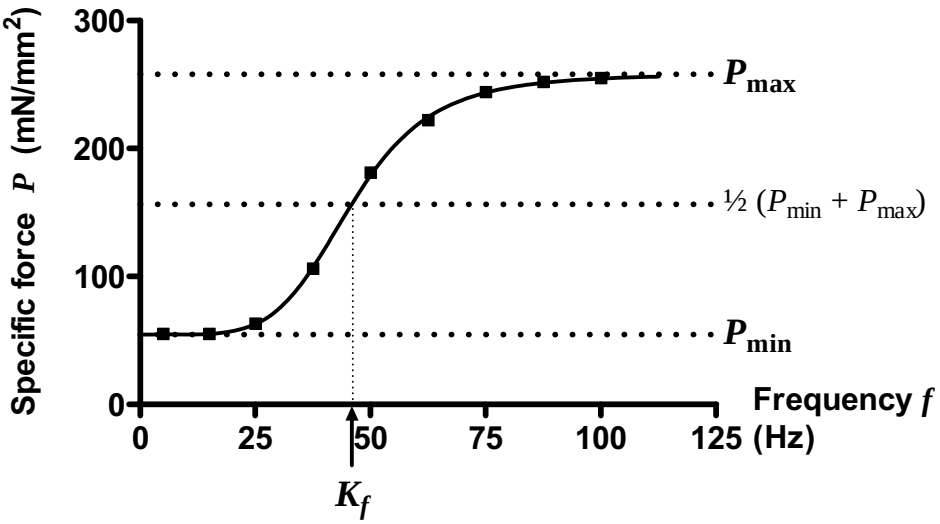

Figure 2.2. A representative force-frequency curve from a 6 week-old control muscle prior to lengthening contractions. Muscle force was measured at different stimulation frequencies, and a sigmoidal curve fitted to the data points. The following measurements were then taken from the fitted curve and used to quantify the muscle's contractile properties: P_{max}, the maximum force; P_{min}, the minimum force; K_f, the half-frequency.

Three contractile properties of the muscle were determined from the fitted parameters of the force-frequency curve: the maximum tetanic force (P_{max}), the twitch to tetanus ratio (P_{min} / P_{max}), and the half-frequency (K_f).

One force-frequency curve was obtained immediately prior to the lengthening contraction protocol. Twenty minutes after the final lengthening contraction, the setting of the optimum length L_0 was repeated, and then a second force-frequency curve was obtained. Muscle damage was assessed functionally, by comparing the abovementioned contractile properties before and after the contraction protocol. Indicators of damage were: the percentage fall in maximum tetanic force, the percentage change in half-frequency and the percentage change in twitch-to-tetanus ratio. The primary indicator of damage was the percentage fall in maximum tetanic force, which will be referred to as the force deficit.

To facilitate comparison between different muscles, forces are expressed as force per cross-sectional area (units mN/mm^2). Cross-sectional area was calculated by dividing the muscle's mass by the product of its optimum length and the density of mammalian muscle ($1.06\ mg/mm^3$).

Muscle stiffness

To assess differences in stiffness between muscles, we analysed the change in force during the ramp phase of the first lengthening contraction in each muscle. Some muscles reached a force that exceeded the capacity of the force transducer during the ramp phase, so we limited our analysis to the first part of the ramp (until the muscle reached 108% of optimum length). Stiffness was assessed by dividing the percentage change in force over this time by the percentage change in length.

Statistical analyses

Analyses were conducted using 2-way ANOVA. The null hypothesis was that the effect of dystrophin deficiency is the same in both "younger" and "older" mice; that is, the effect of dystrophin deficiency is independent of age. Post-tests, comparing *mdx* with control within each age group, were performed using the Bonferroni correction for multiple comparisons. All tests were conducted at a significance level of 5%. All statistical analyses, plus the fitting of the force-frequency curve, were performed using a standard statistical software package (GraphPad Prism Version 4.00 for Windows, GraphPad Software, San Diego California USA). Means are presented as mean ± SEM.

Muscle fibre morphology

Immediately following experimentation, the muscles were digested to yield individual fibres. The solution used for the digestion was Krebs solution containing 3 mg/mL collagenase Type I (Sigma) and 1 mg/mL trypsin inhibitor (Sigma), continuously bubbled with 95% O_2-5% CO_2 and maintained at 37°C. After about 30 minutes the muscles were removed from this solution, rinsed in Krebs solution and placed in a relaxing solution with the following composition (concentrations in mM): 117 K^+, 36 Na^+, 1 Mg^{2+}, 60 HEPES (*N*-[2-hydroxyethyl] piperazine-*N'*-[2-ethanesulphonic acid]), 8 ATP, 50 $EGTA^{2-}$ (ethyleneglycol-bis[β-aminoethyl ether] *N*,*N*,*N'*,*N'*-tetraacetic acid) and free Ca^{2+} of 10^{-7} M, the free calcium was determined after titrating the solution with $CaCl_2$ in order to determine the excess EGTA. The muscle was then gently agitated using pipette suction, releasing some individual fibres from the muscle mass.

Individual fibres were examined either with a light microscope (Olympus BX60) or a laser-scanning confocal microscope (Leica TCS SP). The extent of fibre branching was assessed by counting the number of fibres that were branched and, for those fibres that were branched, counting the number of branches.

Results

Length, mass and cross-sectional area

Muscles from older mice (~ 6 to 7 months old) were longer than muscles from younger mice (~ 1 to 2 months old), but there were no differences in length between *mdx* and controls in each age group (**Figure 2.3(A)**). In younger mice, *mdx* muscles were similar to control muscles in both mass and cross-sectional area, while in older mice, the mass and cross-sectional area of *mdx* muscles were around 60% higher than those of control muscles (**Figure 2.3(B)** and **(C)**). Over the approximate five-month period separating the two age groups of mice used in this study, the mass and cross-sectional area of littermate control muscles increased by around 5% per month, while those of *mdx* muscles increased by around 15% per month. Hence, in our new colony of dystrophin-deficient *mdx* mice with littermate controls, dystrophin deficiency is associated with a higher rate of growth in the physical bulk of muscles. Similar findings were reported for the original colony of *mdx* mice when compared with age matched wild-type controls from a separate colony (Lynch *et al.*, 2001).

Contractile properties before lengthening contractions

The contractile properties of the muscles before lengthening contractions are shown in **Figure 2.4**. **Figure 2.4(A)** shows the maximum tetanic force expressed as an absolute force (not corrected for cross-sectional area). The absolute forces of control and *mdx* muscles were similar in each age group. However, when corrected for cross-sectional area, the specific force

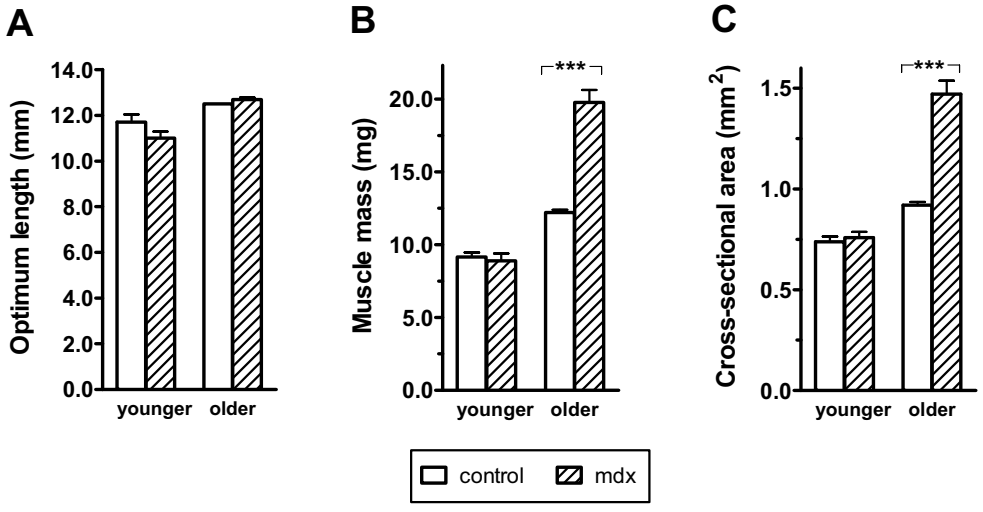

Figure 2.3. Length, mass and cross-sectional area. **(A)** length, **(B)** mass, **(C)** cross-sectional area. (Stars over a pair of bars indicate a significant difference between *mdx* and control in that particular age group; *** means $p<0.001$; $n = 5$ muscles for younger control, $n = 6$ for younger *mdx*, $n = 4$ for older control, $n = 8$ for older *mdx*.).

produced by *mdx* muscles was significantly lower than controls in each age group (**Figure 2.4(B)**). In younger mice the specific force produced by *mdx* muscles was about 15% lower than controls, and in older mice about 30% lower than controls. In both age groups the difference was statistically significant. These results show that as the *mdx* animal ages, the impairment of specific force generation becomes more marked, although the animal is able to compensate for this by muscle hypertrophy, thus maintaining absolute forces at normal levels. The values of specific force obtained here are comparable to those obtained in other studies (for example, in Consolino & Brooks (2004): 235 mN/mm^2 for control, 173 mN/mm^2 for *mdx*, in EDL muscles of ~20 week old mice).

The twitch to tetanus ratios were similar across all the muscles studied (**Figure 2.4(C)**) and were comparable to the value of about 0.2 normally found in mammalian muscle (Keynes & Aidley, 1991).

Figure 2.4(D) shows the half-frequency, which is the stimulation frequency at which the force generated was halfway between the twitch force and the maximum tetanic force. This is an indicator of the muscle's responsiveness to increases in frequency. A higher half-frequency means that the force-frequency curve has shifted to the right (see Figure 2.2), so that the muscle needs higher stimulation frequencies to produce the same amount of force. The half-frequency of *mdx* muscles was similar to controls in each age group. However, older muscles had higher half-frequencies than younger muscles, suggesting that as the animal grows older, its muscles become less responsive to increases in frequency.

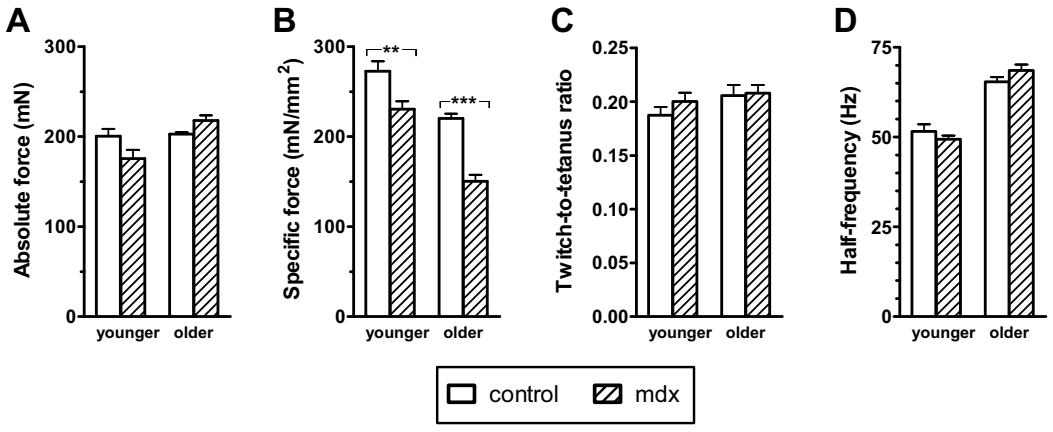

Figure 2.4. Contractile properties before lengthening contractions. (*A*) maximum tetanic force, expressed as an absolute force (no correction for cross-sectional area); (*B*) maximum tetanic force, expressed as a specific force (corrected for cross-sectional area); (*C*) twitch to tetanus ratio; (*D*) the half-frequency. (Stars over a pair of bars indicate a significant difference between *mdx* and control in that particular age group; *** means $p<0.001$, ** means $0.001<p<0.01$; $n = 5$ muscles for younger control, $n = 6$ for younger *mdx*, $n = 4$ for older control, $n = 8$ for older *mdx*.).

Damage following lengthening contractions

The muscles were subjected to a lengthening contraction protocol of 15% strain. A mild strain was used so that any differences in fragility between normal and dystrophic muscles could be determined (see Table 2.1). Various contractile properties were measured before and after the contractions, and the changes in these properties were used as functional indicators of the extent of damage. The results are shown in **Figure 2.5**.

The force deficit, or the reduction in maximum tetanic force following lengthening contractions, was the primary indicator of muscle damage in this study (**Figure 2.5(A)**). The force deficit is the most reliable and reproducible indicator of damage following lengthening contractions (Brooks & Faulkner, 1996). In younger mice, the force deficit for *mdx* muscles (7.3 ± 4.8%, *n*=6) was not significantly different from the force deficit for control muscles (−1.2 ± 3.5%, *n*=5), suggesting that dystrophin deficiency did not increase the susceptibility of younger muscles to contraction-induced damage. However, in older mice, the force deficit for *mdx* muscles (58.0 ± 5.0%, *n*=8) was significantly higher ($p < 0.001$) than the force deficit for controls (24.8 ± 5.3%, *n*=4), suggesting that dystrophin deficiency did increase the

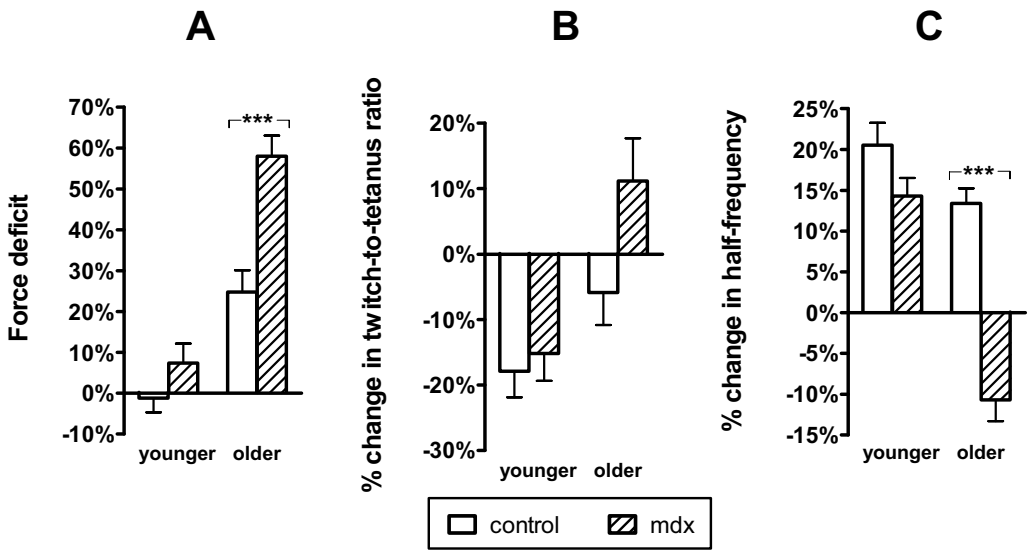

Figure 2.5. Damage following lengthening contractions. (A) force deficit, or the fall in maximum tetanic force; **(B)** percentage change in twitch to tetanus ratio; **(C)** percentage change in half-frequency. These results demonstrate a susceptibility of older *mdx* muscles to contraction-induced damage. (Stars over a pair of bars indicate a significant difference between *mdx* and control in that particular age group; *** means $p<0.001$; $n = 5$ muscles for younger control, $n = 6$ for younger *mdx*, $n = 4$ for older control, $n = 8$ for older *mdx*.).

susceptibility of older muscles to contraction-induced injury. Hence the effect of dystrophin deficiency on a muscle's vulnerability to damage was dependent on age, with the effect being more pronounced at older ages.

Our secondary indicators of muscle damage were the change in twitch-to-tetanus ratio and the change in half-frequency following lengthening contractions. For the twitch-to-tetanus ratio, the change in ratio for older *mdx* muscles was opposite in direction to the change in ratio for all the other muscles (**Figure 2.5(B)**). However, none of the comparisons made between muscles were statistically significant. For the half-frequency, the change in older *mdx* muscles was opposite in direction from the changes in all other muscles (**Figure 2.5(C)**). The half-frequency decreased in older *mdx* muscles, whereas in all other muscles it increased. In this case, the comparison between *mdx* and control in the older age group was statistically significant ($p < 0.001$). These secondary measures of muscle damage suggest that the older *mdx* muscles have been affected differently from all the other muscles, and add further to the suggestion from the force deficit results that older *mdx* muscles are more susceptible to injury.

Muscle fibre morphology

No branched fibres were found among the 151 fibres (63 younger, 88 older) examined from littermate control muscles. The results for *mdx* muscles are shown in **Figure 2.6**. Each of the fibres was categorised according to the number of branch points it contained (none, 1, 2, 3 or 4+). **Figure 2.6(A)** shows the proportion of fibres in each category, while **Figure 2.6(B)** shows the absolute numbers in each category. Of the 176 *mdx* fibres (106 younger, 70 older) examined, only 17% of the younger *mdx* fibres contained branch points, while 89% of the older *mdx* fibres were branched (**Figure 2.6(A)**). Not only did older *mdx* muscles contain more branched fibres than younger *mdx* muscles, they also had more branch points on these fibres. The branched fibres in young *mdx* muscle usually had just one branch point on a fibre, while the branched fibres in older *mdx* muscle usually had multiple branch points on a fibre.

In addition to having more branched fibres and more branches per fibre, the branching patterns in older *mdx* fibres were also more complex than those in younger *mdx* fibres, as is evident from comparing **Figure 2.7** with **Figure 2.8**. There appeared to be three basic patterns of branching: (i) a small branch leaving the main fibre, as in **Figure 2.7(C)**; (ii) the main fibre dividing into two similarly sized branches, as in **Figure 2.8(A)**; and (iii) the two branches rejoining into one fibre again, as in **Figure 2.7(D)**. The branches in younger *mdx* fibres are shorter and smaller than in the older *mdx* fibres. In addition, some older *mdx* fibres displayed branching so complex that it was difficult to classify them into any of the above patterns.

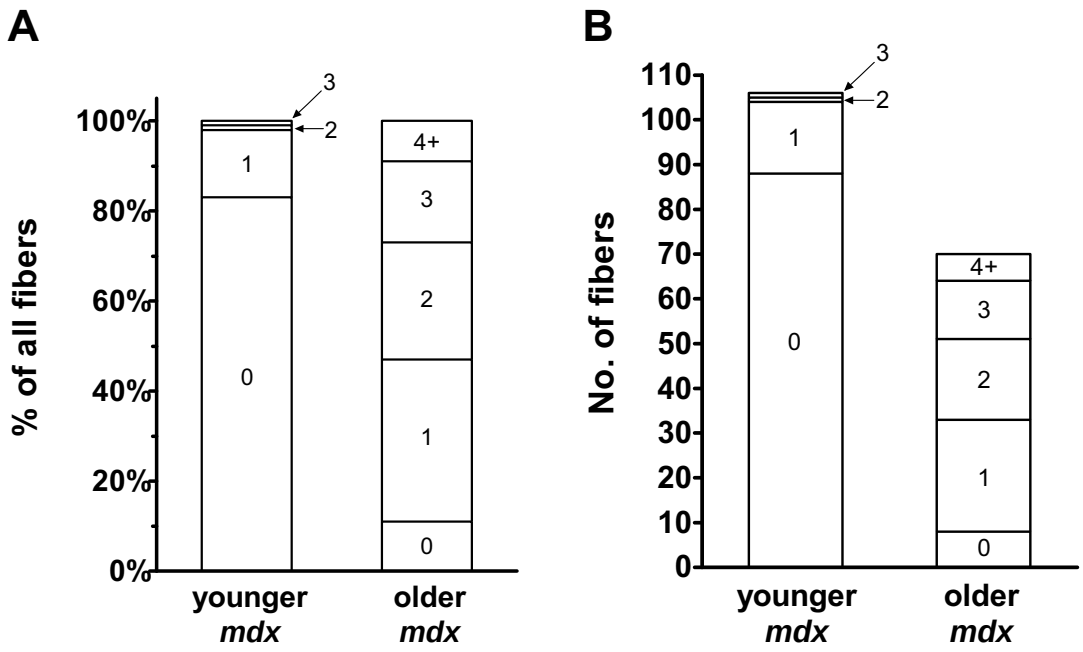

Figure 2.6. Fibre branching in younger and older *mdx* muscles. Fibres were categorised according to the number of branch points they displayed (0, 1, 2, 3 or 4+). **(A)** Proportion of fibres in each category. **(B)** Absolute number of fibres in each category. Compared to younger *mdx* muscles, older *mdx* muscles had a greater number of branched fibres and a greater number of fibres with multiple branches.

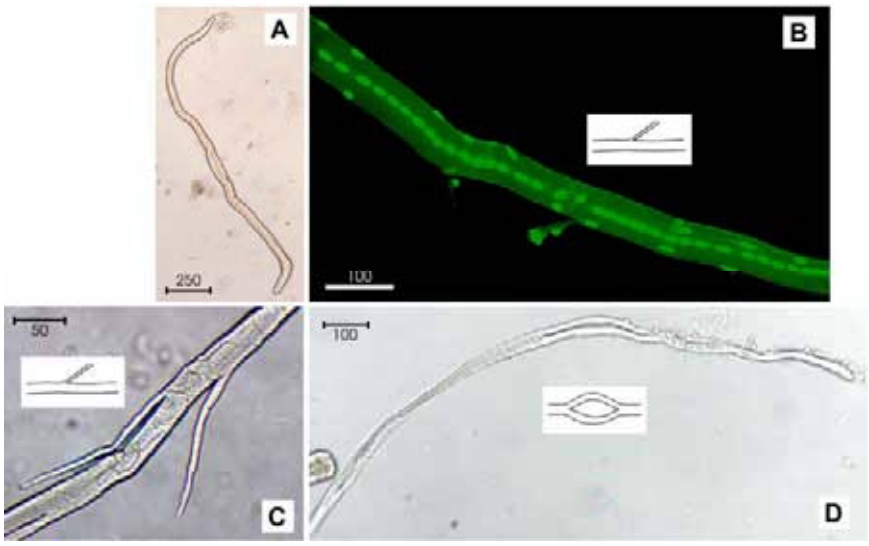

Figure 2.7. Low power images of enzymatically dispersed single muscle fibres from younger *mdx* mice (1-2 months of age). (A) an example of an unbranched EDL fibre; **(B)** an image from a confocal laser scanning microscope with the fibre stained with ethidium bromide to label the nuclei which are predominantly in the centre of the fibre; this fibre has one small central branch; **(C)** a fibre with two small sprouts coming off the middle and a larger fissure lower left; **(D)** a fibre with a split which reconnects. Scale bar measurements are in microns. The inserts are diagrammatic representations of the main deformity displayed by the fibre.

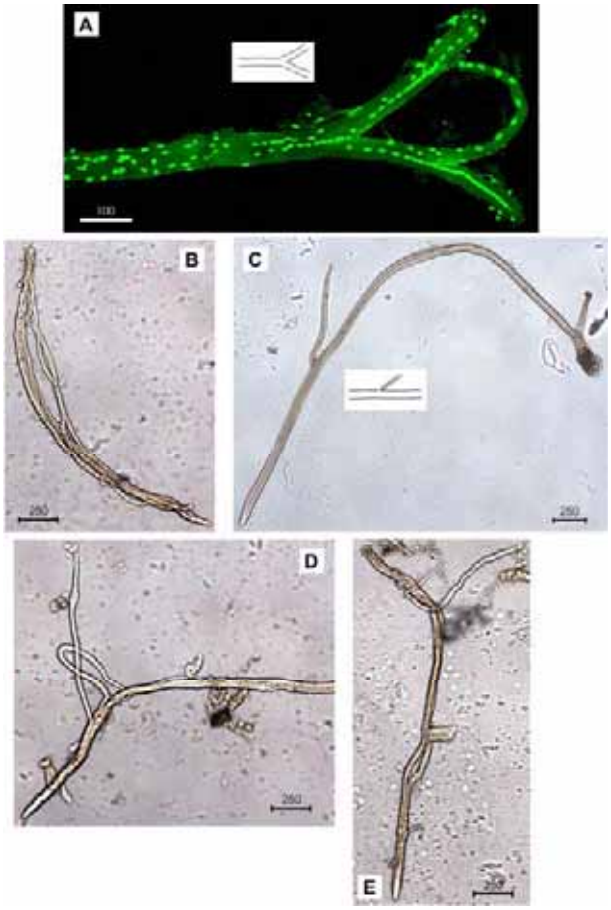

Figure 2.8. Low power images of enzymatically dispersed single muscle fibres from older *mdx* mice (6-7 months of age). (A) an image from a confocal laser scanning microscope with the fibre stained with ethidium bromide to label the nuclei which are predominantly in the centre of the fibre; this fibre has two major and two minor branch points; **(B,D,E)** fibres with extraordinarily complex patterns of morphological abnormalities; **(C)** a fibre which branches into two parts of unequal diameter at two different points. Scale bar measurements are in microns.

Muscle stiffness

To ascertain whether the differences between muscles in their susceptibility to damage might be due to differences in the stiffness of the sarcomeres, we analysed the ramp phase of the lengthening contractions, measuring the change in force as the muscle was stretched from 100% to 108% of its optimal length. The results are displayed in **Figure 2.9**, which shows the percentage increase in force for each 1% increase in length. No significant differences were found between *mdx* and controls in either age group. However, older muscles showed significantly larger increases in force than younger muscles, in both *mdx* and controls, suggesting that the sarcomeres of older muscles have more stiffness than those of younger muscles.

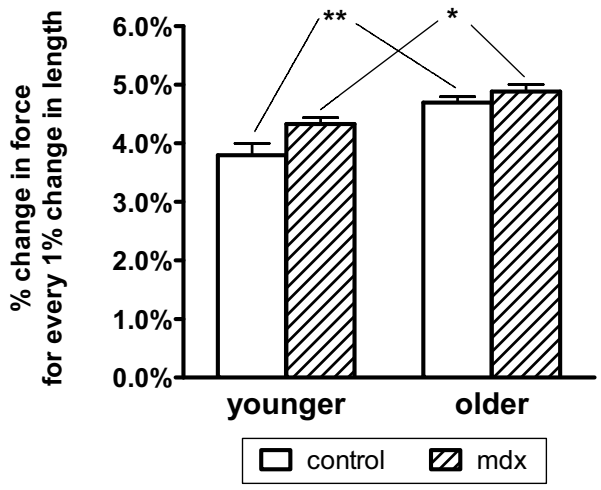

Figure 2.9. **Muscle stiffness**, as measured by the percentage change in force for every 1% change in length during the ramp phase of the lengthening contractions. There were no differences between *mdx* and control in either age group, but older muscles showed significantly more stiffness than younger muscles, in both *mdx* and controls. (** means $0.001<p<0.01$, * means $0.01<p<0.05$; $n = 5$ muscles for younger control, $n = 6$ for younger *mdx*, $n = 3$ for older control, $n = 8$ for older *mdx*.)

Discussion

We have demonstrated that a lengthening contraction protocol of 15% strain causes more damage to muscles of *mdx* mice aged 6 to 7 months than to muscles of *mdx* mice aged 1 to 2 months, relative to age-matched littermate controls. Our results demonstrate that dystrophin deficiency has little effect on the vulnerability of the younger muscles to injury; however, it significantly increases the vulnerability of the older muscles to injury.

Why should dystrophin deficiency have a greater effect on skeletal muscle's vulnerability to damage as age increases? One possible reason, suggested by our fibre morphology results, is that the fibre branching associated with the dystrophic process becomes more extensive as the dystrophic animal ages. It has been demonstrated previously that fibres containing branches are more liable to be damaged during contraction than fibres without branches (Head *et al.*, 1990). Compared with younger *mdx* muscles, older *mdx* muscles had more branched fibres, more branch points on each fibre and greater complexity of branching patterns. These morphological changes mean that the potential number of "weak" branch points is substantially greater in older *mdx* animals, rendering them susceptible to damage by contractions that would not damage either normal (non-branched) dystrophin-positive skeletal muscle or skeletal muscle from younger (non-branched) dystrophin-negative *mdx* animals.

The observed association between the degree of damage and the extent of branching has implications for the interpretation of past studies involving lengthening contractions in the *mdx* mouse. The studies in Table 1 which found larger force deficits for *mdx* muscles all used mice that were older than the 6 to 8 week-old mice of our study. Given that, in our study, 17% of fibres were already branched at 6 to 8 weeks, and 89% were branched by 27 to 31 weeks, the muscles in these other studies may have contained a significant proportion of branched fibres. This means that at least part of the force deficits observed in *mdx* muscle may have been associated with the presence of the branched fibres, rather than the absence of dystrophin.

To remove the potential confounding effect of branched fibres, and to gain a clearer understanding of what is the primary effect of the lack of dystrophin, we can look at muscles in which fibre branching is minimal. One study by Grange *et al.* (2002) used dystrophic mouse pups 9-12 days old. This is much younger than any of the studies listed in Table 1 and hence the effect of fibre branching would be minimised. They found that the extent of membrane damage (as measured by dye uptake) was no different between dystrophic and control

animals following lengthening contractions. This suggests that a lack of dystrophin does not in itself weaken the sarcolemma. In contrast to the present study, Yeung *et al.* (2003) used unbranched single fibres from the flexor digitorum brevis muscle and found that unbranched *mdx* fibres had slightly higher force deficits than controls following lengthening contractions. Interestingly, however, this difference was eliminated when specific blockers of stretch-activated ion channels were added to the unbranched single fibres, suggesting that the primary effect of dystrophin deficiency may be the malfunctioning of ion channels rather than a fragile sarcolemma.

Hence, in these studies, it does not appear that dystrophin's primary role is to mechanically strengthen the sarcolemma, and that the initiating event in the dystrophic process may not necessarily be mechanical damage during contraction. Popular alternative candidates for the initial step are a pathological calcium homeostasis due to one or more of the following; aberrant ion channel functioning; sarcolemmal ion channel dysfunction, especially with reference to mechanosensitive channels; and ROS activity (Allard, 2006; Whitehead *et al.*, 2006; Deconinck & Dan, 2007).

Interestingly the aged control muscles were also somewhat damaged by the lengthening contractions. This finding is consistent with those of Brooks & Faulkner (1996) who found that aged mice about 24 months old were more susceptible to contraction-induced damage than younger mice. Our analysis of muscle stiffness provides a possible explanation of this. We found that older muscles had increased stiffness compared to younger muscles. This may mean that older muscles are less compliant and less able to absorb the strain as the muscle is stretched, rendering it more susceptible to damage.

In summary, we have observed that the force deficits in *mdx* muscle following mild lengthening contractions are associated with the degree of fibre branching. Given this association, it is important to isolate the possible effects of fibre branching from the direct effects of dystrophin deficiency when interpreting the results of similar studies in *mdx* mice. The effect of fibre branching can be removed by using mice that are as young as possible or by using individual fibres that have no branches. In this way, the direct effect of dystrophin deficiency can be more easily seen and provide a clearer understanding of what is the primary initiating event in the pathogenesis of muscular dystrophy.

Acknowledgements

This work was supported by a grant from the Muscular Dystrophy Association, New South Wales, Australia.

Paper B

Declaration

This chapter is a reproduction of the published paper:

> Chan S, Seto JT, MacArthur DG, Yang N, North KN & Head SI (2008). A gene for speed: contractile properties of isolated whole EDL muscle from an α-actinin-3 knockout mouse. *American Journal of Physiology Cell Physiology* 295: C897-C904.

Current status

Published.

Author contributions

The contribution of S.C. to this paper was 70%, and consisted of designing and performing the experiments, analysing the data, and writing the paper.

Note on format

The paper as presented in this chapter is a reproduction of the final manuscript submitted to the publisher on 21st July 2008. This was the manuscript that was accepted for publication. In reproducing this manuscript here, only the spelling, referencing style, and the numbering style of figures and tables have been modified. This has been done to achieve consistency with the rest of the thesis. Some figures have also been reproduced in colour where appropriate. References are listed with all other references at the end of the thesis.

The paper is reprinted in its published format in the "Publications" section at the end of the thesis.

Abstract

The actin-binding protein α-actinin-3 is one of the two isoforms of α-actinin that are found in the Z-discs of skeletal muscle. α-Actinin-3 is exclusively expressed in fast glycolytic muscle fibres. Homozygosity for a common polymorphism in the ACTN3 gene results in complete deficiency of α-actinin-3 in about 1 billion individuals worldwide. Recent genetic studies suggest that the absence of α-actinin-3 is detrimental to sprint and power performance in elite athletes and in the general population. In contrast, α-actinin-3 deficiency appears to be beneficial for endurance athletes. To determine the effect of α-actinin-3 deficiency on the contractile properties of skeletal muscle, we studied isolated extensor digitorum longus (fast-twitch) muscles from a specially developed α-actinin-3 knockout (KO) mouse. α-Actinin-3-deficient muscles showed similar levels of damage to wild-type (WT) muscles following lengthening contractions of 20% strain, suggesting that the presence or absence of α-actinin-3 does not significantly influence the mechanical stability of the sarcomere in the mouse. α-Actinin-3 deficiency does not result in any change in myosin heavy chain expression. However, compared with α-actinin-3-positive muscles, α-actinin-3-deficient muscles displayed longer twitch half-relaxation times, better recovery from fatigue, smaller cross-sectional areas and lower twitch-to-tetanus ratios. We conclude that α-actinin-3 deficiency results in fast-twitch, glycolytic fibres developing slower-twitch, more oxidative properties. These changes in the contractile properties of fast-twitch skeletal muscle from α-actinin-3-deficient individuals would be detrimental to optimal sprint and power performance, but beneficial for endurance performance.

Introduction

The α-actinins are a group of actin-binding proteins. In skeletal muscle, they are found in the Z-disc, where they cross-link the thin actin filaments of adjacent sarcomeres. The two isoforms found in the Z-disc are α-actinin-2 and α-actinin-3. α-Actinin-2 is the predominant isoform found in oxidative muscle fibres, while α-actinin-3 is restricted mainly to fast glycolytic fibres (MacArthur & North, 2004).

It is estimated that around 1 billion individuals worldwide completely lack α-actinin-3, due to homozygosity for a common polymorphism in the α-actinin-3 gene (MacArthur *et al.*, 2007). α-Actinin-3 deficiency is not associated with any disease phenotype, suggesting that its absence may largely be compensated for by the closely related protein, α-actinin-2 (Mills *et al.*, 2001). However, the genomic region surrounding the polymorphism shows low levels of genetic variation and recombination in individuals of certain populations, consistent with strong, recent positive selection (MacArthur *et al.*, 2007). This suggests that α-actinin-3 deficiency does have an important effect on skeletal muscle, and that muscles lacking α-actinin-3 must be different in some way from muscles that have the protein.

A study of athletes at the Australian Institute of Sport (Yang *et al.*, 2003) found that those engaged in sprint or power activities had a lower incidence of α-actinin-3 deficiency than the general population (6% compared with 18%). In fact, among Olympic sprint athletes, there were no cases of α-actinin-3 deficiency. Endurance athletes, in contrast, tended to have a higher incidence of α-actinin-3 deficiency, although this trend was only statistically significant in females. The reduced incidence of α-actinin-3 deficiency among elite sprint and power athletes has since been observed in other independent studies (Niemi & Majamaa, 2005; Papadimitriou *et al.*, 2008; Roth *et al.*, 2008). α-Actinin-3 deficiency has also been associated with reduced muscle strength (Clarkson *et al.*, 2005) and poorer sprinting performance (Moran *et al.*, 2007) in non-athletes. These data strongly suggest that a lack of α-actinin-3 affects skeletal muscle in a way that is detrimental to sprint and power performance but beneficial for endurance activities.

Studies on a specially generated α-actinin-3 knockout mouse (MacArthur *et al.*, 2007) lend support to these findings in humans. In an endurance test in which mice were run on a motorized treadmill, knockouts were found to run 33% further than wild-types before exhaustion (MacArthur *et al.*, 2007), supporting the finding of a higher incidence of α-actinin-3 deficiency in female endurance athletes. Knockouts also had reduced grip strength, lower muscle weights and smaller fast fibre diameters than wild-types (MacArthur *et al.*, 2008),

supporting the finding that α-actinin-3 deficient individuals are under-represented in strength and power activities.

There are various hypotheses as to why α-actinin-3 deficiency might adversely affect power performance and benefit endurance performance. One hypothesis is that α-actinin-3 serves to stabilise the sarcomere when muscles are exercised to maximal or near-maximal capacity as in sprinting. In its absence, the sarcomere might be weakened and more likely to be damaged during extreme athletic activity. Such a role is suggested by the protein's location in the Z-disc and its actin-binding properties.

Another hypothesis is that α-actinin-3 influences fibre-type differentiation towards a fast-twitch, glycolytic profile that is beneficial for sprint performance, while its absence would lead to differentiation towards a slower oxidative profile that is beneficial for endurance performance. Such a role is suggested by the restricted distribution of the protein, which is confined to fast glycolytic fibres, and by molecular studies which indicate that the sarcomeric α-actinins interact with signalling proteins involved in fibre-type differentiation and with metabolic enzymes involved in glycogenolysis (MacArthur & North, 2004). Under this hypothesis, one might expect that fast glycolytic fibres would adopt slower, more oxidative properties when α-actinin-3 is absent. Indeed, the activity of key oxidative enzymes in the α-actinin-3 knockout mouse is significantly higher than in wild-type controls, although there is no change in fibre types as defined by myosin heavy chain composition (MacArthur *et al.*, 2007, MacArthur *et al.*, 2008).

In this present study we examined some physiological properties of isolated, whole α-actinin-3-deficient muscles from the α-actinin-3 knockout mouse to gain greater insight into the likely functions of this protein. For comparison, we used littermate wild-type controls which were homozygous for the α-actinin-3 gene. We chose to analyse the extensor digitorum longus (EDL) muscle from the hindlimb, because α-actinin-3 is found predominantly in fast glycolytic fibres (MacArthur & North, 2004), and the mouse EDL muscle contains a high proportion of these fibres. Thus any consequences of α-actinin-3 deficiency will be most apparent in this muscle.

To see whether α-actinin-3 plays a mechanical role in stabilizing the sarcomere, we measured the muscle damage resulting from eccentric contractions of 20% strain, and also examined the morphology of individual fibres for evidence of repetitive muscle injury. To see whether α-actinin-3 influences fibre-type differentiation and metabolism, we measured some basic contractile properties and also examined the responses of the muscles to a fatigue protocol.

Methods

Animals used

Use of animals was approved by the University of New South Wales Animal Care and Ethics Committee. 12 knockout mice and 12 wild-type mice aged 8 to 10 weeks, plus 1 knockout and 1 wild-type aged ~6 months, were used. All mice were males.

Muscle preparation

All animals were anaesthetised with halothane and sacrificed by cervical dislocation. The extensor digitorum longus (EDL) muscle was dissected from the hindlimb and tied by its tendons to a force transducer (World Precision Instruments, Fort 10) at one end and a linear tissue puller (University of New South Wales) at the other, using silk suture (Deknatel 6.0). It was placed in a bath continuously superfused with Krebs solution, with composition (mM): 4.75 KCl, 118 NaCl, 1.18 KH_2PO_4, 1.18 $MgSO_4$, 24.8 $NaHCO_3$, 2.5 $CaCl_2$ and 10 glucose, with 0.1% fetal calf serum and continuously bubbled with 95% O_2-5% CO_2 to maintain pH at 7.4. The muscle was stimulated by delivering a supramaximal current between two parallel platinum electrodes, using an electrical stimulator (A-M Systems). At the start of the experiment, the muscle was set to the optimum length L_0 that produced maximum twitch force. All experiments were conducted at room temperature (~ 22°C to 24°C).

Force-frequency curve

A force-frequency curve was then obtained by delivering 500 ms stimuli of different frequencies (2, 15, 25, 37.5, 50, 75, 100, 125 and 150 Hz), and measuring the force produced at each frequency of stimulation. A 30 second rest was allowed between each frequency. A curve relating the muscle force P to the stimulation frequency f was fitted to these data. The curve had the following equation:

$$P = P_{\min} + \frac{P_{\max} - P_{\min}}{1 + \left(\frac{K_f}{f}\right)^h}$$

The values of r^2 for the fitting procedure were never lower than 99.3%. From the fitted parameters of the curve, the following contractile properties were obtained: maximum force (P_{max}), half-frequency (K_f), Hill coefficient (h) and twitch-to-tetanus ratio (P_{min}/P_{max}).

Eccentric contractions

The muscle was then subjected to a series of eccentric (lengthening) contractions. At time = 0 ms, the muscle was stimulated by supramaximal pulses of 1 ms duration and 125 Hz frequency. At time = 250 ms, after it had attained its maximum isometric force, the muscle was stretched at a speed of $0.2L_0$ per second until it was 20% longer than its optimum length, held at this length for 0.5 seconds, then returned at the same speed to its original position. The electrical stimulus was stopped at time = 2000 ms. This eccentric contraction was performed 5 times, at intervals of 2 minutes. After a 15 minute recovery period, the optimum length was reset and a second force-frequency curve was obtained.

Muscle mass

Finally, the muscle was removed from the bath. The tendons were trimmed and the muscle was lightly blotted on filter paper and then weighed. An estimate of the cross-sectional area was obtained by dividing the muscle's mass by the product of its optimum length and the density of mammalian muscle (1.06 mg/mm^3) (Brooks *et al.*, 1995).

Muscle stiffness

To estimate muscle stiffness, we divided the change in muscle force (as a percentage of isometric force) by the change in muscle length (as a percentage of optimum length) during the first eccentric contraction. We only measured up to the point where the muscle reached 109% of optimum length; beyond this length, many muscles developed forces that exceeded the measurement capacity of the force transducer.

Fatigue

In a separate set of experiments using different muscles from those used for eccentric contractions, muscles were examined for their responses to a fatiguing protocol. Muscles were set up as described above and a force frequency curve was obtained as described above, except that the duration of stimulation at each frequency was only 250 ms. After 5 minutes, the fatigue protocol was started. The muscle was given a one-second, 100-Hz tetanus every 2 seconds over a period of 30 seconds. The muscle was then allowed to recover for a period of 30 minutes, during which force recovery was monitored with a brief (250 ms) 100-Hz tetanus every 5 minutes. Additional force-frequency curves were obtained 90 seconds after the end of the fatigue protocol, and 1 minute after the final recovery tetanus.

The 30 minute recovery period was chosen due to time constraints. At this time, recovery in the muscles ranged from 74% to 92% of pre-fatigue force. The experiment would have been too prolonged if the muscle had been left to recover to 100%; in any case it is

unlikely that complete recovery would have occurred due to the possible development of an anoxic core during the very vigorous stimulation protocol.

Muscle fibre morphology

Individual fibre morphology was examined in the EDL muscles of 1 wild-type and 1 knockout mouse aged ~6 months. Animals were anaesthetised with halothane and sacrificed by cervical dislocation. The extensor digitorum longus (EDL) muscle was dissected from the hindlimb. Following dissection, the muscles were digested to yield individual fibres. The solution used for the digestion was Krebs solution containing 3 mg/mL collagenase Type I (Sigma) and 1 mg/mL trypsin inhibitor (Sigma), continuously bubbled with 95% O_2-5% CO_2 and maintained at 37°C. After about 30 minutes the muscles were removed from this solution, rinsed in Krebs solution and placed in a relaxing solution with the following composition (concentrations in mM): 117 K^+, 36 Na^+, 1 Mg^{2+}, 60 HEPES (*N*-[2-hydroxyethyl] piperazine-*N'*-[2-ethanesulphonic acid]), 8 ATP, 50 $EGTA^{2-}$ (ethyleneglycol-bis[β-aminoethyl ether] *N*,*N*,*N'*,*N'*-tetraacetic acid) and free Ca^{2+} of 10^{-7} M. The muscle was gently agitated using pipette suction, releasing some individual fibres from the muscle mass.

Individual fibres were examined either with a light microscope (Olympus BX60) or a laser-scanning confocal microscope (Leica TCS SP).

Statistical analyses

Data are presented as Mean ±S.E.M.. For the contractile properties and eccentric contraction data, two-tailed *t*-tests were used. For the fatigue data, the Mann-Whitney U test was used because of smaller sample sizes. All tests were conducted at a significance level of 5%. All statistical tests and curve fitting were performed using a standard statistical software package (GraphPad Prism Version 4.00 for Windows, GraphPad Software, San Diego California USA).

Results

Sample sizes and ages

The results presented below for general physical properties, maximum forces, force-frequency characteristics, twitch characteristics and eccentric contractions were all obtained from one experimental group consisting of 8 wild-type muscles and 10 knockout muscles. Each muscle was taken from a different mouse. Animals were male mice aged 8 to 10 weeks.

The fibre morphology was performed on EDL muscles from one wild-type and one knockout mouse, both males aged about 6 months.

The fatigue experiments were performed on 6 wild-type muscles and 8 knockout muscles. Each muscle was taken from a different mouse. Animals were male mice aged 8 to 10 weeks.

General physical properties

The general physical properties of wild-type and knockout muscles are shown in **Table 3.1**. While their optimum lengths were virtually identical to those of wild-type muscles, α-actinin-3-deficient muscles were 9% lighter than α-actinin-3-positive muscles, with a corresponding 9% reduction in cross-sectional area.

Maximum forces generated by muscles

Table 3.1 shows the forces generated by the muscles when stimulated at maximum frequency. There were no statistically significant differences between wild-types and knockouts in either absolute force (without correcting for cross-sectional area) or specific force (after correcting for cross-sectional area).

To see whether there were any differences at sub-maximal levels of stimulation, we analysed the forces produced at 100 Hz (about 67% of maximum frequency) by the cohort of muscles used in the fatigue experiments (to be described later). The 100-Hz absolute forces of knockouts were 10.9% lower than wild-types (p = 0.008, Mann-Whitney test), but there was no difference in 100-Hz specific forces.

Force-frequency characteristics

Table 3.1 shows various contractile properties derived from the force-frequency curves of individual muscles. The half-frequency is the stimulation frequency at which the muscle develops a force which is halfway between its minimum and maximum forces. The Hill coefficient is a measure of the slope of the curve. The half-frequency and Hill coefficient indicate the sensitivity of the contractile proteins to calcium. The lower the half-frequency and

	Wild-types	Knockouts	*P*-value
General physical properties			
Optimum length (mm)	11.9 ± 0.1	11.9 ± 0.2	
Mass (mg)	9.7 ± 0.4	8.8 ± 0.2	0.035
Cross-sectional area (mm^2)	0.77 ± 0.02	0.70 ± 0.01	0.015
Maximum forces			
Absolute force (mN)	202 ± 5.4	189 ± 5.5	
Specific force (mN/mm^2)	262 ± 5.5	271 ± 7.8	
Force-frequency characteristics			
Half-frequency (Hz)	56.4 ± 0.5	55.0 ± 1.1	
Hill coefficient	5.0 ± 0.1	5.5 ± 0.2	0.048
Twitch-to-tetanus ratio (%)	20.1 ± 0.5	18.3 ± 0.5	0.027

Table 3.1 Properties of wild-type and α-actinin-3 knockout muscles. Values are Mean ± S.E.M.. *P*-values are shown where there was a significant difference between wild-types and knockouts.

the higher the Hill coefficient, the greater the sensitivity. The twitch-to-tetanus ratio measures the minimum force as a proportion of the maximum force.

The half-frequency in wild-type muscles was not significantly different from the half-frequency in knockouts. The Hill coefficient was significantly higher in knockouts than in wild-types. The twitch-to-tetanus ratio in knockouts was significantly lower than the ratio in wild-types.

The effects of these differences on the shape of the force-frequency curve are shown in **Figure 3.1**, in which individual force-frequency data for wild-types and knockouts have been aggregated into single curves. At low frequencies, the curve for knockouts is depressed slightly compared with wild-types, reflecting the lower twitch-to-tetanus ratio in knockouts. Over middle frequencies, where the curves are rising steeply, the curve for knockouts has a slightly steeper slope than the curve for wild-types, reflecting the higher Hill coefficient in knockouts.

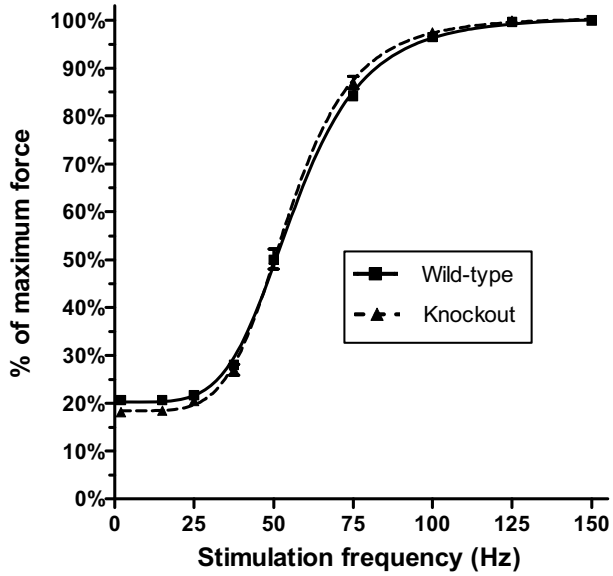

Figure 3.1. Aggregated force-frequency curves. Force-frequency data from individual muscles were aggregated to produce a single curve for wild-types (full line) and a single curve for knockouts (dashed line). Compared with the curve for wild-types, the curve for knockouts is slightly depressed at low frequencies, reflecting the lower twitch-to-tetanus ratio, and rises more steeply, reflecting the higher Hill coefficient. (*n* = 8 muscles for WT, *n* = 10 muscles for KO.

Eccentric contractions

The muscles were subjected to eccentric contractions of 20% strain to determine whether there were any differences between wild-types and knockouts in their susceptibility to eccentric damage. **Figure 3.2** shows results from these experiments. Before the contraction protocol, a force-frequency curve was obtained. This pre-contraction curve is the full line shown in **(A)** for wild-types and in **(B)** for knockouts. The muscle was then subjected to the eccentric contraction protocol. Force tracings obtained during the 5 contractions in an individual wild-type muscle are shown in **(C)**, and force tracings for one knockout muscle are shown in **(D)**. Following the eccentric contractions, the muscle was allowed to recover for 15 minutes and its optimum length reset. Then a second force-frequency curve was obtained, shown by the dashed line in (A) for wild-types and in (B) for knockouts.

By comparing the "Before" and "After" curves, it can be seen that muscle damage is reflected in three changes to the force-frequency relationship: (i) a fall in maximum force; (ii) a rightward shift of the curve, meaning that the half-frequency has increased; and (iii) a reduction in the steepness of the curve, meaning that the Hill coefficient has decreased. The rightward shift and reduced steepness of the force-frequency curve is commonly observed following eccentric contractions, and could indicate some damage to the excitation-contraction coupling mechanism.

The extent of each of these three changes was used to assess the degree of muscle damage in wild-types and knockouts, and the results are shown in **Figure 3.3**. **(A)** shows the force deficit, or the percentage fall in maximum force. This was 1.6 ± 2.0% in wild-types and 2.6 ± 1.5% in knockouts. **(B)** shows the percentage increase in half-frequency, or the extent of the rightward shift of the curve. This was 15.2 ± 0.6% in wild-types and 12.9 ± 1.1% in knockouts. **(C)** shows the percentage decrease in the Hill coefficient, or the extent of the reduction in the curve's steepness. This was 10.1 ± 1.5% in wild-types and 12.4 ± 1.4% in knockouts. There were no statistically significant differences between wild-types and knockouts in any of these measures.

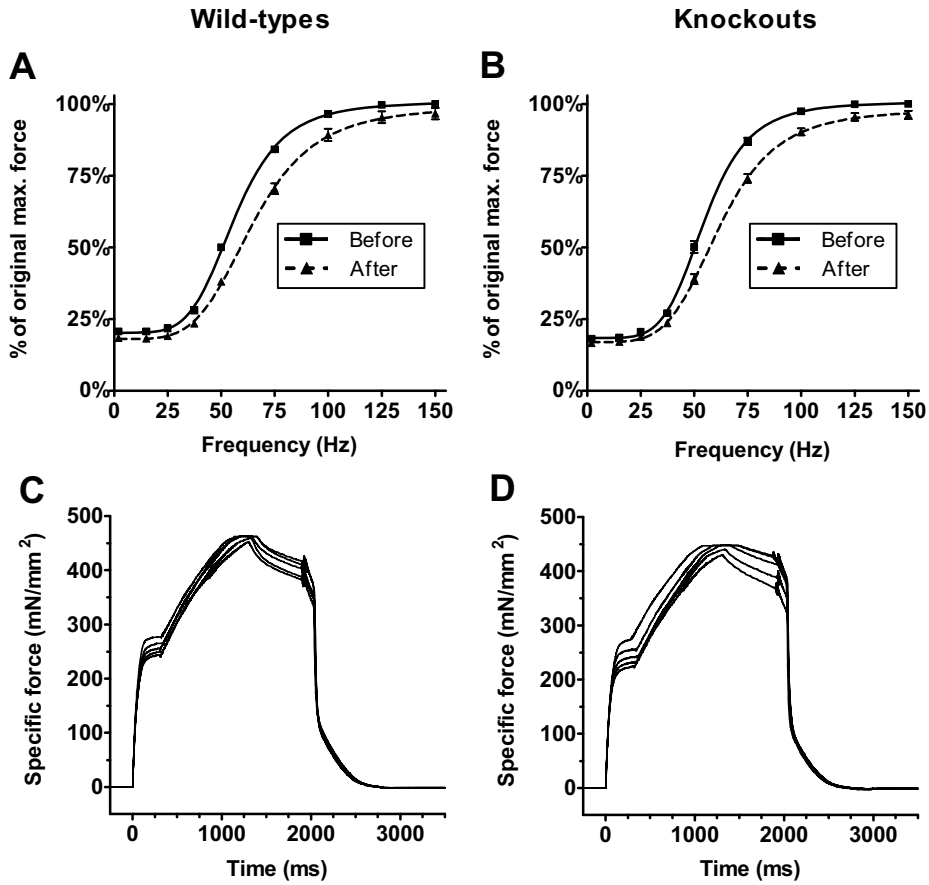

Figure 3.2. Eccentric contractions. **(A)** and **(B)** show force-frequency curves obtained before (full line) and after (dashed line) the eccentric contraction protocol. **(A)** shows aggregated data for wild-types and **(B)** shows aggregated data for knockouts (*n* = 8 muscles for WT, *n* = 10 muscles for KO). The eccentric contractions have caused a fall in maximum force, a rightward shift of the force-frequency curve and a reduction in steepness of the curve. Also shown are the force tracings obtained during the 5 eccentric contractions in one particular wild-type muscle **(C)** and one particular knockout muscle **(D)**. The force tracing for each contraction is slightly lower than that of the preceding contraction.

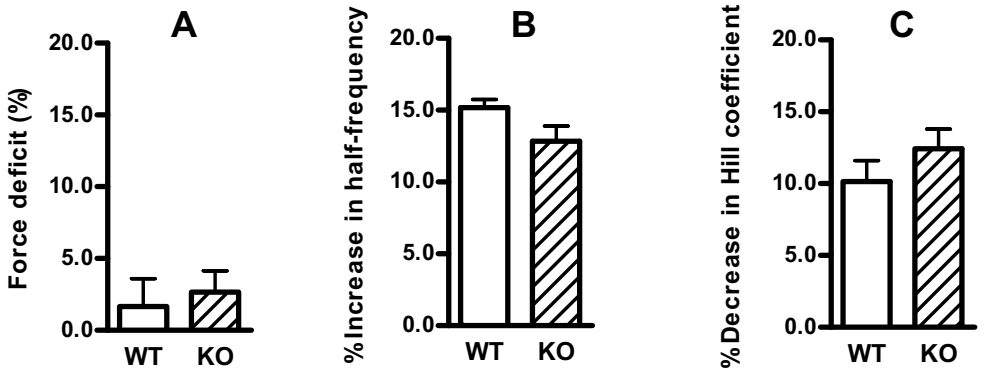

Figure 3.3. Measures of damage from eccentric contractions. Three measures were used to assess the extent of damage from eccentric contractions: **(A)** the force deficit, which is the percentage fall in maximum force; **(B)** the percentage increase in the half-frequency, which measures the extent of rightward shift of the force-frequency curve; and **(C)** the percentage decrease in the Hill coefficient, which measures the reduction in steepness of the force-frequency curve. There were no statistically significant differences between wild-types (WT) and knockouts (KO) in any of these measures. (*n* = 8 muscles for WT, *n* = 10 muscles for KO)

Muscle stiffness

The stiffness of wild-type and knockout muscles was compared by measuring the percentage change in muscle force as the muscle was stretched from 100% to 109% of its optimum length during the first eccentric contraction. A stiffer muscle would be expected to exhibit a greater change in force for a given change in length. **Figure 3.4** shows the change in muscle force (expressed as a percentage of isometric force) for every 1% increase in muscle length. There were no significant differences between wild-types and knockouts, suggesting that the stiffness of both groups of muscles was similar.

Fibre morphology

A feature of repetitive muscle damage is the development of muscle fibres which are branched, or split (Tamaki & Akatsuka, 1994). Branched fibres are found in processes involving continuous degeneration and regeneration of muscle, such as in the X-linked recessive condition of Duchenne muscular dystrophy. In mice with an equivalent condition, muscles contain a large proportion of branched fibres, and these fibres have centrally located nuclei, another feature of regenerating muscle (Head *et al.*, 1992).

A muscle which was particularly susceptible to eccentric injury might be expected to develop a large number of branched fibres over time. We thus examined the individual fibre morphology from muscles of older mice (~6 months old) to see whether there was any fibre branching indicative of repetitive muscle damage.

Individual fibres from the EDL muscles of one wild-type and one knockout mouse were examined by laser-scanning confocal microscopy. Examples of fibres are shown in **Figure 3.5**. Almost all fibres were normal, with no branches and with peripherally located nuclei, as shown in **(A)**. Branching was detected in a very small number of knockout fibres, such as the one shown in **(B)**. All the branched fibres had peripherally located nuclei. Hence any morphological evidence of fibre damage was minimal, and was not sufficient to suggest that knockouts were any more susceptible than wild-types to eccentric muscle injury.

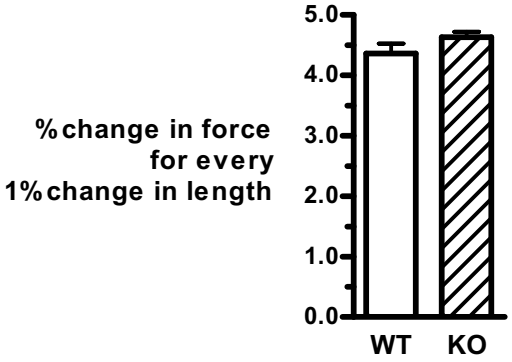

Figure 3.4. Muscle stiffness. The graph shows the change in force (expressed as a percentage of isometric force) for every 1% increase in muscle length during the first eccentric contraction. This was used as an indicator of muscle stiffness. There were no significant differences in stiffness between wild-type and knockout muscles. (*n* = 8 muscles for WT, *n* = 10 muscles for KO)

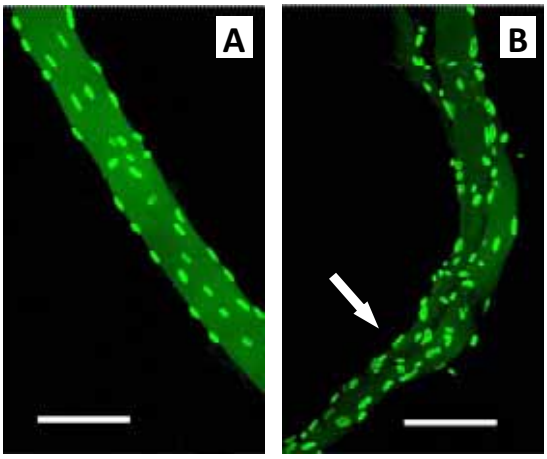

Figure 3.5. Fibre morphology. Individual muscle fibres from ~6-month-old animals were examined by confocal microscopy. All fibres from the wild-type mouse, and almost all fibres from the knockout mouse, had an appearance similar to **(A)**, which shows a portion of a fibre with no branches and with peripherally located nuclei. A very small number of fibres from the knockout mouse were split, and an example is shown in **(B)**. The arrow indicates the site where the single fibre divides into two separate branches. The nuclei, however, are still peripherally located. (Scale bars represent 100 microns.)

Fatigue

Muscles were subjected to a fatigue protocol in which they were given a one-second, 100-Hz tetanus every 2 seconds over a period of 30 seconds. The muscles were then allowed to recover for a period of 30 minutes, during which force recovery was monitored with a brief 100-Hz tetanus every 5 minutes.

Figure 3.6 shows the results obtained from 6 wild-type muscles and 8 knockout muscles. The descending part of the curve shows the decline in 100-Hz force with each successive tetanus during the 30-second fatigue protocol. By the end of this fatigue protocol, 100-Hz force had declined to 45.1 ± 1.3% of original in wild-types and to 42.9 ± 4.5% of original in knockouts. These values were not significantly different (Mann-Whitney test). The ascending part of the curve shows the recovery in 100-Hz force over the 30 minutes following the fatigue protocol. By the end of this period, knockouts had recovered to 86.1 ± 1.1% of their original force, but wild-types recovered to only 78.4 ± 1.9% of original. These values were significantly different (p = 0.013, Mann-Whitney test), indicating that recovery of 100-Hz force following fatigue was better in knockouts than in wild-types. The difference in 30-minute recovery has previously been presented in MacArthur *et al.* (2008), but the full data is included here so as to show the time course of the changes in force during fatigue and recovery.

In addition to measurements of 100-Hz force, force-frequency curves were also obtained for each muscle at various stages of the experiment. The times at which they were obtained are indicated by the shaded regions in Figure 3.6. The first curve (FF1) was obtained just prior to the start of the fatigue protocol, the second (FF2) shortly after the end of the fatigue protocol and the third (FF3) at the end of the 30-minute recovery period.

These force-frequency curves are shown in **Figure 3.7**, **(A)** and **(B)**. Here, data from individual muscles have been aggregated and forces expressed as a percentage of the pre-

fatigue maximum to facilitate comparison. Wild-type muscles are shown in (A) and knockouts in (B). The fatiguing protocol produced a rightward shift of the force-frequency curve, as is evident from the rightward displacement of FF2 compared to FF1 in both wild-types and knockouts. Right-shifting of the force-frequency curve is commonly found after fatigue and may indicate some impairment of the excitation-contraction coupling mechanism. The magnitude of the rightward shift can be quantified as the percentage increase in half-frequency between FF1 and FF2. This percentage increase is shown in **(C)**. There was a 33.7 ± 2.8% increase in half-frequency for wild-types and a 23.3 ± 4.0% increase for knockouts, but this difference was not statistically significant (Mann-Whitney test).

After 30 minutes recovery, the force-frequency curve shifts back slightly to the left, as can be seen by comparing FF3 with FF2 in Figure 3.7, (A) and (B). However, FF3 is still noticeably displaced to the right of FF1. The magnitude of this displacement is shown in **(D)**. In wild-types, the half-frequency for FF3 is still 32.2 ± 1.8% higher than the half-frequency for FF1, while in knockouts the increase is only 19.7 ± 1.3%. Here, the difference between wild-types and knockouts is significant (p = 0.048, Mann-Whitney test), suggesting that, after the 30-minute recovery period, the extent of right-shifting of the force-frequency curve is more pronounced in wild-types than in knockouts, and hence the knockout muscles have recovered better than the wild-type muscles.

By comparing FF3 with FF1 in Figure 3.7, (A) and (B), it can be seen that after 30 minutes, the force at very low and very high frequencies is very close to pre-fatigue levels; it is only over the middle frequencies that force remains significantly depressed. This is illustrated in **Figure 3.8**, where the force at each frequency following 30 minutes' recovery is expressed as a percentage of the force generated at that frequency before the muscle was fatigued. At very low and very high frequencies, the post-recovery force is around 90% of the pre-fatigue force. However, over middle frequencies, this percentage is considerably lower. Another feature of the graph is that, at very high and very low frequencies, the percentages for both wild-types and knockouts are similar, but over intermediate frequencies, wild-types have not recovered to the same degree as knockouts. At 37.5, 50, 75 and 100 Hz, the recovery in wild-types is significantly less than in knockouts (2-way ANOVA with Bonferroni post-tests). As maximum force was usually reached at about 150 Hz, these frequencies represent a range that is around 25% to 67% of maximum stimulation frequency.

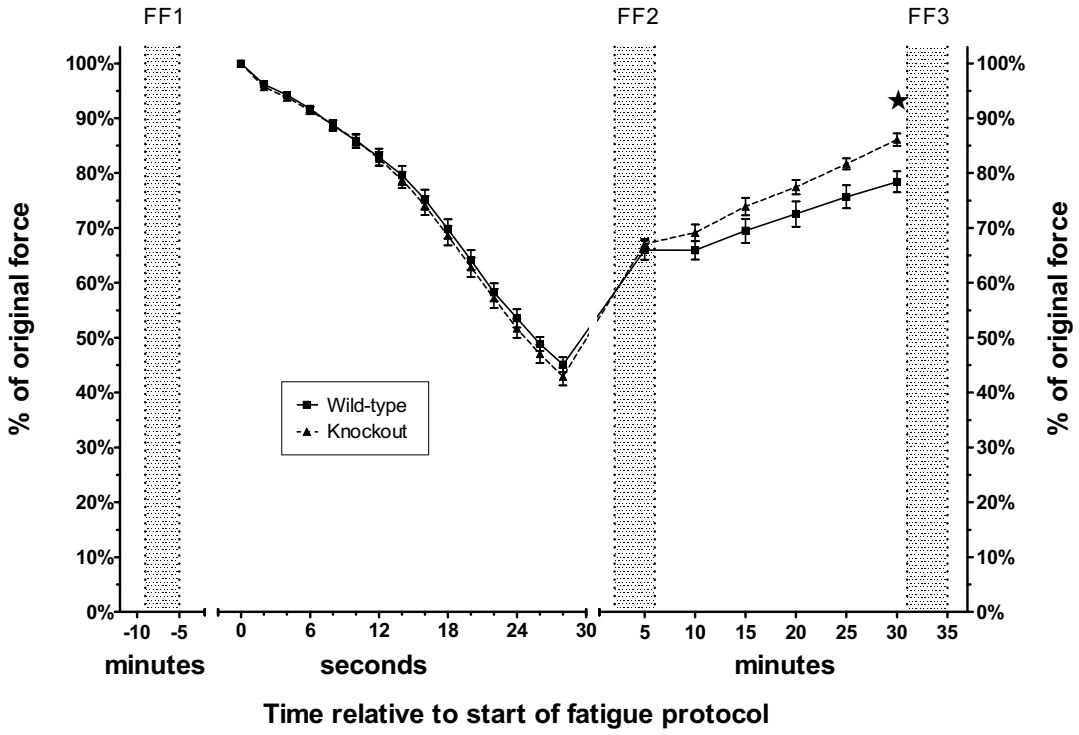

Figure 3.6. Changes in 100-Hz force during fatigue and recovery. Muscles were subjected to a fatigue protocol consisting of a one-second, 100-Hz tetanus every 2 seconds for 30 seconds. The descending part of the curve shows the decline in 100-Hz force over the duration of the fatigue protocol. Muscles were then allowed to recover for a period of 30 minutes. The ascending part of the curve shows the recovery in 100-Hz force during the recovery period (n = 6 muscles for WT, n = 8 muscles for KO). The star indicates a significant difference in force between wild-types and knockouts at 30 minutes (p = 0.013). The shaded regions represent 4-minute time intervals during which force-frequency curves were obtained for each muscle. The three curves (FF1, FF2 and FF3) are shown in Figure 3.7.

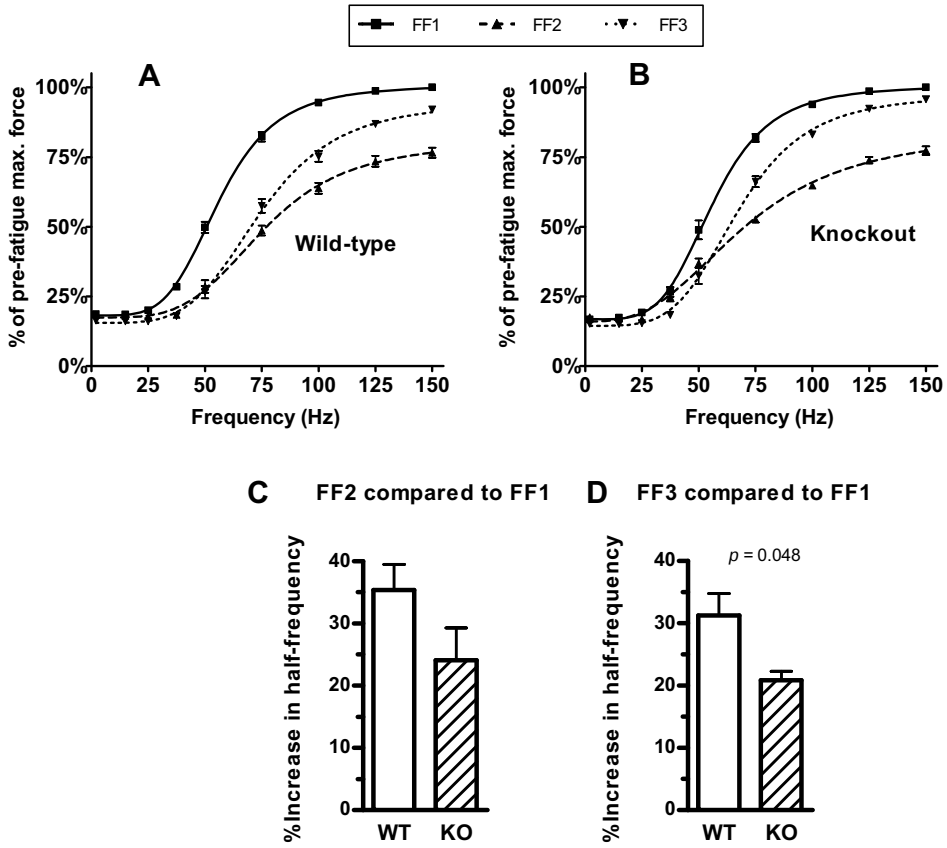

Figure 3.7. Force-frequency characteristics at various stages of fatigue experiments. (A) and **(B)** show, for wild-types and knockouts respectively, the changes in the shape of the force-frequency curve over time. FF1 (full line) is the pre-fatigue curve. FF2 (dashed line) is the curve shortly after the fatigue protocol has ended. It is right-shifted compared to FF1. FF3 (dotted line) is the curve at the end of the 30-minute recovery period. It has moved back slightly towards the pre-fatigue curve, but is still noticeably right-shifted compared with FF1. The fatigue-induced rightward shift of the force-frequency curve is reflected in increased half-frequencies for FF2 and FF3 compared with FF1. The percentage increase in half-frequency indicates the extent of the shift and is shown in **(C)** for FF2 and in **(D)** for FF3. In both these cases, wild-types had larger increases in half-frequency than knockouts, but this was only statistically significant in the case of FF3. (*n* = 6 muscles for WT, *n* = 8 muscles for KO. *p*-values are shown where there are significant differences between WT and KO.)

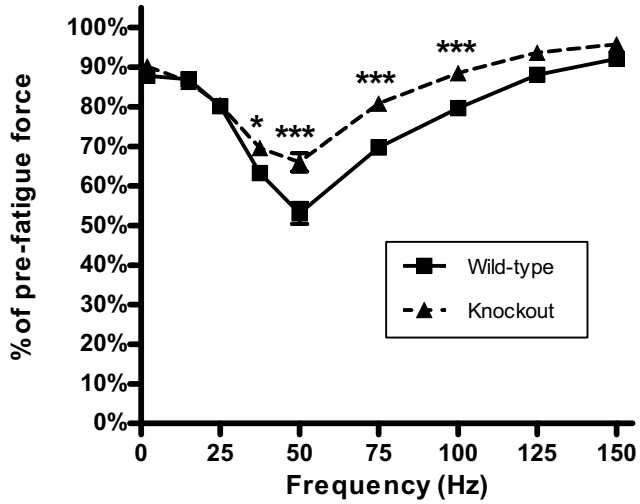

Figure 3.8. Post-recovery force as a percentage of pre-fatigue force. Each data point shows the force developed at a particular frequency following 30 minutes' recovery, expressed as a percentage of the force generated at that frequency before the fatigue protocol. At very low and very high frequencies, the post-recovery force is around 90% of the pre-fatigue force. However, over middle frequencies, force was still considerably lower than pre-fatigue levels. Also, at frequencies of 37.5, 50, 75 and 100 Hz, the loss of force was significantly greater in wild-types than in knockouts. (n = 6 muscles for WT, n = 8 muscles for KO. Stars indicate significant differences between WT and KO using 2-way ANOVA with Bonferroni post-tests. "*" indicates $0.01<p<0.05$, "***" indicates $p<0.001$.)

Discussion

Our current knowledge about the functions of α-actinin-3 is still in an early stage. We do know that its expression is confined largely to fast glycolytic muscle fibres and that its presence is somehow beneficial for power and sprint athletes at the elite level. One of the proposed roles for this protein is as a mechanical stabiliser of the sarcomere, while another possible function may be as an influencer of signalling and metabolic pathways, enabling a muscle fibre to differentiate towards a fast-twitch, glycolytic profile. This present study, and the one by MacArthur *et al.* (2008), represent the first investigations of the physiological properties of isolated skeletal muscle in the α-actinin-3 knockout mouse, and provide some data against which to evaluate these hypotheses about the protein's functions.

Our findings in the eccentric contraction studies do not appear to support the hypothesis that α-actinin-3 mechanically strengthens the sarcomere during extreme muscle activity. Following an eccentric contraction protocol with a large (20%) strain, knockout muscles did not show any more damage than wild-type muscles in any of the measures of damage. Moreover, morphological analysis of muscle fibres of older mice did not reveal any major evidence of repetitive injury in knockout muscles, apart from a very small number of split fibres.

One complicating factor in interpreting these results is the size of the muscle fibres. Fast glycolytic fibres in knockout mice have reduced fibre diameters compared with wild-types (MacArthur *et al.*, 2008), so there would be less shear stress on the fast fibres in knockouts, thus protecting them from eccentric damage (Karpati *et al.*, 1988). Hence it is still possible that sarcomeres are inherently weaker when they lack α-actinin-3, but that this is masked by the protective effect of smaller fibre diameter.

Our measurements of muscle stiffness concur with our eccentric contraction studies as no difference was found in muscle stiffness between wild-types and knockouts, suggesting that α-actinin-3 deficiency did not affect the strength or stiffness of the muscle as a whole.

Besides their interactions with actin, the sarcomeric α-actinins are also known to interact with cell-signalling proteins that are involved in fibre type differentiation, and with enzymes involved in metabolic pathways. This raises the possibility that one role of α-actinin-3 could be to influence fibre type differentiation towards a fast-twitch, glycolytic profile. While there is no evidence of a shift in myosin heavy chain composition from IIB to other isoforms in α-actinin-3-deficient muscle, there is evidence that α-actinin-3-deficient fibres have higher levels of oxidative enzymes than would be expected in a fast glycolytic fibre (MacArthur *et al.*, 2007). Enzyme assays reveal that the activity of key enzymes involved in oxidative

metabolism, such as citrate synthase, SDH and cytochrome *c* oxidase, is significantly higher in knockouts than in wild-types, while the anaerobic pathway enzyme, lactate dehydrogenase, has significantly lower activity in knockouts (MacArthur *et al.*, 2008). Thus it may also be hypothesised that α-actinin-3 somehow helps fast glycolytic fibres to use more anaerobic pathways, and in its absence these fibres resort to more oxidative pathways.

In this study, we found some features of the knockout muscle that were consistent with the hypothesis that α-actinin-3-deficient fibres are more oxidative than normal. These features were smaller cross-sectional areas, lower twitch-to-tetanus ratios and better recovery from fatigue.

We found that α-actinin-3-deficient muscles had a 9% smaller cross-sectional area than α-actinin-3-positive muscles. This is consistent with the fact that the diameter of fast glycolytic fibres is smaller in knockouts than in wild-types (MacArthur *et al.*, 2008), and supports the hypothesis that these fibres take on more oxidative characteristics when α-actinin-3 is absent, because oxidative fibres have smaller diameters than fast glycolytic fibres.

Slow-twitch motor units tend to have lower twitch-to-tetanus ratios than fast-twitch motor units (Celichowski & Grottel, 1993). Our finding that knockout muscles had lower twitch-to-tetanus ratios than wild-type muscles is therefore consistent with the α-actinin-3-deficient fast glycolytic fibres changing to a more slow-twitch, oxidative profile.

Knockout muscles also recovered better from fatigue than wild-type muscles. At the end of the 30-minute recovery period, knockouts had recovered significantly more of their original 100-Hz force than wild-types, and the rightward shift of the force-frequency curve, thought to represent impairment of excitation-contraction coupling due to fatigue, was much less pronounced in knockouts than in wild-types. The difference in recovery between wild-types and knockouts was most apparent at stimulation frequencies which were between 25% and 67% of maximum. At these frequencies, knockouts were able to develop a much higher percentage of their pre-fatigue force than wild-types. The improved recovery from fatigue in knockouts is consistent with the notion that α-actinin-3-deficient fibres may change towards the properties of more oxidative fibre types, which are more fatigue-resistant than glycolytic fibres. This also lends support to earlier findings that knockout mice can run 33% further than wild-types before exhaustion when subjected to treadmill running (MacArthur *et al.*, 2008), and may be one factor behind the increased incidence of α-actinin-3 deficiency in endurance athletes (Yang *et al.*, 2003).

Although wild-types and knockouts showed differences in their rates of recovery from fatigue, it can be seen from Figure 3.6 that there were no differences in their rates of force decline during the 30 seconds of fatiguing stimulation. One explanation for this may be the

accumulation of extracellular K^+ that occurs when muscles are subjected, as they were in this study, to intense, repeated stimulation *in vitro* (Allen *et al.*, 2008). Although only small amounts of K^+ leave the muscle fibre during each action potential, repeated action potentials can significantly increase the $[K^+]$ inside the lumen of the t-tubules, which comprise only 1% of the total fibre volume but 80% of the total membrane surface area. The increased extracellular $[K^+]$ and reduced intracellular $[K^+]$ result in membrane depolarisation and a reduction of membrane excitability (Allen *et al.*, 2008).

It is possible that this impaired excitability is the predominant factor underlying the reduction in force during the fatigue protocol in our study. This may have masked any differences in metabolic efficiency between wild-types and knockouts during the fatiguing stimulation, so that their forces declined at similar rates. However, $[K^+]$ and membrane potential rapidly return to normal once stimulation is stopped (Allen *et al.*, 2008), so the differences we observed between wild-types and knockouts during recovery are likely to be due to metabolic factors, and these differences are consistent with α-actinin-3 deficient fibres developing more oxidative properties, enabling knockout muscles to recover more quickly from fatigue.

There is one further piece of evidence suggesting that the contractile properties of α-actinin-3-deficient fibres may change towards those of a slower-twitch, more oxidative fibre type. This is the 2.6 ms increase in the twitch half-relaxation time of knockout muscles compared to wild-types, as we reported earlier in experiments on the same set of muscles (MacArthur *et al.*, 2008). Such a change is consistent with the observation that elite sprinters have a very low incidence of α-actinin-3 deficiency. Lack of this protein would significantly prolong the time taken for muscles to relax and thus be detrimental to activities requiring repeated rapid contractions, such as sprinting (Allen *et al.*, 1995).

To summarise, this present study has provided an overview of some basic contractile properties of the EDL muscle in a new knockout mouse, together with data on its responses to eccentric contractions and fatiguing stimulation. While these data do not appear to support the hypothesis that α-actinin-3 provides mechanical protection to the muscle fibre during strenuous physical activity, some results are consistent with the hypothesis that α-actinin-3 plays an important role in the differentiation of the fibre towards a fast-twitch, glycolytic profile, and that in its absence the fibre may tend towards a slower-twitch, more oxidative profile. This paper demonstrates that α-actinin-3 deficiency does have important effects on physiological function in muscle, and since α-actinin-3 deficiency is common in humans, it will be important to determine the effects of such deficiency in situations such as ageing and congenital muscle disease.

Grants

This project was funded in part by a grant (301590) from the Australian National Health and Medical Research Council. D.G.M. and J.T.S. were supported by Australian Postgraduate Awards.

Appendix to Paper B

One result from the set of studies forming *Paper B* has not been published in this paper. It has instead been published in the paper: MacArthur DG, Seto JT, Chan S, Quinlan KG, Raftery JM, Turner N, Nicholson MD, Kee AJ, Hardeman EC, Gunning PW, Cooney GJ, Head SI, Yang N & North KN (2008). An *Actn3* knockout mouse provides mechanistic insights into the association between α-actinin-3 deficiency and human athletic performance. *Human Molecular Genetics* 17: 1076-1086.

This result is the twitch half-relaxation time. It will be presented here in this appendix so that this result, along with those reported in *Paper B*, form a complete picture of the contractile properties examined in this cohort of muscles.

Method

The muscle was stimulated with a supramaximal pulse of 1 ms duration and the resulting twitch recorded. The twitch data was smoothed by averaging the raw data over 2.5 ms intervals, and from the resulting smoothed data the half-relaxation time (time taken to relax to half of peak twitch force) was obtained.

Result

Knockout muscles had a significantly longer half-relaxation time than wild-type muscles (**Table 3.2**). This is another feature suggesting a shift towards slower-twitch properties in the absence of α-actinin-3.

	Wild-type	Knockout	*P*-value
Twitch half-relaxation time, ms	13.2 ± 0.6	15.7 ± 0.6	0.008

Table 3.2 Twitch half-relaxation time.

Paper C

Declaration

This chapter is a reproduction of the submitted paper:

Chan S, Seto JT, Houweling PJ, Yang N, North KN & Head SI. Contractile properties of EDL muscle and skinned fibres from α-actinin-3 KO mice of various ages.

Current status

Under review as at December 2009. Submitted to *Experimental Physiology* on 26th November 2009.

Author contributions

The contribution of S.C. to this paper was 70%, and consisted of designing and performing the experiments, analysing the data, and writing the paper.

Abstract

α-Actinin-3 is a protein found in the Z-disc of fast glycolytic skeletal muscle fibres. An estimated 1 billion people worldwide are deficient in this protein due to a common null polymorphism in the ACTN3 gene. This gene has been termed the "gene for speed". α-Actinin-3 deficiency is associated with poorer sprint performance and enhanced endurance performance in athletes. Whole EDL muscles from *Actn3* knockout mice display physiological characteristics that suggest a change towards a slower-twitch, more oxidative profile. In this study we examine the properties of the contractile proteins and sarcoplasmic reticulum (SR) in fast-twitch EDL muscle fibres deficient in α-actinin-3. By examining caffeine-induced Ca^{2+} release in mechanically skinned fibres from the *Actn3* knockout mouse, we found that the SR of α-actinin-3-deficient fibres loads Ca^{2+} more slowly than wild-types. The Ca^{2+} and Sr^{2+} activation characteristics of chemically skinned fibres were also different between *Actn3* knockouts and wild-types, with knockouts exhibiting steeper force-pCa curves than wild-types and a higher frequency of myofibrillar oscillations. Whole knockout *Actn3* knockout muscles were found to have longer twitch and tetanus relaxation times than wild-types, reduced mass and cross-sectional area, steeper force-frequency curves and lower twitch-to-tetanus ratios. Overall, these changes in the properties of skinned fibres and whole muscles are consistent with a switch towards slower-twitch characteristics in fast-twitch fibres lacking α-actinin-3.

Introduction

The α-actinins are a group of actin-binding proteins found in the Z-discs of skeletal muscle sarcomeres. Two isoforms are found in the Z-disc: α-actinin-2, which occurs in all muscle fibres, and α-actinin-3, which is restricted mainly to fast glycolytic fibres (MacArthur & North, 2004).

An estimated 18% of individuals worldwide completely lack α-actinin-3, due to homozygosity for a common polymorphism in the ACTN3 gene (MacArthur *et al.*, 2007). This gene has become known colloquially as the "gene for speed". α-Actinin-3 deficiency is not associated with any disease phenotype. However, elite sprint and power athletes have a reduced frequency of α-actinin-3 deficiency (Yang *et al.*, 2003; Niemi & Majamaa, 2005; Papadimitriou *et al.*, 2008; Roth *et al.*, 2008), while there is a tendency towards a higher frequency of α-actinin-3 deficiency among elite endurance athletes (Yang *et al.*, 2003; Eynon *et al.*, 2009). In non-athlete polpulations, α-actinin-3 deficiency has been associated with reduced muscle strength (Clarkson *et al.*, 2005) and poorer sprinting performance (Moran *et al.*, 2007). Taken overall, these data indicate that a lack of α-actinin-3 is detrimental to sprint and power performance but beneficial for endurance activities.

We have generated an *Actn3* knockout mouse (MacArthur *et al.*, 2007) which displays a phenotype consistent with that observed in humans. Knockout mice were able to run 33% further than wild-types on a motorised treadmill endurance test (MacArthur *et al.*, 2007), but had lower grip strength and lower muscle weights than wild-types (MacArthur *et al.*, 2008). The *Actn3* knockout mouse is thus an appropriate model for examining the effects of α-actinin-3 deficiency.

Our earlier studies on the *Actn3* knockout mouse provide insights into the mechanisms by which α-actinin-3 deficiency might lead to reduced sprinting performance and enhanced endurance performance. We have found that knockout muscles display characteristics that are more slow-twitch and oxidative than wild-type muscles. Compared to wild-type muscles, knockout muscles have slower twitch half-relaxation times, smaller fast-fibre diameters, higher activity of oxidative enzymes, lower activity of anaerobic enzymes and quicker recovery of force following fatiguing stimulation (MacArthur *et al.*, 2008; Chan *et al.*, 2008). Such changes would be a disadvantage in activities requiring repeated rapid contractions, such as sprinting (Allen *et al.*, 1995), but would be beneficial for activities dependent on aerobic metabolism, such as endurance sports.

These findings suggest that α-actinin-3 may play a role in the development of fast-twitch, glycolytic properties in a muscle fibre, and that in its absence slower-twitch, more oxidative properties may develop. At a subcellular level many factors contribute to the characterisation of a fibre as fast-twitch or slow-twitch. These include: (i) the sensitivity of the contractile apparatus to Ca^{2+}; and (ii) the rate of release and re-uptake of Ca^{2+} by the sarcoplasmic reticulum (SR) (Bottinelli & Reggiani, 2000). Our first aim in this present study is to find out what changes occur at the level of the contractile proteins and SR when α-actinin-3 is absent. Using individual fibres from the extensor digitorum longus (EDL) muscles of *Actn3* knockout and wild-type mice, we employ the skinned fibre technique to examine: (i) the Ca^{2+} loading properties of the SR; and (ii) the Ca^{2+} and Sr^{2+} activation characteristics of the contractile filaments. The skinned fibre technique is widely used for elucidating mechanisms at the level of the contractile proteins and SR (Bakker *et al.*, 1998).

As the *Actn3* knockout mouse is a newly developed model of α-actinin-3 deficiency, it is useful to characterise the contractile properties of whole fast-twitch muscles from this mouse. This was previously done in an adult male cohort (Chan *et al.*, 2008); in this present study we are also interested in whether these characteristics vary with age and gender. Hence in this study our second aim is to characterise the contractile properties of whole EDL muscles from male and female *Actn3* knockout mice in two age groups: adult (2 to 6 months old) and aged (19 to 22 months old).

Methods

Animals used

Use of animals was approved by the Animal Care and Ethics Committees of the Children's Medical Research Institute and Children's Hospital at Westmead and the University of New South Wales. 9 male mice (4 WT, 5 KO) aged 10 to 11 months were used for the skinned fibre experiments. Mice used in the whole muscle experiments were in two age groups: adult mice (2 to 6 months old) and aged mice (19 to 22 months old). Adult mice consisted of 24 males (12 WT, 12 KO) and 15 females (8 WT, 7 KO). Aged mice consisted of 14 males (7 WT, 7 KO) and 12 females (6 WT, 6 KO).

Fibre preparation – skinned fibre experiments

All animals were anaesthetised with halothane and sacrificed by cervical dislocation. The EDL muscle was dissected from the hindlimb. Individual fibres were isolated and mechanically skinned in paraffin oil and mounted on a force transducer to monitor isometric force (Bakker *et al.*, 1998). The length and diameter of each fibre were measured at slack length, and the fibre was then stretched by 20% to maximise the force responses.

Ca^{2+} loading of sarcoplasmic reticulum

The fibre was first depleted of Ca^{2+} by exposure for 2 minutes to a K^+-HDTA solution containing low Mg^{2+} (0.25 mM) and 30 mM caffeine, to maximally release Ca^{2+} from the SR, and 0.25 mM EGTA, to chelate all released Ca^{2+} and prevent SR Ca^{2+} reaccumulation. The fibre was then loaded with Ca^{2+} for a predetermined period of time by exposure to a highly buffered Ca^{2+} solution (pCa 6.57) made by combining solutions *A* and *B* at a ratio of 0.85:1.15 (see "Contractile apparatus" below for compositions of solutions *A* and *B*). Loading was rapidly terminated at the end of the loading period by a brief exposure (~1–2 s) to solution *A*, after which the fibre was washed (for 6 s) in a K^+-HDTA solution to remove excess EGTA. The fibre was then re-exposed to the caffeine solution (above), and the force response was measured. This procedure was repeated using different loading times to generate a series of caffeine-induced force response curves. Before exposure to the caffeine solution, the fibre was incubated for 30 s in a K^+-HDTA solution containing 0.25 mM EGTA to allow time for the EGTA to equilibrate within the fibre. The K^+-HDTA solution was of a similar composition to solution *A* (see "Contractile apparatus" below), with the exception that EGTA was replaced by HDTA.

The area under each caffeine-induced force response curve was used as a measure of the amount of Ca^{2+} released, and hence of the amount of Ca^{2+} loaded by the SR during the

loading period. For any particular fibre, the area under the curve for a particular loading time was expressed as a percentage of the maximum area measured out of all the force response curves for that fibre. This relative area indicates the amount of Ca^{2+} loaded by the SR during that time, relative to the maximum amount that it could load. Some investigators adjust these relative areas by a correction factor which ensures direct proportionality between the relative areas and the SR Ca^{2+} content (Macdonald & Stephenson, 2001; Macdonald & Stephenson, 2006). However, because we were only interested in differences between knockouts and wild-types in their rates of Ca^{2+} uptake, rather than the exact rates of Ca^{2+} uptake, we did not apply this correction factor in the analysis of our Ca^{2+} loading data.

Contractile apparatus

Following the Ca^{2+} loading experiments, the fibre was placed for 10 mins in solution *A* (see below) with 2% Triton X-100 added to chemically skin all remaining membranous cell elements. The fibre was then exposed to a series of solutions of different free Ca^{2+} concentrations. The strongly buffered Ca^{2+} solutions were prepared by mixing specific proportions of EGTA-containing solution (solution *A*) and CaEGTA-containing solution (solution *B*). Solution *A* contained (in mM) 117 K^+, 36 Na^+, 8 ATP (total), 1 free Mg^{2+}, 10 creatine phosphate, 50 EGTA (total), 60 HEPES, and 1 NaN_3 at pH 7.10. Solution *B* was similar to solution *A*, with the exception that the EGTA and CaEGTA concentrations of solution *B* were 0.3 and 49.7 mM, respectively. The free Ca^{2+} concentrations of the solutions were calculated using a $K_{apparent}$ for EGTA of $4.78 \times 10^6\ M^{-1}$ (Head *et al.*, 1990). Maximal force was determined by exposure to solution *B*, containing a free Ca^{2+} concentration of 3.5×10^{-5} M. Force was returned to baseline after maximal activation by exposure to solution *A*. The plateaus of the force responses elicited by exposure to solutions of increasing free Ca^{2+} concentration were expressed as a percentage of maximum Ca^{2+}-activated force and plotted as a function of pCa. The fibres were then similarly activated by exposure to a series of Sr^{2+} solutions, made by combining solution *A* with a solution containing 9.5 mM EGTA and 40.0 mM SrEGTA. Differences between the force-pCa and force-pSr curves can provide a rough indication of fibre type (Fink *et al.*, 1986; Bortolotto *et al.*, 2000). The data were fitted with Hill curves and the following fitted parameters determined: (i) n_{Ca} and n_{Sr}, the cooperativity of Ca^{2+} and Sr^{2+} binding sites; (ii) pCa_{50} and pSr_{50}, the sensitivity to Ca^{2+} and Sr^{2+}; and (iii) pCa_{50}-pSr_{50}, the relative sensitivity to Ca^{2+} and Sr^{2+}.

Muscle preparation – whole muscle experiments

The EDL muscle was dissected as described above, then tied by its tendons to a force transducer (World Precision Instruments, Fort 10) at one end and a fixed metal hook at the other, using silk suture (Deknatel 6.0). It was placed in a bath continuously superfused with Krebs solution, with composition (mM): 4.75 KCl, 118 NaCl, 1.18 KH_2PO_4, 1.18 $MgSO_4$, 24.8 $NaHCO_3$, 2.5 $CaCl_2$ and 10 glucose, with 0.1% fetal calf serum and continuously bubbled with 95% O_2-5% CO_2 to maintain pH at 7.4. The muscle was stimulated by delivering a supramaximal current between two parallel platinum electrodes, using an electrical stimulator (A-M Systems). At the start of the experiment, the muscle was set to the optimum length L_0 that produced maximum twitch force. All experiments were conducted at room temperature (~22°C to 24°C).

Twitch relaxation

The muscle was stimulated with a supramaximal pulse of 1 ms duration and the resulting twitch recorded. The twitch data was smoothed by averaging the raw data over 2.5 ms intervals, and from the resulting smoothed data the half-relaxation time (time taken to relax to half of peak twitch force) was obtained. Some muscles were also subjected to a strenuous fatigue protocol, after which another twitch was recorded and measured as described above. The fatigue protocol consisted of a one-second, 100-Hz tetanus every 2 seconds over a period of 30 seconds.

Force-frequency curve

A force-frequency curve was obtained by delivering 500 ms stimuli of different frequencies (2, 15, 25, 37.5, 50, 75, 100, 125 and 150 Hz), and measuring the force produced at each frequency of stimulation. A 30 second rest was allowed between each frequency. A curve relating the muscle force P to the stimulation frequency f was fitted to these data. The curve had the following equation (Motulsky & Christopoulos, 2003):

$$P = P_{\min} + \frac{P_{\max} - P_{\min}}{1 + \left(\frac{K_f}{f}\right)^h}$$

The values of r^2 for the fitting procedure were never lower than 99.3%. From the fitted parameters of the curve, the following contractile properties were obtained: maximum force (P_{max}), half-frequency (K_f), Hill coefficient (h) and twitch-to-tetanus ratio (P_{min}/P_{max}). Some muscles were also subjected to a strenuous fatigue protocol (described in "Twitch relaxation" above), after which a second force-frequency curve was obtained.

Tetanus relaxation

Tetanus relaxation consists of a slow linear phase followed by a fast exponential phase. The linear phase is the easier to interpret as relaxation during this phase is homogeneous along the fibre, whereas in the exponential phase some parts of the fibre are lengthening and others are shortening (Westerblad & Lännergren, 1991). In our measurements, the start of the linear phase was defined to be the point at which force began to fall following cessation of stimulation. Linear regression was then performed between this point and all subsequent points. The point at which the linear regression began to yield an r^2 of less than 98.5% was defined to be the end of the linear phase. We used the duration of this linear phase and the rate of force decline over this phase as measures of the rate of relaxation following a tetanus. The tetanus analysed was the 125-Hz tetanus from the force-frequency curve.

Mass and cross-sectional area

At the end of the whole muscle experiment, the muscle was removed from the bath. The tendons were trimmed and the muscle was lightly blotted on filter paper and then weighed. An estimate of the cross-sectional area was obtained by dividing the muscle's mass by the product of its optimum length and the density of mammalian muscle (1.06 mg/mm^3).

Statistical analyses

Data are presented as Mean ± S.E.M.. For the skinned fibre data, the statistical tests used were two-tailed *t*-tests at a significance level of 5%. For the whole muscle data, we were comparing *Actn3* knockouts versus wild-types in younger and older animals. Hence for all comparisons we used 2-way ANOVA in which genotype (wild-type or knockout) and age (adult or aged) were the two factors. Comparison of wild-type versus knockout in each age group was made using Bonferroni post-tests with an overall significance level of 5%. All statistical tests and curve fitting were performed using a standard statistical software package (GraphPad Prism Version 5 for Windows, GraphPad Software, San Diego California USA).

Results

Ca^{2+} loading of the sarcoplasmic reticulum

In previous studies of the *Actn3* knockout mouse we observed that whole fast-twitch muscles from the knockout mouse showed a shift towards more slow-twitch characteristics (MacArthur *et al.*, 2008; Chan *et al.*, 2008). At the individual fibre level, one distinguishing feature between fast-twitch and slow-twitch fibres is the rate of Ca^{2+} uptake by the sarcoplasmic reticulum (SR) (Bottinelli & Reggiani, 2000). Hence we compared SR Ca^{2+} uptake in *Actn3* knockout and wild-type fibres, to see whether any differences here might be contributing to the slower-twitch phenotype of whole knockout muscle. We used an established procedure for investigating SR Ca^{2+} loading, where the SR of mechanically skinned fibres is loaded with Ca^{2+} for a predetermined period of time and then depleted of all releasable Ca^{2+} with caffeine (Bakker *et al.*, 1998; Trinh & Lamb, 2006).

Figure 4.1(A) shows an example of the process. At the outset we depleted the SR of all its endogenous Ca^{2+} by exposing the fibre to a caffeine-EGTA solution. The first curve shows the force response during this exposure. It can be seen that the caffeine-EGTA solution fully empties the SR of all Ca^{2+} because when the fibre is re-exposed to the caffeine-EGTA solution without any intervening exposure to the Ca^{2+}-loading solution, there is no force response. After depleting the SR of all endogenous Ca^{2+} we then carried out repeating cycles of load and release, where the SR was loaded with Ca^{2+} by exposing the fibre to a low-[Ca^{2+}] solution for a known length of time, then fully depleted of Ca^{2+} by exposing the fibre to the caffeine-EGTA solution. The subsequent curves show the force responses during exposure to the caffeine-EGTA solution. The area under the curve of the force response was used as a measure of the amount of Ca^{2+} released, and hence of the amount of Ca^{2+} loaded into the SR during the time of exposure to the low-[Ca^{2+}] solution.

Figure 4.1(B) shows the results for our sample of fibres. Each point on the graph shows the amount of Ca^{2+} loaded into the SR during a particular loading duration, expressed as a percentage of maximum Ca^{2+} loaded. It can be seen that maximum loading is achieved by 10 seconds in both wild-type and *Actn3* knockout fibres. For any particular loading time shorter than this, the SR in knockout fibres is able to load less Ca^{2+} than the SR in wild-type fibres, indicating that Ca^{2+} uptake by the SR in α-actinin-3-deficient fibres is slower than in wild-type fibres.

Another factor which could affect how quickly a fibre relaxes is the rate of dissociation of Ca^{2+} from troponin C. As an estimate of the relative rates at which Ca^{2+} dissociates from the

myofilaments in knockout and wild-type fibres, we compared the half-relaxation times of their force response curves following maximum loading. In terms of Figure 4.1(A), this is the half-relaxation time of the force response curve after loading for 10s. The rationale here is that the EGTA in the caffeine solution would chelate all the Ca^{2+} released from the SR and the rate of relaxation would reflect the rate of Ca^{2+} removal from the myofilaments. We found that on average, the half-relaxation times in *Actn3* knockout fibres was 40% longer than in wild-type fibres, suggesting that in α-actinin-3-deficient fibres the kinetics of Ca^{2+} dissociation from the myofilaments is slower than in wild-type fibres.

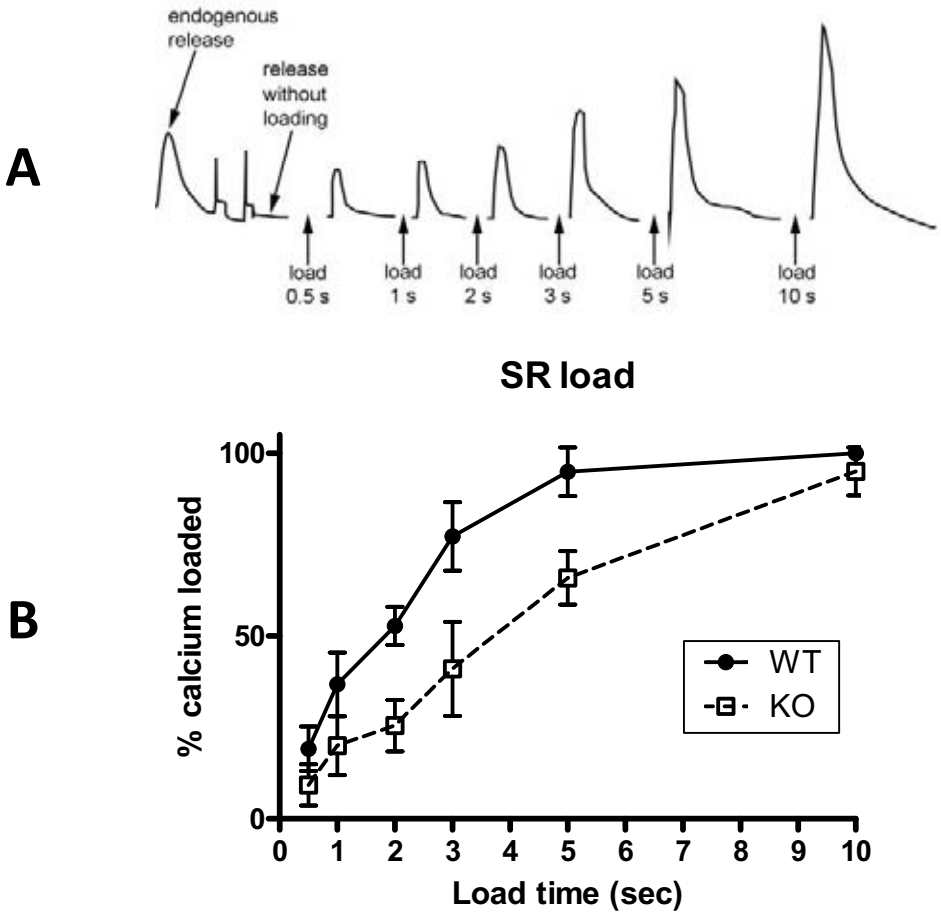

Figure 4.1. Ca^{2+} loading of the sarcoplasmic reticulum. (A) shows representative force responses produced in a fibre from the muscle of a knockout animal when exposed to a caffeine-EGTA solution to empty the sarcoplasmic reticulum (SR) of all releasable Ca^{2+}. Firstly, the SR was emptied of all endogenous Ca^{2+} ("endogenous release" curve). To illustrate that the SR was completely emptied, when this fibre was then re-exposed to the caffeine-EGTA solution without loading, there was zero force response (indicated by "release without loading"). The fibre was then exposed for differing lengths of time to a low-[Ca^{2+}] solution to load the SR with Ca^{2+}. After each loading, the SR was emptied by exposing the fibre to the caffeine-EGTA solution (subsequent force response curves). The loading time is indicated before each curve. The area under each curve gives an indication of the amount of Ca^{2+} released, and hence of the amount loaded during the loading period. **(B)** shows the amount of Ca^{2+} loaded by the SR over different loading times, expressed as a percentage of maximum loading. The full line is for wild-type fibres, the dashed line for knockout fibres. It is apparent that the SR in knockouts loads Ca^{2+} more slowly than the SR in wild-types.

Ca^{2+} and Sr^{2+} activation characteristics of individual skinned fibres

Another distinguishing feature between fast-twitch and slow-twitch fibres is the Ca^{2+} sensitivity of the contractile proteins (Bottinelli & Reggiani, 2000). To investigate the possibility that α-actinin-3 deficiency may change the properties of the contractile proteins and contribute to a slower-twitch phenotype in whole muscle, we examined the Ca^{2+} and Sr^{2+} activation characteristics of individual skinned fibres.

Following the SR loading experiments, muscle fibres were chemically skinned with Triton X-100 and then exposed to a series of highly buffered Ca^{2+} solutions of increasing concentrations. The force produced by the fibre in this series of solutions is shown in the left of **Figure 4.2(A)** for a representative fibre. Forces were then expressed as a percentage of maximum and a force-pCa curve was fitted to the data points. The force-pCa curves for wild-types and knockouts are the left pair of curves shown in **Figure 4.2(B)**. Force-pSr curves were also produced for each fibre by exposure to a series of Sr^{2+} solutions. The force produced in this series of Sr^{2+} solutions is shown in the right of Figure 4.2(A) for a representative fibre, and the resulting force-pSr curves for wild-types and knockouts are the right pair of curves shown in Figure 4.2(B). From the fitted force-pCa and force-pSr curves, it was possible to determine the following parameters: (i) n_{Ca} and n_{Sr}, the cooperativity of Ca^{2+} and Sr^{2+} binding sites, which reflects the degree to which the various subunits of the thin and thick filaments and thin-filament regulatory proteins interact to produce tension (Moss *et al.*, 1995); (ii) pCa_{50} and pSr_{50}, the sensitivity of the contractile apparatus to Ca^{2+} and Sr^{2+}, respectively (Fink et al., 1986); and (iii) pCa_{50}-pSr_{50}, the relative sensitivity of a particular fibre to Ca^{2+} and Sr^{2+} (Fink et al., 1986).

The values of these parameters in wild-type and knockout EDL fibres are shown in **Figure 4.2(C)**. Knockout fibres had significantly higher n_{Ca} and n_{Sr} values than wild-types, indicative of a higher cooperativity of the contractile filaments in *Actn3* knockouts. There was no difference between wild-types and knockouts in their sensitivity to Ca^{2+} as measured by the pCa_{50}. There was a statistically significant difference in pSr_{50} between wild-types and knockouts, but this difference was extremely small. There was no difference between wild-types and knockouts in their pCa_{50}-pSr_{50}, indicating the lack of a gross difference in myosin heavy chain isoform compositions.

Specific forces upon maximal Ca^{2+} activation were 302 ± 48 mN/mm^2 in *Actn3* knockout fibres and 314 ± 50 mN/mm^2 in wild-type fibres. These were not significantly different between wild-types and knockouts. These values are consistent with maximum specific forces of whole EDL muscles in our study (327 ± 10 mN/mm^2 for knockouts, 302 ± 7.6 mN/mm^2 for wild-types, p>0.05).

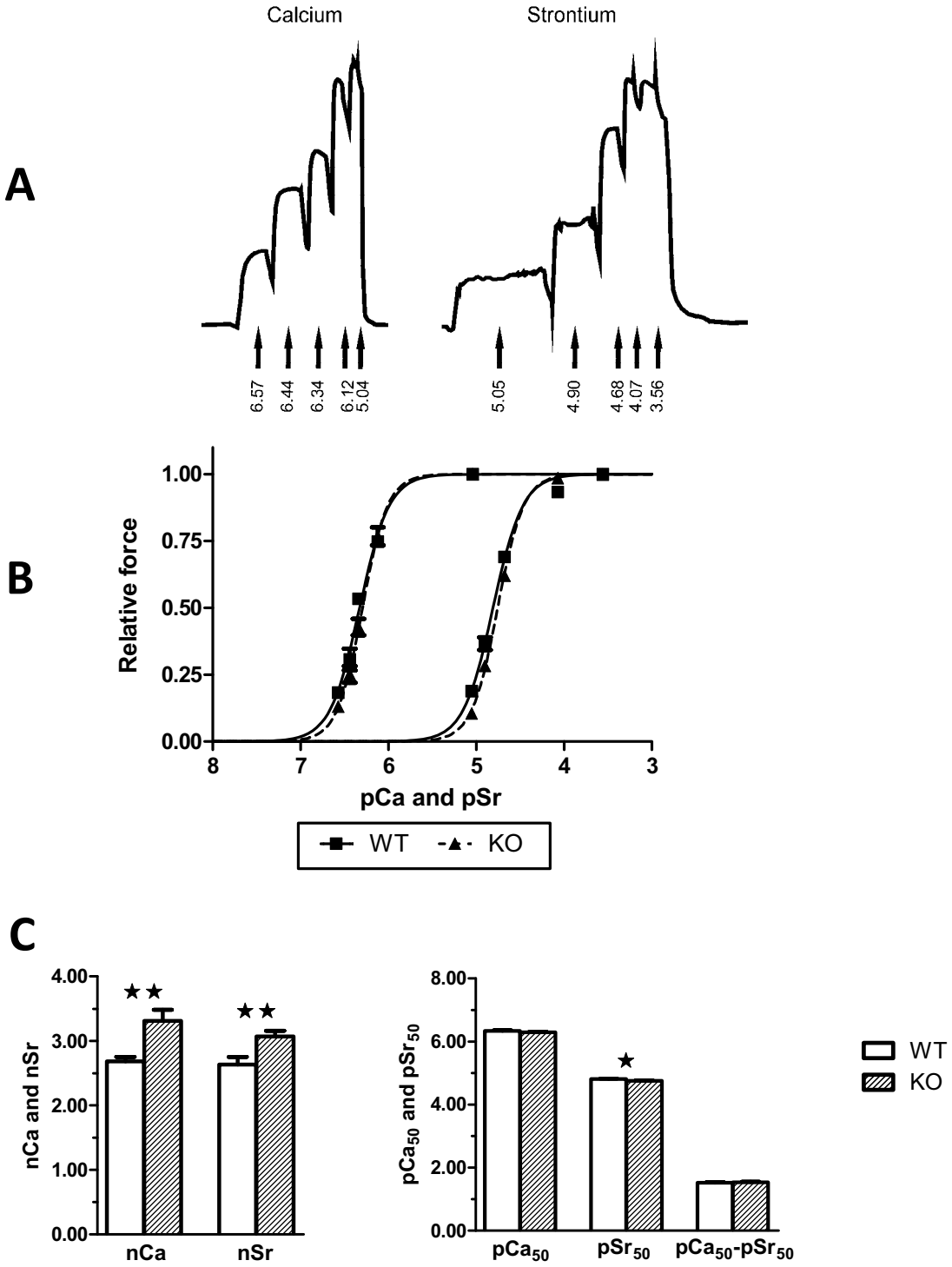

Figure 4.2. Ca^{2+} and Sr^{2+} activation characteristics of individual skinned fibres. (A) shows representative force responses in an individual skinned fibre when exposed to a series of solutions of increasing [Ca^{2+}] (left) and increasing [Sr^{2+}] (right). [Ca^{2+}] and [Sr^{2+}] are indicated under the curves (expressed as pCa and pSr). The force-pCa curves and force-pSr curves for wild-types and knockouts are shown in **(B)**. The left pair of curves is for pCa, the right pair is for pSr. The values of parameters derived from these curves are shown in **(C)**. Knockout fibres had significantly higher n_{Ca} and n_{Sr} values than wild-types. There was also a statistically significant difference in their pSr_{50} values, but this difference was extremely small. There was no difference between wild-types and knockouts in their pCa_{50}-pSr_{50}. (Sample sizes – 17 WT fibres, 18 KO fibres. ★★ indicates $0.001<p<0.01$, ★ indicates $0.01<p<0.05$.)

Frequency of myofibrillar oscillations

At submaximal levels of activation by Ca^{2+} or Sr^{2+}, skinned fibres exhibit characteristic oscillations in force (Stephenson & Williams, 1982; Fink *et al.*, 1986; Williams *et al.*, 1993). We also observed these oscillations in our skinned fibres during the generation of the force-pCa and force-pSr curves. These oscillations appear to be a property of the contractile apparatus and reflect the nature of the interaction between actin filaments and the myosin heads (Smith & Stephenson, 2009). Hence it is possible that subtle alterations to actin-myosin affinity in the absence of α-actinin-3 might show up as changes in the frequency of myofibrillar oscillations.

We thus analysed all myofibrillar oscillations observed in our skinned fibre preparations when activated by Ca^{2+} and Sr^{2+}. **Figure 4.3(A)** shows examples of oscillations observed in a wild-type fibre and in a knockout fibre. In **Figure 4.3(B)**, the frequency of oscillation has been plotted against the percentage of maximally activated force at which the oscillation occurred. Oscillations typically occurred at less than 40% of maximum activation, although some occurred at up to 60% of maximum activation. It can be seen that higher-

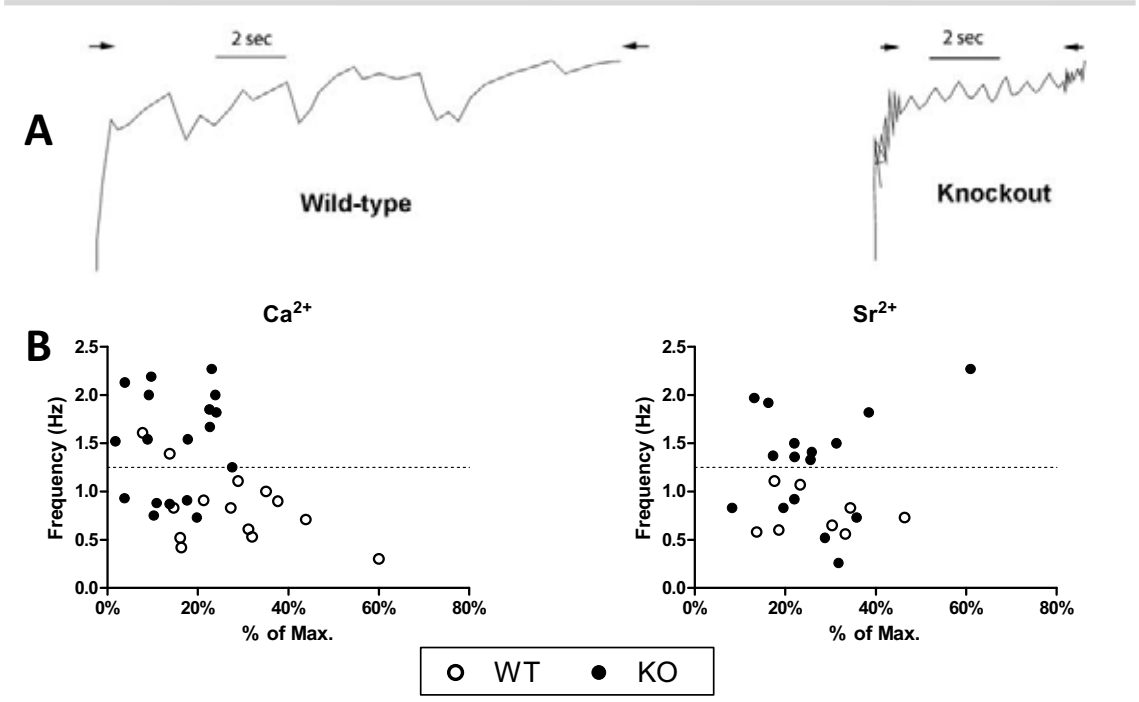

Figure 4.3. Myofibrillar oscillations in Ca^{2+} and Sr^{2+} solutions. (A) shows examples of oscillations occurring in a wild-type fibre (left) and a knockout fibre (right). These occurred at 27% of maximum force in the wild-type fibre and at 31% of maximum force in the knockout fibre. The space between the arrows is where the chart recorder was run at maximum speed. **(B)** shows the frequency of oscillation plotted against the percentage of maximally activated force at which the oscillation occurred. Each circle represents one instance of oscillations occurring. The left diagram shows instances of oscillations in the Ca^{2+} solutions and the right diagram shows instances of oscillations in the Sr^{2+} solutions. Open circles are for wild-type fibres, closed circles for knockout fibres. A line has been drawn at 1.25 Hz to show that higher-frequency oscillations generally occurred only in knockout fibres, as can be seen from the points that lie above this line.

frequency oscillations generally occurred in only the knockout fibres. Of those cases where oscillation frequency exceeded 1.25 Hz in the Ca^{2+} solutions, only 2 were in wild-type fibres, whereas 12 were in knockout fibres. In the Sr^{2+} solutions, only knockout fibres displayed oscillation frequencies exceeding 1.25 Hz. These data suggest that fibres in *Actn3* knockout muscles may have altered actin-myosin affinity, giving rise to higher oscillation frequencies that do not occur in the fibres of wild-type muscles.

Mass and cross-sectional area

As the *Actn3* knockout mouse is a newly developed model of α-actinin-3 deficiency, we wished to characterise the contractile properties of whole EDL muscle from both male and female mice in two age groups: adult (2 to 6 months old) and aged (19 to 22 months old). **Figure 4.4** shows the mass and cross-sectional area of EDL muscles from wild-type and *Actn3* knockout animals. The mass and cross-sectional area in adult male mice was 9% lower in knockouts than in wild-types ($0.001<p<0.01$). In adult female mice, knockout muscles had 11% lower mass and 13% smaller cross-sectional area than wild-types ($0.001<p<0.01$). In aged animals however, these differences were no longer apparent. There were no significant differences between *Actn3* knockouts and wild-types in either aged male mice or aged female mice. Hence α-actinin-3 deficiency is associated with a reduction in EDL muscle mass and cross-sectional area in both males and females, but only in adult animals.

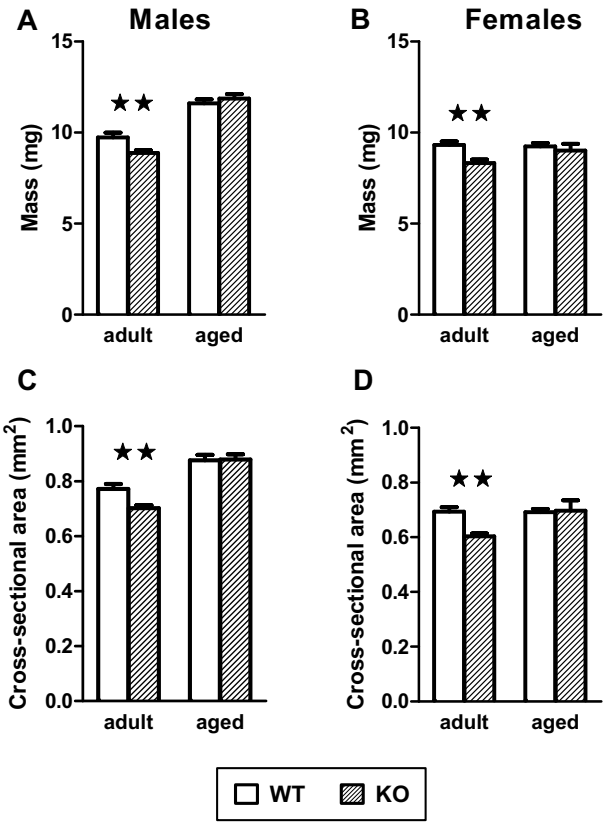

Figure 4.4. Mass and cross-sectional area. Mass is shown in **(A)** for males and **(B)** for females. Cross-sectional area is shown in **(C)** for males and **(D)** for females. In adult male and adult female mice, EDL muscles had significantly lower mass and cross-sectional area than wild-types. However, no differences were apparent in aged muscles (>19 months old). (Sample sizes: adult males – 17 WT, 22 KO; aged males – 11 WT, 9 KO; adult females – 13 WT, 10 KO; aged females – 6 WT, 6 KO. ★★ indicates $0.001<p<0.01$.)

Twitch relaxation

Figure 4.5(A) shows the time course of relaxation during an isometric twitch, both in unfatigued EDL muscles and in muscles fatigued by repetitive stimulation (see *Methods* for fatigue protocol). Twitch relaxation data for individual EDL muscles were expressed as a percentage of peak twitch force and aggregated into single curves for each age/gender group. It can be seen that in all cases, except for unfatigued muscles from adult female mice, the relaxation curves for *Actn3* knockouts lie to the right of those for wild-types, suggesting that *Actn3* knockout muscles relax at a slower rate. An example of this slowing in a knockout muscle compared to a wild-type muscle is shown in **Figure 4.5(B)**.

In unfatigued muscles from adult male mice, the half-relaxation time (time taken to fall to 50% of peak twitch force) was significantly longer in knockouts than in wild-types (2.2 ms longer, $p<0.001$). In fatigued muscles from the same group of mice, there was an even greater difference, with the half-relaxation time of knockout muscles being 7.7 ms longer than that of wild-types ($p<0.001$). Additionally, in the muscles of adult female mice, the half-relaxation time for knockouts was 3.6 ms longer than for wild-types ($0.01<p<0.05$). Although the curves for aged males and aged females also suggest a slowing of relaxation in knockouts, this was not statistically significant.

Tetanus relaxation

Relaxation following an isometric tetanic contraction can be divided into two phases: a slow linear phase in which relaxation is homogeneous along the muscle fibre, followed by a fast exponential phase in which some parts of the fibre shorten and others lengthen (Westerblad & Lännergren, 1991). **Figure 4.6(A)** shows the decline in force over time following a maximal tetanic contraction in an EDL muscle. We defined the linear phase to be that part of the curve where a linear regression yielded an r^2 of greater than 98.5% (see *Methods* for more details). We measured the duration of this linear phase (**Figure 4.6(B)**) and the rate of force decline during this linear phase (**Figure 4.6(C)**), both in unfatigued muscles and in muscles that had been fatigued by repetitive stimulation.

The results in Figure 4.6(B) and Figure 4.6(C) show that *Actn3* knockout muscles have a longer duration of the linear phase, and a slower rate of force decline, than wild-type muscles, suggesting that knockout muscles relax more slowly than wild-types following a tetanus. The longer duration in knockouts was statistically significant in unfatigued muscles of adult males (2.1 ms longer than wild-types, $0.01<p<0.05$) and unfatigued muscles of adult females (3.3 ms longer, $0.001<p<0.01$). The slower rate of force decline in knockouts was statistically significant in unfatigued muscles of adult males (0.16 mN/ms slower than wild-types, $p<0.001$),

unfatigued muscles of adult females (0.15 mN/ms slower, $p<0.001$) and fatigued muscles of adult females (0.10 mN/ms slower, $0.01<p<0.05$). No statistically significant differences were found in aged muscles.

Force-frequency characteristics

Figure 4.7 shows the force-frequency curves for males and females, by age. Force-frequency data for individual EDL muscles were expressed as a percentage of maximum force and aggregated into single curves for each age/gender group.

In all groups, the rapidly rising portion of the curve (~37.5 to 75 Hz) is slightly steeper for knockouts than for wild-types as a result of a higher Hill coefficient in *Actn3* knockout EDL muscles. The higher Hill coefficient in knockouts was statistically significant in adult males (Hill coefficient of 5.60 ± 0.17 for KO vs. 5.01 ± 0.07 for WT, $0.01<p<0.05$) and aged females (5.15 ± 0.23 for KO vs. 4.46 ± 0.23 for WT, $0.01<p<0.05$).

Another feature of the force-frequency curves is that, with the exception of aged females, the curve for *Actn3* knockouts starts at a lower level than the curve for wild-types, as a result of a lower twitch-to-tetanus ratio in knockout EDL muscles. The lower twitch-to-tetanus ratio was statistically significant in adult males (twitch-to-tetanus ratio of 18.4 ± 0.4% for KO vs. 20.3 ± 0.4% for WT, $0.01<p<0.05$).

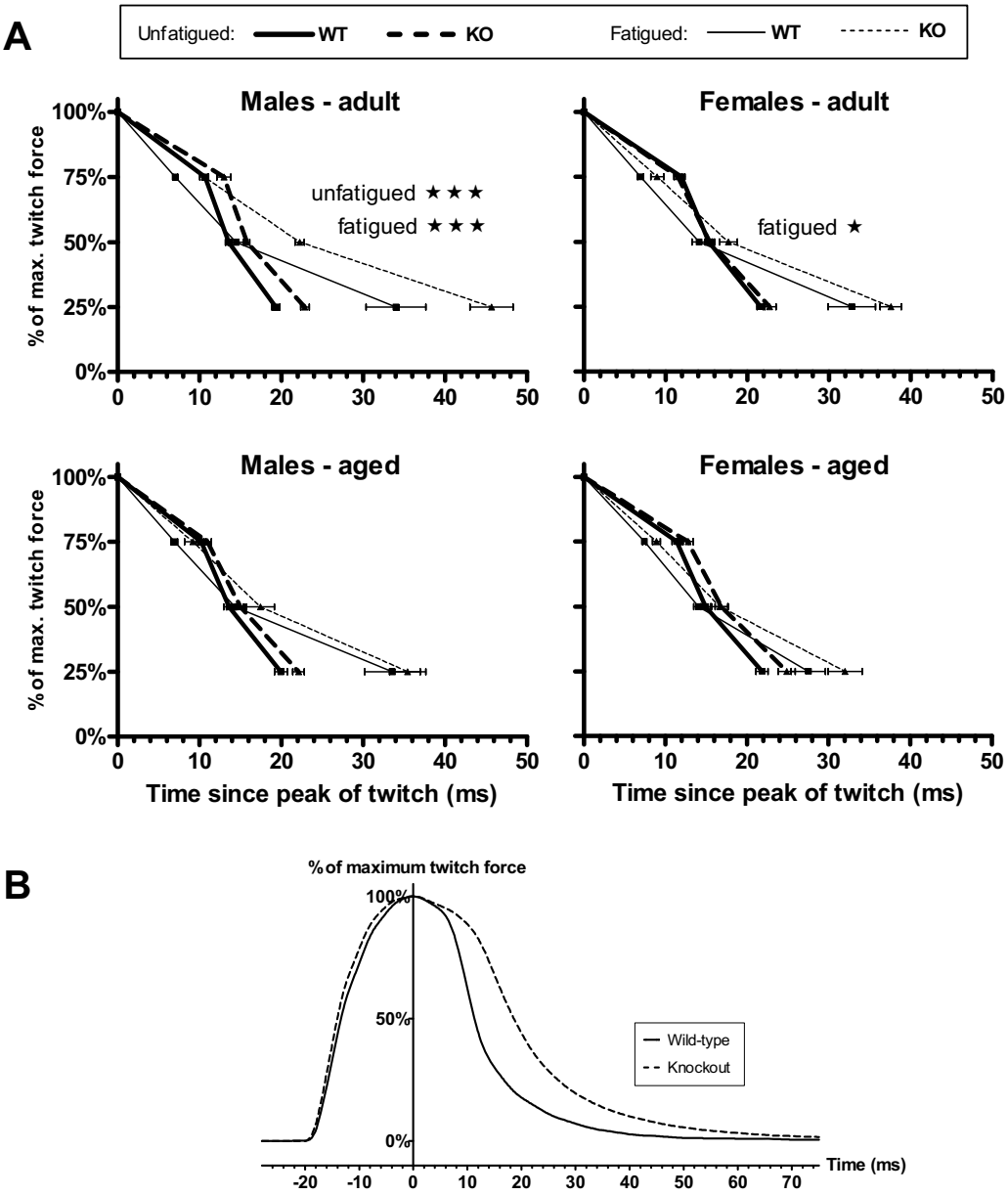

Figure 4.5. Twitch relaxation. The time course of relaxation during an isometric twitch is shown in **(A)** for each of the four age/gender groups. Twitch relaxation data from individual EDL muscles have been expressed as a percentage of peak twitch force and aggregated into single curves for each age group. Each line shows the time taken to relax to 75%, 50% and 25% of peak twitch force. The thicker lines show relaxation of unfatigued muscles. The thinner lines show relaxation of muscles that had just been subjected to a strenuous fatigue protocol. Full lines are for wild-types, dashed lines are for knockouts. In all cases except for unfatigued muscles from adult females, the curves for knockouts are shifted to the right of those for wild-types, suggesting a slowing of twitch relaxation in knockouts. This was statistically significant in unfatigued muscles from adult males, fatigued muscles from adult males and fatigued muscles from adult females (using half-relaxation time as a measure of relaxation rate). **(B)** shows an example of slowed relaxation in a twitch from a knockout EDL muscle (dashed line) compared to a twitch from a wild-type muscle (full line). Both muscles were from the adult male group. (Sample sizes – *for unfatigued muscles*: adult males – 17 WT, 22 KO; aged males – 11 WT, 9 KO; adult females – 13 WT, 10 KO; aged females – 5 WT, 6 KO; *for fatigued muscles*: adult males – 6 WT, 8 KO; aged males – 5 WT, 4 KO; adult females – 6 WT, 5 KO; aged females – 5 WT, 6 KO. ★★★ indicates $p<0.001$, ★ indicates $0.01<p<0.05$.)

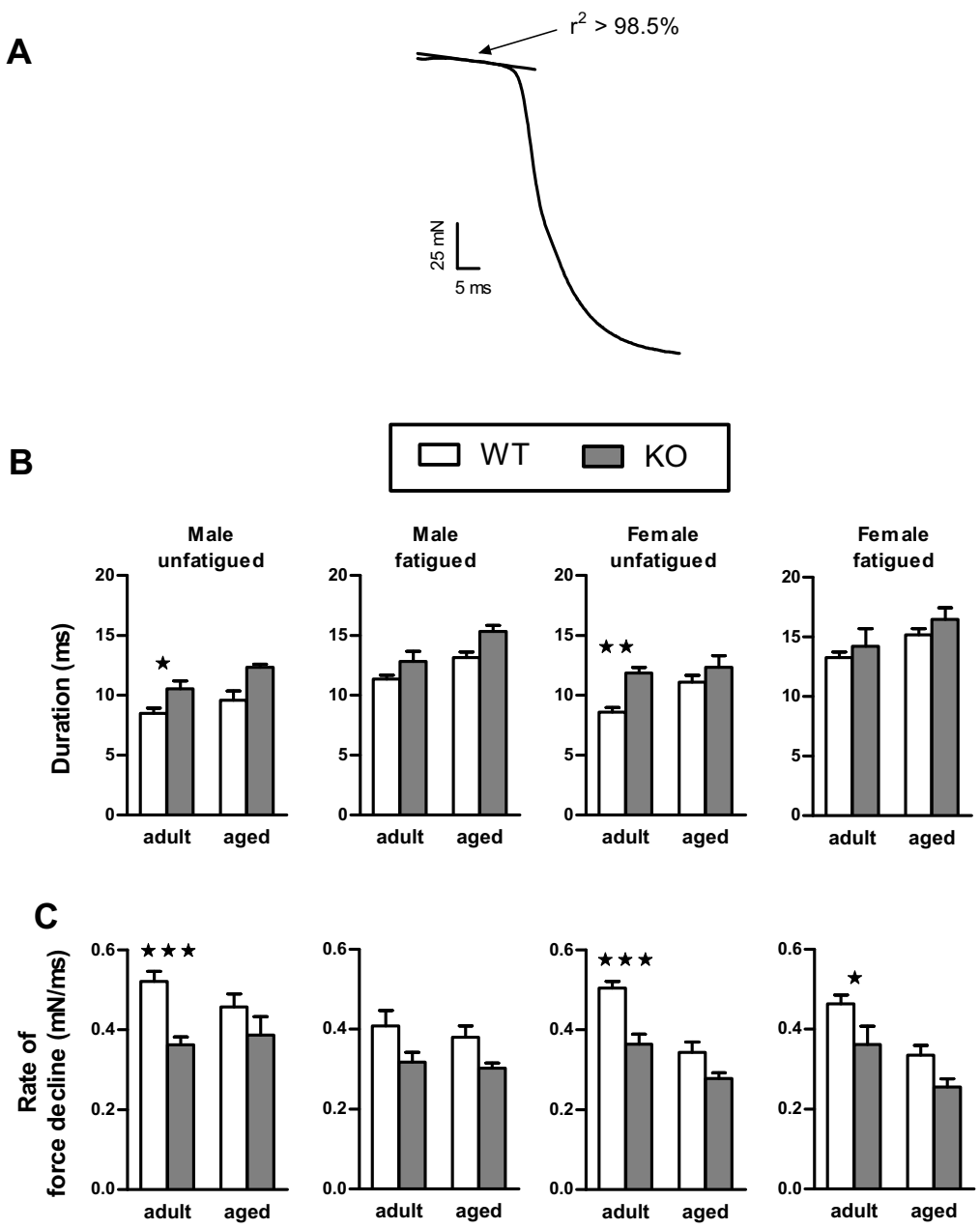

Figure 4.6. Tetanus relaxation. The two phases of relaxation following a tetanus are shown in **(A)**. We defined the initial linear phase to be that part of the curve where the r^2 value for linear regression was greater than 98.5% (see *Methods*). We measured the duration **(B)** and rate of force decline **(C)** of this linear phase. The duration of this linear phase is greater in knockouts than in wild-types and the rate of force decline is lower in knockouts than in wild-types, suggesting a slowing of relaxation in knockouts compared to wild-types following a tetanic contraction. Statistically significant differences between knockouts and wild-types are indicated. (Sample sizes – for unfatigued muscles: adult males – 6 WT, 8 KO; aged males – 4 WT, 3 KO; adult females – 6 WT, 5 KO; aged females – 6 WT, 6 KO; for fatigued muscles: adult males – 6 WT, 8 KO; aged males – 5 WT, 4 KO; adult females – 6 WT, 5 KO; aged females – 6 WT, 6 KO. ★★★ indicates $p<0.001$, ★★ indicates $0.001<p<0.01$, ★ indicates $0.01<p<0.05$.)

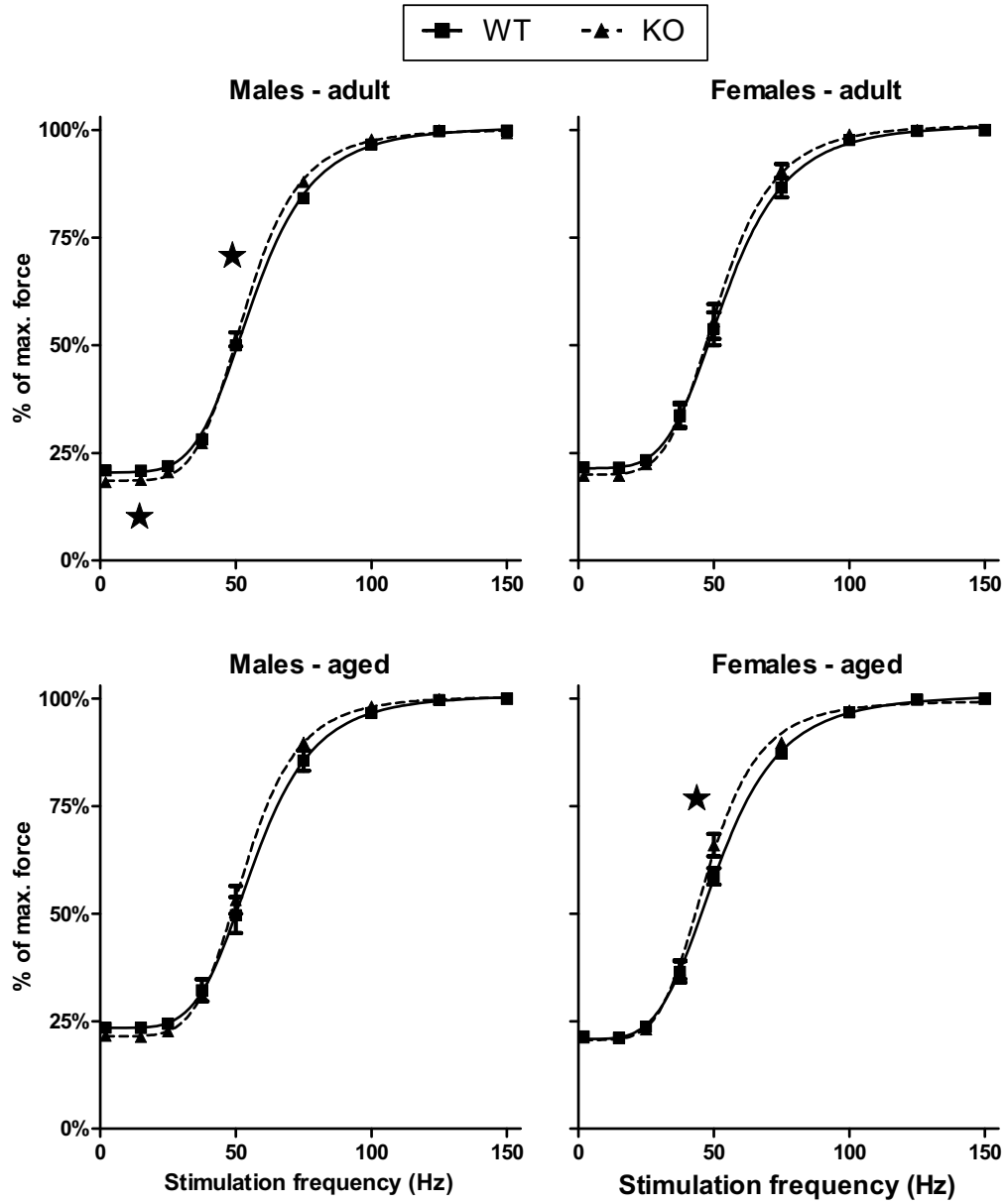

Figure 4.7. Force-frequency characteristics. Force-frequency data from individual EDL muscles have been aggregated to form single curves for each age/gender group. The curve for knockouts (dashed line) rises more steeply than the curve for wild-types (full line) in all age groups, indicative of a higher Hill coefficient in knockouts. The curve for knockouts starts at a lower level than the curve for wild-types in all groups except aged females, indicative of a lower twitch-to-tetanus ratio in knockout EDL muscles. However, these differences were not statistically significant in all cases. A star on the steep portion of the curve indicates a statistically significant difference in Hill coefficient and a star under the start of the curve indicates a significant difference in twitch-to-tetanus ratio. (Sample sizes: adult males – 11 WT, 14 KO; aged males – 6 WT, 4 KO; adult females – 7 WT, 5 KO; aged females – 6 WT, 6 KO. ★ indicates $0.01<p<0.05$.)

Discussion

Muscles lacking α-actinin-3 display a shift from fast-twitch towards slower-twitch characteristics (MacArthur *et al.*, 2008; Chan *et al.*, 2008). The location of α-actinin-3 within the Z-disc of fast-twitch muscle fibres, where it interacts with a multitude of structural, signalling and metabolic proteins (MacArthur & North, 2004; Frey *et al.*, 2008), suggests that at a subcellular level it may influence the properties which distinguish fast-twitch and slow-twitch fibres. At a subcellular level, two important factors which characterise a fibre as fast-twitch or slow-twitch are: (i) the properties of the contractile filaments; and (ii) the rate at which the sarcoplasmic reticulum (SR) resequesters the Ca^{2+} released during excitation (Bottinelli & Reggiani, 2000).

Hence our first aim in this study was to use the skinned fibre technique to examine whether there were any differences in these two factors between wild-types and knockouts which might contribute to the slower-twitch characteristics of *Actn3* knockout muscles. The skinned fibre technique has been widely used to characterise the properties of the contractile filaments and SR in skeletal muscle, and is the most sensitive probe with which to elucidate mechanisms at the level of contractile proteins and SR (Bakker *et al.*, 1998).

To examine the rate of Ca^{2+} uptake by the SR, we looked at the force responses generated by caffeine-induced Ca^{2+} release from the SR of mechanically skinned fibres following predetermined loading periods. This is an established technique for investigating Ca^{2+} uptake by the SR (Bakker *et al.*, 1998; Trinh & Lamb, 2006) and has the advantage of being able to directly probe SR re-uptake mechanisms in the absence of any sarcoplasmic contents or differing phosphorylation levels which could confound the investigation of the basic mechanisms of SR Ca^{2+} uptake. Our major finding from these studies was that the SR in knockout fibres loads Ca^{2+} more slowly than the SR in wild-type fibres. For any particular duration of loading, the amount of Ca^{2+} loaded by the SR, expressed as a percentage of the maximum amount it could load, was lower in knockout fibres than in wild-types (Figure 4.1(B)).

This alteration in SR Ca^{2+} uptake is evidence of a shift at a subcellular level towards slower-twitch characteristics in the absence of α-actinin-3. It is well established that the uptake of Ca^{2+} by the SR is considerably slower in slow-twitch than in fast-twitch fibres. This is due to slow-twitch fibres having a smaller surface area of SR membrane and a two- to threefold lower density of Ca^{2+}-ATPase pumps in the SR membrane (Pette & Staron, 1990). In addition, the maximum Ca^{2+} capacity of the SR in slow-twitch fibres is only about one-third of that in fast-twitch fibres, due to smaller amounts of calsequestrin being available to buffer

rises in [Ca^{2+}] (Fryer & Stephenson, 1996). This inhibits the ability of the Ca^{2+}-ATPase to pump Ca^{2+} back into the SR lumen (Fryer & Stephenson, 1996). It is possible that factors such as these underlie the slower Ca^{2+} uptake by the SR in *Actn3* knockout fibres, and that α-actinin-3 deficiency may be associated with smaller SR membrane surface area, lower Ca^{2+}-ATPase pump density, or lower SR Ca^{2+} capacity and calsequestrin levels. It should also be noted that an increased rate of Ca^{2+} leakage from the SR would also reduce the rate of Ca^{2+} loading (Bakker *et al.*, 1998), and we cannot rule out the possibility that Ca^{2+} leakage is increased in the SR of knockout fibres.

Trinh & Lamb (2006), in a study on the properties of the SR, found that fast fibers from the rat took a comparatively long time (approximately 25-90 s) to reload the SR to half-maximum capacity. Our fast fibers loaded significantly faster (approximately 2-5 s to reach 50%, see Fig.1*B*), which is most likely a reflection of the different [Ca^{2+}] in the loading solutions. Our loading solution contained 50 mM EGTA, compared with 1mM EGTA in the loading solution used by these other investigators. While the low [EGTA] used by Trinh & Lamb was useful in indicating the maximum absolute Ca^{2+} capacity of the SR, our high [EGTA] loading solution was designed to measure the rate at which the SR could pump Ca^{2+}.

The characterisation of a fibre as fast-twitch or slow-twitch is also influenced by the properties of the contractile filaments. To investigate the effects of α-actinin-3 deficiency on the properties of the contractile filaments, we chemically skinned the fibres following the SR loading experiments and exposed them to solutions of varying [Ca^{2+}] and [Sr^{2+}] to generate force-pCa and force-pSr curves. The value of pCa_{50}-pSr_{50} was virtually identical in knockouts and wild-types (Figure 4.2(C)), suggesting an absence of any gross shift in myosin heavy chain isoform composition in α-actinin-3-deficient fibres. This result is consistent with our earlier immunohistochemical studies which showed that the proportions of fibres staining for fast or slow MHC isoforms was virtually the same in EDL muscles of wild-type and knockout mice (MacArthur *et al.*, 2008).

The force-pCa and force-pSr curves were steeper for knockouts than for wild-types, as indicated by the higher n_{Ca} and n_{Sr} values in knockout fibres (Figure 4.2(C)). The n_{Ca} and n_{Sr} values are indicators of the degree of cooperativity between subunits of the thick and thin filaments in producing tension (Moss *et al.*, 1995), and suggest that there is a greater cooperativity of the contractile filaments in the absence of α-actinin-3. Cooperativity is influenced by the particular isoforms of the myofibrillar proteins expressed by a fibre. These proteins include troponin C, troponin T, tropomyosin and myosin light chain (Moss *et al.*, 1995; Bortolotto *et al.*, 2000). It is possible that absence of α-actinin-3 could alter the isoforms of

these proteins that are expressed by a fibre, thus affecting cooperativity, but this would need to be examined in future studies by direct analysis of the isoforms by Western blot.

Actin-myosin crossbridge interactions can also influence cooperativity (Bottinelli & Reggiani, 2000). The binding of myosin heads to actin facilitates further binding and stabilises the thin filament in a state of higher Ca^{2+} sensitivity (Bottinelli & Reggiani, 2000). This is relevant to our finding that knockout fibres exhibited myofibrillar oscillations of a higher frequency than those in wild-type fibres when submaximally stimulated by Ca^{2+} and Sr^{2+} (Figure 4.3(B)). Myofibrillar oscillations are a reflection of crossbridge interactions; the higher frequency in knockout fibres could be explained if the properties of myosin had changed in such a way that either the rate of detachment of the myosin heads had increased or the rate of attachment had increased (Smith & Stephenson, 2009). The altered myosin-actin interaction suggested by the change in frequency of myofibrillar oscillations could be a factor contributing to the altered cooperativity observed in *Actn3* knockout fibres.

The *Actn3* knockout mouse is a newly generated model of α-actinin-3 deficiency (MacArthur *et al.*, 2007), so it is important to characterise the contractile properties of whole fast-twitch muscle from this mouse model. This has so far been done only in an adult male cohort of mice (Chan *et al.*, 2008), and it is not known whether these properties vary with age and gender. This information would be a valuable database for future studies into the mechanisms which produce the altered muscle characteristics of *Actn3* knockout fast-twitch muscle. Hence our second aim in this study was to examine the contractile properties of whole *Actn3* knockout EDL muscle from males and females in two age groups: adult (2 to 6 months old) and aged (19 to 22 months old).

In the muscles of adult males and adult females, we found a significant slowing of relaxation in *Actn3* knockouts for both a twitch (Figure 4.5(A)) and a tetanus (Figure 4.6(A) and (B)). In light of our skinned fibre results, this is most likely due to the slower uptake of Ca^{2+} by the SR in α-actinin-3-deficient fibres. Another contributing factor could be the slower kinetics of dissociation of Ca^{2+} from the contractile filaments that we found in α-actinin-3-deficient fibres. The effect of a steeper force-pCa curve in *Actn3* knockout fibres is more difficult to interpret. A steeper curve should in fact cause faster relaxation because a given drop in $[Ca^{2+}]$ will be accompanied by a larger drop in force. The fact that relaxation is actually slower in knockout muscles suggests that the effect of slower Ca^{2+} uptake by the SR outweighs the effect of a steeper force-pCa relationship. Another factor which could contribute to the slowing of twitch and tetanus relaxation is a reduction in the levels of myoplasmic Ca^{2+} buffers such as parvalbumin (Stephenson *et al.*, 1998). Our skinned fibre experiments were designed to specifically investigate the properties of the contractile proteins and SR, without the

confounding effects of factors such as parvalbumin which would be present in an intact fibre preparation. Hence, in addition to the contractile protein and SR properties which we have examined in the current study, it must be noted that if there is a slight reduction in parvalbumin levels in α-actinin-3-deficient fibres this would also contribute to slower relaxation times and we cannot rule out a contribution from this source.

We also found changes in the force-frequency curves of whole *Actn3* knockout EDL muscles (Figure 4.7). In adult males and aged females the force-frequency curves were significantly steeper for knockouts than for wild-types. This parallels the steeper force-pCa and force-pSr curves of *Actn3* knockout fibres, and in the same way could reflect a greater cooperativity of the contractile proteins in producing tension. It may also be a consequence of longer twitch relaxation times in knockout muscles; all other factors being equal, longer relaxation times would lead to twitch summation at earlier frequencies of stimulation and a steeper force-frequency relationship. We also found that the twitch-to-tetanus ratio of knockout muscles was significantly lower than wild-types in adult males. This is consistent with a shift towards slower-twitch properties in α-actinin-3-deficient muscle as slow-twitch motor units have lower twitch-to-tetanus ratios than fast-twitch motor units (Burke *et al.*, 1973).

The mass and cross-sectional areas of whole *Actn3* knockout EDL muscles also show a shift towards slow-twitch characteristics. Slow-twitch fibres have smaller cross-sectional areas than fast-twitch fibres (Hamalainen & Pette, 1993; MacArthur *et al.*, 2008), and we have shown that there is in fact a reduction in fast-fibre diameter in muscles from the *Actn3* knockout mouse (MacArthur *et al.*, 2008). This would explain the significantly smaller cross-sectional areas of *Actn3* knockout EDL muscles from adult males and adult females.

Overall there was little difference between males and females in the effects of α-actinin-3 deficiency on whole EDL muscle. Changes in mass, cross-sectional area, twitch relaxation, tetanus relaxation and force-frequency characteristics in the absence of α-actinin-3 were found in both males and females. However, there is some reduction in the effects of α-actinin-3 deficiency with age. There has been a shift in the whole muscle phenotype of the *Actn3* knockout mouse with age, with statistically significant differences found in adult animals no longer being found in aged animals. The reduction in the effect of α-actinin-3 deficiency as the animal ages could be due to the fact that motor units within a muscle undergo significant remodelling with age, with a marked reduction in the number of fast fatiguable motor units (Kadhiresan *et al.*, 1996). These motor units are comprised of fast glycolytic fibres, which is the type of fibre in which α-actinin-3 is expressed. Loss of these fibres as the animal ages means that the effects of α-actinin-3 deficiency would become less pronounced over time.

In conclusion, our data provide further insight into the mechanisms underlying changes in skeletal muscle performance associated with α-actinin-3 deficiency. Our skinned fibre data show that a slowing of Ca^{2+} re-uptake by the sarcoplasmic reticulum in α-actinin-3-deficient fibres is one factor contributing to the slower relaxation of whole knockout muscles following both a twitch and a tetanus. In whole knockout EDL muscle, we found changes in mass, cross-sectional area, twitch relaxation, tetanus relaxation and force-frequency characteristics that are consistent with a shift towards a slower-twitch profile in fast-twitch muscles lacking α-actinin-3. There is a clear amelioration of the *Actn3* knockout phenotype with age. In contrast, gender did not affect the *Actn3* knockout phenotype. These changes to the properties of fast glycolytic muscle fibres and fast-twitch muscle would be detrimental to sprint and power activities as has been observed in both athlete and non-athlete human cohorts.

Author contributions

S.C., K.N.N. and S.I.H. designed the experiments and wrote the paper; S.C. and S.I.H. performed the experiments and analysed the data; J.T.S., P.J.H. and N.Y. developed and maintained the *Actn3* knockout mice and critically evaluated the manuscript.

Acknowledgements

We acknowledge Ms M. B. Arber for her expert technical assistance and for analysing the skinned fibre data. We thank Professor George Stephenson for his evaluation of the oscillations obtained in the skinned fibre study.

Appendix to Paper C

To complete the whole muscle phenotype of the *Actn3* knockout mouse reported in *Paper C*, two further results will be presented in this Appendix. These are the maximum force and the response to fatiguing stimulation. These results were obtained as part of the experiments in *Paper C*, but they are intended to be published in another forthcoming paper.

Methods

Maximum force was taken to be the P_{max} of the fitted force-frequency curve. For the derivation of the force-frequency curve, please refer to "Force-frequency characteristics" in the *Methods* section of *Paper C*. For examination of response to fatiguing stimulation, muscles were given a one-second, 100-Hz tetanus every 2 seconds over a period of 30 seconds. Muscles were then allowed to recover for a period of 30 minutes, during which force recovery was monitored with a brief (250 ms) 100-Hz tetanus every 5 minutes.

Results – maximum forces

Maximum forces are presented in **Figure 4.8** below. Both absolute force and specific force (corrected for cross-sectional area) are shown. There were no significant differences between wild-types and knockouts in aged males, adult females and aged females, but in adult male mice, knockout EDL muscles generated 7% less absolute force than wild-type muscles. However, because of the smaller cross-sectional area of the knockout muscles (Figure 4.4),

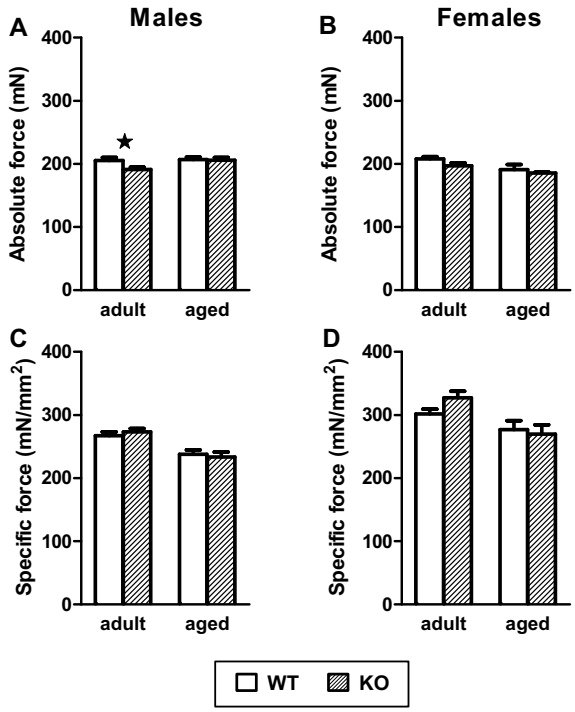

Figure 4.8 Maximum force generation. Absolute force is shown in **(A)** for males and **(B)** for females. Specific force is shown in **(C)** for males and **(D)** for females. In adult males, knockout EDL muscles generated significantly less absolute force than wild-types. No other differences were found between wild-types and knockouts in other age/gender groups. (Sample sizes:adult males – 17 WT, 22 KO; aged males – 11 WT, 9 KO; adult females – 13 WT, 10 KO; aged females – 6 WT, 6 KO. ★ indicates $0.01<p<0.05$.)

there was no significant difference in specific force in adult males.

This reduction in absolute force in *Actn3* knockout muscle from adult males is another example of a shift towards slower-twitch characteristics when α-actinin-3 is lost, as slow-twitch fibres generate less force than fast-twitch fibres. It should be noted that in *Paper B*, knockout muscles from adult male mice also showed lower absolute forces than wild-type muscles, but this difference was not statistically significant (see Table 3.1, p.53). The result presented here in this appendix was statistically significant, most likely because a larger sample of muscles was used (17 WT, 22 KO compared with 8 WT, 10 KO in *Paper B*).

These results also illustrate a diminishing effect of α-actinin-3 deficiency with age, as observed in other contractile characteristics. The reduction in absolute force was only observed in the adult males, and not in the aged male or aged female mice.

Results – fatigue

EDL muscles were subjected to a strenuous fatigue protocol as described above. The decline in force over the 30-second fatigue protocol, and the subsequent recovery over 30 minutes, are depicted in **Figure 4.9** for each of the four groups of muscles. At the end of the 30-second fatigue protocol, there was no significant difference between wild-types and knockouts in the amount of force decline, both having lost about 50% of their original force. However, over the 30 minute recovery period, the graphs show that knockouts recover more quickly than wild-types in all four groups of muscles. After 30 minutes' recovery, the force produced by the muscles as a percentage of their pre-fatigue force was greater in knockouts than in wild-types, and this difference was statistically significant in all groups. In muscles from adult males, knockouts were producing 7.7% more of their pre-fatigue force than wild-types after 30 minutes' recovery. In aged males the difference was 8.6%, in adult females the difference was 12.4%, and in aged females the difference was 9.5%. These results indicate that α-actinin-3 deficiency is associated with improved recovery from fatigue.

Slow-twitch fibres recover more quickly from fatigue than fast-twitch fibres due to their greater use of oxidative metabolism (Brooks, 2003). Hence these results are further evidence that fast-twitch, glycolytic fibres shift towards slower-twitch, more oxidative characteristics in the absence of α-actinin-3. They are consistent with enzyme assays showing that *Actn3* knockout muscles have a reduced activity of enzymes involved in anaerobic glycolysis, and an increased activity of enzymes involved in oxidative metabolism (MacArthur *et al.*, 2007; MacArthur *et al.*, 2008).

In one respect, however, these results for fatiguing stimulation differ from the other aspects of the *Actn3* knockout phenotype described in *Paper C*. These results show that in the

case of recovery from fatigue, the effects of α-actinin-3 deficiency persist with age. Statistically significant improvements in fatigue recovery were found in the knockout muscles of both adult and aged animals, whereas with most other aspects of the *Actn3* knockout phenotype, statistically significant differences were only found in adult animals.

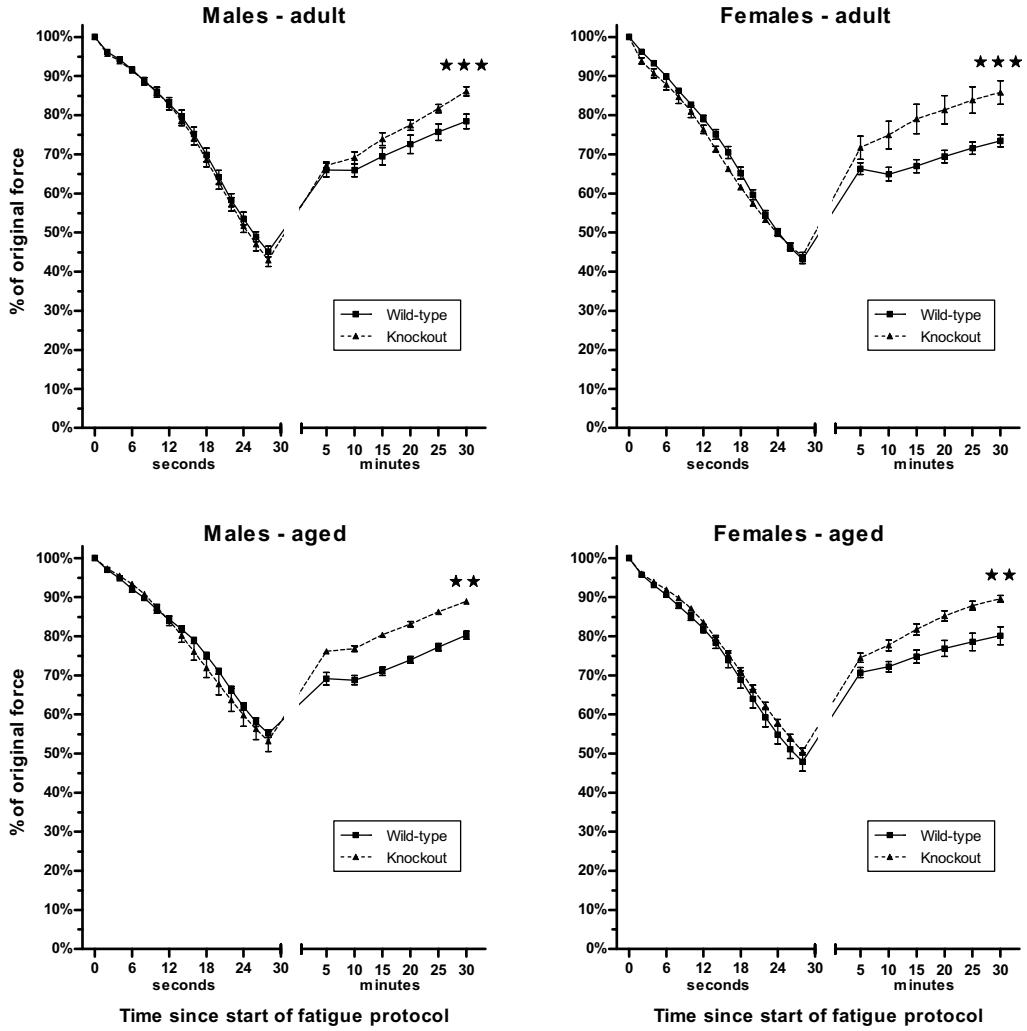

Figure 4.9 Fatigue. Muscles were subjected to a strenuous fatigue protocol of repeated 100-Hz tetani over 30 seconds. The left part of each graph shows the decline in force with each tetanus over this 30-second period, while the right part of each graph shows the recovery in force over 30 minutes. At the end of the 30-minute recovery period, knockout EDL muscles had recovered significantly more of their pre-fatigue force than wild-types in all age/gender groups. (Sample sizes: adult males – 6 WT, 8 KO; aged males – 5 WT, 4 KO; adult females – 6 WT, 5 KO; aged females – 6 WT, 6 KO. ★★★ indicates $p<0.001$, ★★ indicates $0.001<p<0.01$.)

Conclusion

In the Introduction, the aims of this thesis were stated as a series of four questions. Here I shall summarise the main findings in regards to these four questions.

1. Are dystrophin-deficient fibres more susceptible to contraction-induced injury because dystrophin is absent, or is it also because these fibres have an abnormal branched morphology?

Contraction-induced damage in *mdx* EDL muscle increases as the extent of fibre branching increases (*Paper A*). Younger dystrophin-deficient EDL muscle containing only a moderate proportion of branched fibres (17%, Figure 2.6, p.38) showed force deficits that were no different from control muscles following an eccentric contraction protocol of 15% strain (Figure 2.5(A), p.36). This shows that dystrophin deficiency in itself does not necessarily render a muscle more susceptible to contraction-induced damage. However, in older dystrophin-deficient EDL muscles containing a high proportion of branched fibres (89%, Figure 2.6, p.38), force deficits were more than twice as large as those in control muscles (Figure 2.5(A), p.36). Moreover, the branching patterns in these muscle fibres were much more complex than those observed in the fibres of younger animals (Figure 2.7 and Figure 2.8, p.39).

These results suggest that fibre branching makes an important contribution to the damage seen in dystrophin-deficient muscle following eccentric contractions. Branch points may represent foci of structural weakness, and indeed it has been shown in another dystrophic mouse model that fibres with branches are more liable to be damaged during contraction than fibres without branches (Head *et al.*, 1990). Using an approach based on the fibre examination methodology of *Paper A*, Lovering *et al.* (2009) also found an increase in fibre branching with age. They observed that 6% of EDL muscle fibres from 6 to 9 week-old *mdx* mice were branched, with this proportion rising to 65% in 32 to 38 week-old *mdx* mice. Furthermore, they found that osmotic stress-induced Ca^{2+} spark activity was increased at the branch points, indicating that these points are more sensitive to mechanical stress than other parts of the fibre.

The finding in *Paper A* of an association between *mdx* muscle damage and fibre branching has important implications for the understanding of the pathogenesis of Duchenne muscular dystrophy (DMD). The previous studies listed in Table 2.1 (p.28) have traditionally been interpreted as evidence for the structural hypothesis of dystrophin function. However, this interpretation does not take into account the contribution made by fibre branching to the force deficits in *mdx* muscle. The results of this thesis suggest that fibre deformity, as well as the loss of the functions normally performed by dystrophin, are both contributing factors in the pathogenesis of muscle degeneration in DMD.

Figure 5.1 is an attempt to represent the distinction between these two factors. The immediate consequences of losing dystrophin's normal functions might be referred to for simplicity as a "primary stage" in which the loss of dystrophin initiates muscle damage, in the absence of any pre-existing fibre deformity. The various hypotheses regarding dystrophin's function are hypotheses about the steps that occur in this primary stage and, as the diagram shows, the main theories are the "structural" and "ion channel" hypotheses.

Whatever these initial steps may be, they ultimately lead to muscle degeneration. Attempts at regeneration result in the formation of branched fibres (Schmalbruch, 1984). As shown in *Paper A*, these deformed fibres are susceptible to contraction-induced damage, so muscle contraction leads to further degeneration. This cycle of muscle damage might be referred to for simplicity as a "secondary stage", in which muscle degeneration is perpetuated by contraction-induced damage to structurally weak branched fibres.

Any study that uses *mdx* muscle with a significant proportion of branched fibres would really be examining the secondary stage of this process. To understand the direct function of dystrophin, it is necessary to look at the primary stage, using *mdx* muscle in which fibre branching is minimal. The studies in Table 2.1 (p.28) which found increased force deficits in *mdx* muscle all used mice that were older than the 6 to 8 week-old mice used in *Paper A*. Given that 17% of fibres are already branched at 6 to 8 weeks of age, it is likely that the *mdx* muscles in these other studies contained a significant proportion of branched fibres. Hence they may not have been examining the direct consequences of dystrophin deficiency. This thesis has shown that in order to understand the direct functions of dystrophin, it is most useful to examine *mdx* muscle before it develops significant branching morphology.

Other considerations

(i) The correlation between fibre branching and force deficit

While the results of *Paper A* show a clear correlation between the extent of fibre branching and the size of the force deficit following eccentric contractions, two points may be raised in regards to this correlation. Firstly, in younger *mdx* muscles where 17% of fibres were branched, the force deficit was less than 10%, while in older control muscles where none of the fibres were branched, the force deficit was actually higher (around 25%) (Figure 2.5(A), p.36). Secondly, in the study by Head *et al.*, (1992), both EDL and soleus muscles contained about 90% branched fibres, yet only the EDL muscles showed a loss of force following eccentric contractions. These two points appear to argue against a correlation between fibre branching and force deficits. However, these arguments do not take into account the confounding effects of age and muscle type on a muscle's susceptibility to eccentric damage.

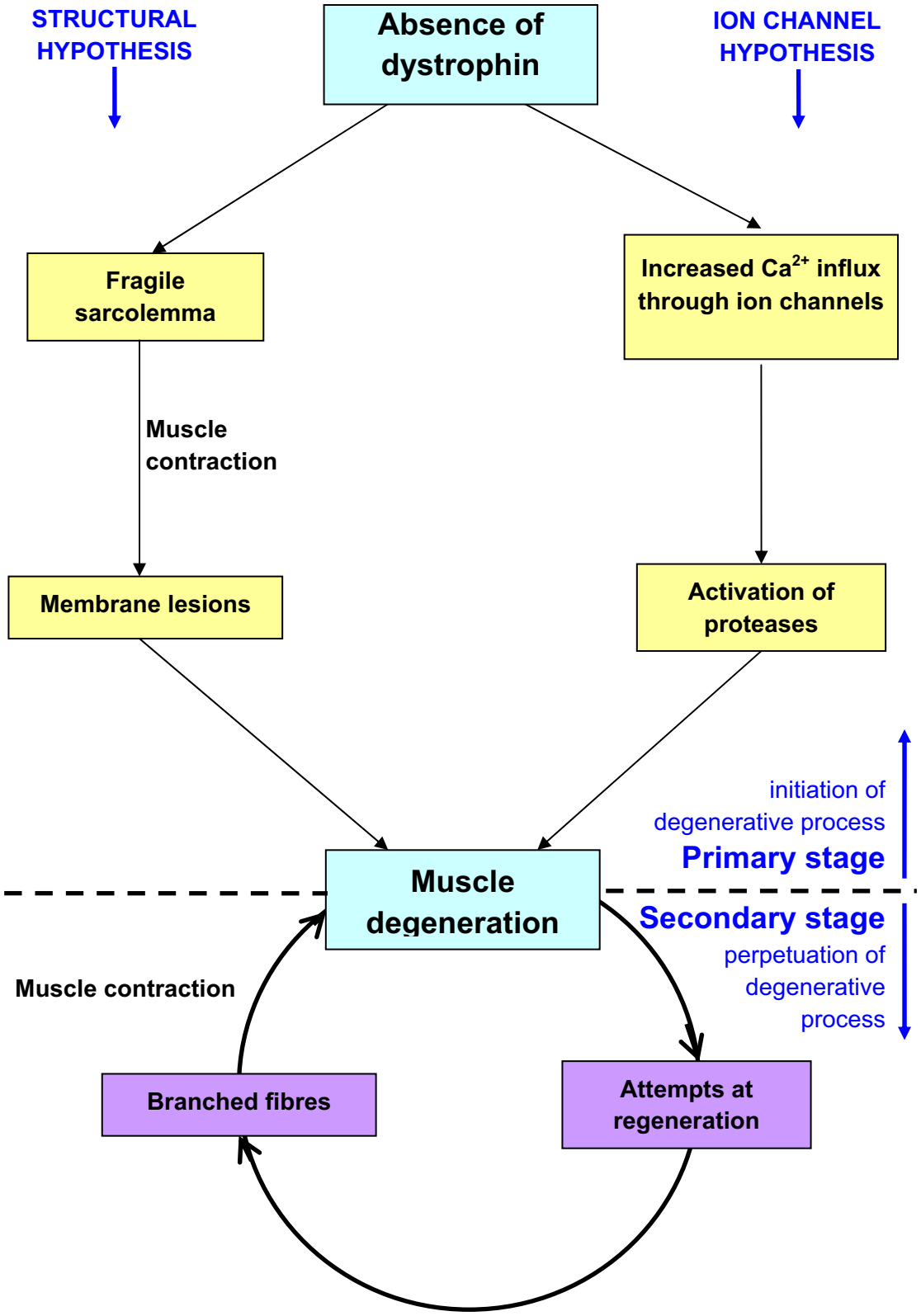

Figure 5.1 Importance of distinguishing between primary and secondary factors in the pathogenesis of DMD. To determine the direct function of dystrophin it is important to examine muscles before they develop significant branching deformities, otherwise it is difficult to tell whether the damage is due to the absence of dystrophin, or to the structurally weak branched fibres.

In regards to the first point, it is questionable whether a muscle with 17% branched fibres should be significantly more prone to eccentric injury than a muscle with no branched fibres. In a study on a laminin-deficient model of muscular dystrophy, Head *et al.*, (2004) found that dystrophic EDL muscles with 34% branched fibres were no more susceptible to eccentric damage than control muscles containing no branched fibres. This suggests that there may be a threshold level of fibre branching at which the proportion of branched fibres becomes large enough to increase a muscle's vulnerability to eccentric damage. Below this threshold, it is possible that there are sufficient numbers of unbranched fibres to support the minority of branched fibres during eccentric contractions (Head *et al.*, 2004). Hence the moderate extent of fibre branching in the younger *mdx* muscles in *Paper A* does not necessarily mean these muscles should have a higher force deficit than the older control muscles.

In fact, the older control muscles had a higher force deficit than the younger *mdx* muscles. This is most likely due to the difference in age between the muscles. It is well established that force deficits following eccentric contractions increase with age (Brooks & Faulkner, 1996; Rader & Faulkner, 2006; Faulkner *et al.*, 2007; Lynch *et al.*, 2008). One possible reason is suggested by our finding that the muscles of older mice were stiffer than those of younger mice (Figure 2.9, p.40) and therefore less capable of absorbing the strain of contraction. However, it is acknowledged that our measure of stiffness is only an indicator and does not distinguish between the stiffness of contractile proteins and non-contractile proteins. Another reason could be that with a slowing of protein turnover with age, "weaker" sarcomeres appear alongside "stronger" ones, and this inhomogeneity of sarcomere strength renders a muscle fibre more susceptible to eccentric injury (Brooks & Faulkner, 1996).

Our study in *Paper A* was designed to exclude the confounding effect of age on the correlation between fibre branching and force deficits. Older *mdx* muscles experienced greater force deficits than younger *mdx* muscles. The difference in force deficit was about 50% (see Figure 2.5(A), p.36). One component of this difference would be attributable to age-related factors such as increasing stiffness and sarcomere inhomogeneity. The difference in force deficit between younger and older control muscles (about 25%; see Figure 2.5(A), p.36) gives an indication of the size of this component. The remaining component (about 25%) must then be due to other differences between younger and older *mdx* muscles. We have shown that the extent of fibre branching is one major point of difference, and thus there is a clear correlation between the degree of fibre branching and the size of the force deficit following eccentric contractions.

In regards to the second point, namely the lack of damage observed in soleus muscle in the study by Head *et al.* (1992), it has been widely reported that fast glycolytic fibres are the fibre type that is most prone to eccentric injury (see Proske & Morgan (2001) for review). Interestingly, they are also the first population of fibres to become necrotic in DMD (Webster *et al.*, 1988). The particular susceptibility of fast glycolytic fibres to eccentric injury could be because this fibre type has the largest diameter, so that it is subject to the largest shear stresses during eccentric contractions (Karpati *et al.*, 1988). Fast glycolytic fibres are absent from soleus muscle but form a significant proportion of the fibres in the EDL muscle (Anderson *et al.*, 1988), so on this basis alone one would expect soleus muscle to be more resistant to eccentric damage than EDL muscle. Hence the observation by Head *et al.* (1992) of lower force deficits in soleus muscle compared with EDL muscle, despite both having similar degrees of fibre branching, does not necessarily discount a correlation between fibre branching and force deficits, but may rather reflect the significant differences in fibre type composition between the two muscles.

(ii) Period of acute myonecrosis in mdx mice

Despite the relatively young age of the younger mice in *Paper A* (6 to 8 weeks), this still falls outside the period of severe muscle necrosis that occurs early in the life of *mdx* mice. Starting at around 21 days in hindlimb muscles, there is an abrupt onset of myonecrosis that affects up to 80% of muscle fibres and stimulates muscle regeneration (Grounds *et al.*, 2008). Necrosis peaks at 25-26 days, then decreases significantly to stabilise by 6 to 8 weeks of age at a low level of active necrosis (and regeneration) that continues throughout life (Grounds *et al.*, 2008). Hence the mice in our study were at the earliest age at which the degenerative-regenerative process in *mdx* muscle reaches a stable level. By using mice of this age, we attempted to minimise the extent of fibre branching, but also ensured that the necrotic-regenerative process was occurring at the same rate as in the older mice in the study. Hence the interpretation of our findings should not be complicated by variations in the level of underlying necrosis between the muscles of younger and older mice.

(iii) Eccentric strain imposed on younger and older muscles in the study

The optimum length of muscles from older *mdx* mice was longer than the muscles from younger *mdx* mice (Figure 2.3, p.34). The muscles were stretched at a velocity of 1 mm/s during the eccentric contraction protocol. This equates to a velocity of 0.21 fibre lengths per second in younger *mdx* muscles and 0.18 fibre lengths per second in older *mdx* muscles (using the fibre length to muscle length ratio of 0.44 as reported by McCully & Faulkner (1986)). Muscle damage following eccentric contractions has been shown to increase with increasing

velocity of stretch, when velocity is measured in terms of fibre lengths per second (McCully & Faulkner, 1986). Hence it is possible that our eccentric contraction protocol was not imposing equivalent strains on the older muscles and the younger muscles. However this is unlikely to have significantly affected our results. In fact, if we had we used the same velocity (in fibre lengths per second) for older muscles as for younger ones, and hence subjected the older muscles to a more severe strain than in the current study, it is likely that we would have observed even larger force deficits in the older *mdx* muscles.

2. Does α-actinin-3 deficiency result in a greater susceptibility to contraction-induced injury?

α-Actinin-3 deficiency did not appear to result in a greater susceptibility to contraction-induced injury. Force deficits in *Actn3* knockout mouse EDL muscle following eccentric contractions of large (20%) strain were no different from controls (Figure 3.3(A), p.55). The stiffness of *Actn3* knockout EDL muscles was no different from controls (Figure 3.4, p.56). In *Actn3* knockout EDL muscle there was very little evidence of the fibre branching that occurs in muscles undergoing repetitive mechanical injury, as in *mdx* muscles (Figure 3.5, p.57).

These results do not support the hypothesis that α-actinin-3 plays a structural role in stabilising the sarcomere during contractile activity, and suggests that the association of the ACTN3 gene with enhanced sprinting performance may not be due to α-actinin-3 providing greater structural integrity to muscle fibres during intense contractile stress.

However, these results do not completely rule out a role for α-actinin-3 in providing mechanical stability to sarcomeres. Fibres deficient in α-actinin-3 have reduced diameters compared with fibres in wild-type animals (MacArthur *et al.*, 2008), and since smaller-diameter fibres are subject to smaller shear stresses during contraction (Karpati *et al.*, 1988), this may have protected *Actn3* knockout fibres from any loss of mechanical stability resulting from the absence of α-actinin-3. Moreover, it is possible that α-actinin-3 does have a structural function, but that it is not a unique function, and can be performed by α-actinin-2 when α-actinin-3 is absent, since *Actn3* knockout muscle shows an upregulation of α-actinin-2 (MacArthur *et al.*, 2007).

Since the reduced fibre diameters may complicate the interpretation of the results from our eccentric contraction studies, it would be useful in future studies to examine the possible structural role of α-actinin-3 using other methods. Because the α-actinins are the major protein component of the Z-disc, and one of the many functions of the Z-disc is to transmit mechanical forces within the myofibril (Frank *et al.*, 2006), changes in the properties of the Z-disc in the absence of α-actinin-3 may suggest that α-actinin-3 has some mechanical

role within the myofibril. One method would be to examine the change in passive tension when the muscle is passively stretched by a certain length. If there is a difference between the muscles of wild-type and *Actn3* knockout mice, this would suggest that there are differences in the properties of the titin filament, and since the titin filament is anchored to the Z-disc (Luther, 2009), this may suggest changes in Z-disc compliance in the absence of α-actinin-3.

Another property that could be examined is the width of the Z-disc. The Z-disc has a precisely defined width that varies between fibre types. Fast fibres have narrow Z-discs (~30 to 50 nm wide) while slow fibres have wider ones (~100 to 140 nm wide), with the difference mainly due to differing numbers of α-actinin layers (Luther, 2009). As Z-disc width is likely to affect the mechanical properties of the sarcomere, a change in the Z-disc width in fast fibres lacking α-actinin-3 could suggest a possible structural role for this protein.

3. What is the phenotype of α-actinin-3 deficient muscle, and do any aspects of this phenotype suggest a shift from fast-twitch towards slower-twitch characteristics?

This thesis has characterised the phenotype of whole EDL muscle from the *Actn3* knockout mouse, a newly generated model of α-actinin-3 deficiency. This phenotype offers important insights into the possible mechanisms underlying the reduced sprinting performance, and enhanced endurance performance, of α-actinin-3-deficient athletes.

Table 5.1 is a summary of the statistically significant differences found between *Actn3* knockout (KO) muscles and wild-type muscles, divided into the four age/gender groups studied (male or female, adult or aged). *Actn3* knockout muscles showed smaller mass and cross-sectional area, lower absolute force production, and slower relaxation of twitch and tetanus than control muscles. Such changes would be detrimental to performance in activities requiring power and rapid contraction and relaxation of muscle. On the other hand, *Actn3* knockout muscles displayed better fatigue recovery than control muscles, and this would benefit performance in endurance activities. The whole muscle phenotype of the *Actn3* knockout mouse thus shows the changes occurring at muscle level to bring about the observed effects of α-actinin-3 deficiency on athletic performance.

Also shown in the last column are the differences that would normally be found in these characteristics between fast-twitch (FT) and slow-twitch (ST) fibres. In all characteristics except for the force-frequency Hill coefficient, the difference between knockout and wild-type muscles is in the same direction as the difference between slow-twitch and fast-twitch fibres. This strongly suggests that loss of α-actinin-3 from fast-twitch fibres results in a shift towards a

Characteristic	Males		Females		Reference	Difference between FT and ST
	Adult (2-6 mth)	**Aged** (19-22 mth)	**Adult** (2-6 mth)	**Aged** (19-22 mth)		
Muscle mass	lower in KO		lower in KO		Table 3.1 (p.53); Figure 4.4 (p.81)	lower in ST[1,2]
Muscle cross-sectional area	smaller in KO		smaller in KO		Table 3.1 (p.53); Figure 4.4 (p.81)	smaller in ST[1,2]
Maximum absolute force	lower in KO				Figure 4.8 (p.93)	lower in ST[1,2,3]
Twitch relaxation	slower in KO		slower in KO		Table 3.2 (p.66); Figure 4.5 (p.84)	slower in ST[4]
Tetanus relaxation	slower in KO		slower in KO		Figure 4.6 (p.85)	slower in ST[4]
Force-frequency Hill coefficient	higher in KO			higher in KO	Table 3.1 (p.53); Figure 4.7 (p.86)	lower in ST[3,5]
Twitch-to-tetanus ratio	lower in KO				Table 3.1 (p.53); Figure 4.7 (p.86)	lower in ST[6]
Fatigue recovery	faster in KO	faster in KO	faster in KO	faster in KO	Figures 3.6, 3.7, 3.8 (p.59-p.61); Figure 4.9 (p.95)	faster in ST[7]

Table 5.1 Main differences between *Actn3* knockout EDL muscles and wild-type muscles. KO – knockouts; FT – fast-twitch; ST – slow-twitch.

Numbers in last column are references as follows: (1) Hamalainen & Pette (1993); (2) MacArthur *et al.* (2008); (3) Bortolotto *et al.* (2000); (4) Moss *et al.* (1995); (5) Fink *et al.* (1986) (6) Burke *et al.* (1973) (7) Brooks (2003).

slower-twitch profile, and supports the hypothesis that α-actinin-3 plays a role in the differentiation of fast-twitch glycolytic fibres.

As shown in the table, differences that were found in male mice were also generally found in female mice. The only exceptions were the differences in absolute force and twitch-to-tetanus ratio. On the whole, α-actinin-3 deficiency appeared to affect male and female mice in the same way. However, the effects of α-actinin-3 deficiency did appear to vary with age. The statistically significant differences between knockouts and wild-types occurred almost exclusively in the adult mice. This apparent amelioration of the *Actn3* knockout phenotype with age may be partly due to the loss of fast glycolytic fibres with age (Kadhiresan

et al., 1996). There was, however, one notable exception. The effect of α-actinin-3 deficiency on fatigue recovery was still strongly evident in aged mice.

4. What changes occur at the level of the contractile proteins and sarcoplasmic reticulum in α-actinin-3-deficient fibres?

If α-actinin-3 is involved in fibre-type differentiation, one would expect certain changes to occur at the subcellular level when α-actinin-3 is absent. Two factors which could be affected at the subcellular level are: (i) the properties of the contractile proteins; and (ii) the rate of Ca^{2+} uptake by the sarcoplasmic reticulum (SR). These factors were examined by the skinned fibre technique in *Paper C*.

The main finding here was that the SR in *Actn3* knockout fibres loaded Ca^{2+} more slowly than the SR in control fibres (Figure 4.1, p.77). This is evidence at a subcellular level of a shift towards slower-twitch characteristics in fibres deficient in α-actinin-3, and suggests a mechanism for the slower twitch and tetanus relaxation observed in whole knockout muscle. Changes were also found in the Ca^{2+} and Sr^{2+} activation characteristics of individual fibres, indicative of changes in the properties of the contractile proteins. The force-pCa relationship was steeper in *Actn3* knockout fibres compared with wild-types (Figure 4.2, p.79) and knockout fibres exhibited myofibrillar oscillations of greater frequency than wild-types (Figure 4.3, p.80). A steeper force-pCa relationship is actually a characteristic of faster-twitch fibres (Fink *et al.*, 1986; Williams *et al.*, 1993), so this result is unusual in light of our other findings. However, the fact that twitch relaxation is slower in *Actn3* knockouts than in wild-types suggests that the effect of slower SR Ca^{2+} uptake must outweigh the effect of a steeper force-pCa relationship and result in slower relaxation overall.

It must be noted that we did not directly examine the MHC isoform compositions of the individual fibres, nor the isoforms of thin-filament regulatory proteins such as troponin C, troponin T, tropomyosin and myosin light chain. Slow-twitch and fast-twitch fibres express different isoforms of these proteins (Moss *et al.*, 1995), so future studies comparing the isoforms expressed in *Actn3* knockout and wild-type animals could provide further valuable information as to whether α-actinin-3 influences fibre-type differentiation.

The phenotype of the *Actn3* knockout mouse at both whole muscle and skinned fibre levels, as characterised in this thesis, provides evidence of a role for α-actinin-3 in promoting the development of fast-twitch, glycolytic properties in muscle fibres. In recent years, the Z-disc of skeletal muscle has come to be viewed as not just a structural component of the sarcomere, but a nodal point for various signalling and metabolic pathways (Frank *et al.*, 2006). This thesis has shown that α-actinin-3, as the major component of the Z-disc, is likely to play an important role in these pathways.

References

Allard B (2006). Sarcolemmal ion channels in dystrophin-deficient skeletal muscle fibres. *Journal of Muscle Research & Cell Motility* 27, 367-373.

Allen DG, Lännergren J & Westerblad H (1995). Muscle cell function during prolonged activity: cellular mechanisms of fatigue. *Experimental Physiology* 80, 497-527.

Allen DG, Lamb GD & Westerblad H (2008). Skeletal muscle fatigue: cellular mechanisms. *Physiological Reviews* 88, 287-332.

Anderson JE, Bressler HH & Ovalle WK (1988). Functional regeneration in the hindlimb skeletal muscle of the *mdx* mouse. *Journal of Muscle Research & Cell Motility* 9, 499-515.

Anderson JL, Head SI & Morley JW (2003). Altered inhibitory input to Purkinje cells of dystrophin-deficient mice. *Brain Research* 982, 280-283.

Bakker AJ, Head SI, Wareham AC & Stephenson DG (1998). Effect of clenbuterol on sarcoplasmic reticulum function in single skinned mammalian skeletal muscle fibers. *American Journal of Physiology Cell Physiology* 274, C1718-C1726.

Boittin F, Petermann O, Hirn C, Mittaud P, Dorchies OM, Roulet E & Ruegg UT (2006). Ca^{2+}-independent phospholipase A_2 enhances store-operated Ca^{2+} entry in dystrophic skeletal muscle fibers. *Journal of Cell Science* 119, 3733-3742.

Bortolotto SK, Cellini M, Stephenson DG & Stephenson GMM (2000). MHC isoform composition and Ca^{2+}- or Sr^{2+}- activation properties of rat skeletal muscle fibers. *American Journal of Physiology Cell Physiology* 279, C1564-C1577.

Bottinelli R & Reggiani C (2000). Human skeletal muscle fibres: Molecular and functional diversity. *Progress in Biophysics and Molecular Biology* 73, 195-262.

Bourke DL & Ontell M (1984). Branched myofibers in long-term whole muscle transplants: a quantitative study. *Anatomical Record* 209: 281-288.

Brooks SV & Faulkner JA (1988). Contractile properties of skeletal muscles from young, adult and aged mice. *Journal of Physiology* 404, 71-82.

Brooks SV, Zerba E & Faulkner JA (1995). Injury to muscle fibres after single stretches of passive and maximally stimulated muscles in mice. *Journal of Physiology* 488, 459-469.

Brooks SV & Faulkner JA (1996). The magnitude of the initial injury induced by stretches of maximally activated muscle fibres of mice and rats increases in old age. *Journal of Physiology* 497, 573-580.

Brooks SV (2003). Current topics for teaching skeletal muscle physiology. *Advances in Physiology Education* 27, 171-182.

Brown SC & Lucy JA (1997). Chapter 7. Functions of dystrophin. In: *Dystrophin: gene, protein, and cell biology*, edited by Brown SC and Lucy JA. Cambridge: Cambridge University Press, p. 163-200.

Burke RE, Levine DN, Tsairis P & Zajac FE (1973). Physiological types and histochemical profiles in motor units of the cat gastrocnemius. *Journal of Physiology* 234, 723-748.

Carlson CG. (1996). Acetylcholine receptor and calcium leakage activity in nondystrophic and dystrophic myotubes (*mdx*). *Muscle & Nerve* 19, 1258-1267.

Carlson CG & Officer T (1996). Single channel evidence for a cytoskeletal defect involving acetylcholine receptors and calcium influx in cultured dystrophic (*mdx*) myotubes. *Muscle & Nerve* 19, 1116-1126.

Carlson CG (1998). The dystrophinopathies: an alternative to the structural hypothesis. *Neurobiology of Disease* 5, 3-15.

Celichowski J & Grottel K (1993). Twitch/tetanus ratio and its relation to other properties of motor units. *Neuroreport* 5, 201-204.

Chan S, Head SI & Morley JW (2007). Branched fibers in dystrophic *mdx* muscle are associated with a loss of force following lengthening contractions. *American Journal of Physiology Cell Physiology* 293, C985-C992.

Chan S, Seto JT, MacArthur DG, Yang N, North KN & Head SI (2008). A gene for speed: contractile properties of isolated whole EDL muscle from an α-actinin-3 knockout mouse. *American Journal of Physiology Cell Physiology* 295, C897-C904.

Clarkson PM, Devaney JM, Gordish-Dressman H, Thompson PD, Hubal MJ, Urso M, Price TB, Angelopoulos TJ, Gordon PM, Moyna NM, Pescatello LS, Visich PS, Zoeller RF, Seip RL & Hoffman EP (2005). ACTN3 genotype is associated with increases in muscle strength in response to resistance training in women. *Journal of Applied Physiology* 99, 154-163.

Consolino CM & Brooks SV (2004). Susceptibility to sarcomere injury induced by single stretches of maximally activated muscles of *mdx* mice. *Journal of Applied Physiology* 96, 633-638.

Deconinck N, Ragot T, Marechal G, Perricaudet M & Gillis JM (1996). Functional protection of dystrophic mouse (*mdx*) muscles after adenovirus-mediated transfer of a dystrophin minigene. *Proceedings of the National Academy of Sciences of the United States of America* 93, 3570-3574.

Deconinck N, Rafael JA, Beckers-Bleukx G, Kahn D, Deconinck AE, Davies KE & Gillis JM (1998). Consequences of the combined deficiency in dystrophin and utrophin on the mechanical properties and myosin composition of some limb and respiratory muscles of the mouse. *Neuromuscular Disorders* 8, 362-370.

Deconinck N & Dan B (2007). Pathophysiology of Duchenne muscular dystrophy: current hypotheses. *Pediatric Neurology* 36, 1-7.

Emery AE. (1993). *Duchenne Muscular Dystrophy*. Oxford University Press, New York.

Emery AE (2002). The muscular dystrophies. *Lancet* 359, 687-695.

Engel AG, Yamamoto M & Fischbeck KH. (1994). Dystrophinopathies. In *Myology, Basic and Clinical*, vol. 2. ed. Engel AG & Franzini-Armstrong C, pp. 1130-1187. McGraw-Hill, New York.

Ervasti JM. (2003). Costameres: the Achilles' heel of Herculean muscle. *Journal of Biological Chemistry* 278, 13591-13594.

Eynon N, Duarte JA, Oliveira J, Sagiv M, Yamin C, Meckel Y, Sagiv M & Goldhammer E (2009). ACTN3 R577X polymorphism and Israeli top-level athletes. *International Journal of Sports Medicine* 30, 695-698.

Faulkner JA, Larkin LM, Claflin DR & Brooks SV (2007). Age-related changes in the structure and function of skeletal muscles. *Clinical and Experimental Pharmacology and Physiology* 34, 1091-1096.

Fink RHA, Stephenson DG & Williams DA (1986). Calcium and strontium activation of single skinned muscle fibres of normal and dystrophic mice. *Journal of Physiology* 373, 513-525.

Fitts RH (1994). Cellular mechanisms of muscle fatigue. *Physiological Reviews* 74, 49-94.

Fong PY, Turner PR, Denetclaw WF & Steinhardt RA (1990). Increased activity of calcium leak channels in myotubes of Duchenne human and *mdx* mouse origin. *Science* 250, 673-676.

Franco A & Lansman JB (1990). Calcium entry through stretch-inactivated ion channels in *mdx* myotubes. *Nature* 344, 670-673.

Frank D, Kuhn C, Katus HA & Frey N (2006). The sarcomeric Z-disc: a nodal point in signalling and disease. *Journal of Molecular Medicine* 84, 446-468.

Frey N, Frank D, Lippl S, Kuhn C, Kögler H, Barrientos T, Rohr C, Will R, Müller O, Weiler H, Bassel-Duby R, Katus HA & Olson EN (2008). Calsarcin-2 deficiency increases exercise capacity in mice through calcineurin/NFAT activation. *Journal of Clinical Investigation* 118, 3598-3608.

Friedrich O, von Wegner F, Chamberlain JS, Fink RHA & Rohrbach P (2008). L-Type Ca^{2+} channel function is linked to dystrophin expression in mammalian muscle. *PLoS ONE* 3(3): e1762. doi:10.1371/journal.pone.0001762.

Fryer MW & Stephenson DG (1996). Total and sarcoplasmic reticulum contents of skinned fibres from rat skeletal muscle. *Journal of Physiology* 493, 357-370.

Gillis JM (1999). Understanding dystrophinopathies: an inventory of the structural and functional consequences of the absence of dystrophin in muscles of the *mdx* mouse. *Journal of Muscle Research and Cell Motility* 20, 605-625.

Girolami UD, Anthony DC & Frosch MP (1999). Peripheral nerve and skeletal muscle. In *Robbins' Pathologic Basis of Disease*. ed. Cotran RS, Kumar V & Collins T, pp. 1269-1291. WB Saunders, Philadelphia.

Grange RW, Gainer TG, Marschner KM, Talmadge RJ & Stull JT (2002). Fast-twitch skeletal muscles of dystrophic mouse pups are resistant to injury from acute mechanical stress. *American Journal of Physiology Cell Physiology* 283, C1090-1101.

Grounds MD, Radley HG, Lynch GS, Nagaraju K & De Luca A (2002). Towards developing standard operating procedures for pre-clinical testing in the *mdx* mouse model of Duchenne muscular dystrophy. *Neurobiology of Disease* 31, 1-19.

Hamalainen N & Pette D (1993). The histochemical profiles of fast fiber types IIB, IID, and IIA in skeletal muscles of mouse, rat and rabbit. *Journal of Histochemistry and Cytochemistry* 41, 733-743.

Head SI, Stephenson DG & Williams DA (1990). Properties of enzymatically isolated skeletal fibres from mice with muscular dystrophy. *Journal of Physiology* 422, 351-367.

Head SI, Williams DA & Stephenson DG (1992). Abnormalities in structure and function of limb skeletal muscle fibres of dystrophic *mdx* mice. *Proceedings of the Royal Society of London Series B: Biological Sciences* 248, 163-169.

Head SI, Bakker AJ & Liangas G (2004). EDL and soleus muscles of the C57BL6J/dy2j laminin-alpha 2-deficient dystrophic mouse are not vulnerable to eccentric contractions. *Experimental Physiology* 89, 531-539.

Kadhiresan VA, Hassett CA & Faulkner JA (1996). Properties of single motor units in medial gastrocnemius muscles of adult and old rats. *Journal of Physiology* 493, 543-552.

Karpati G, Carpenter S & Prescott S (1988). Small-caliber skeletal muscle fibers do not suffer necrosis in *mdx* mouse dystrophy. *Muscle & Nerve* 11, 795-803.

Keynes RD & Aidley DJ (1991). *Nerve and Muscle*. Cambridge: Cambridge University Press.

Khurana TS & Davies KE (2003). Pharmacological strategies for muscular dystrophy. *Nature Reviews. Drug Discovery* 2, 379-390.

Kueh SL, Head SI & Morley JW (2004). A new colony of *mdx* dystrophic mice with genetically identical littermate controls. *Proceedings of the Australian Health and Medical Research Congress 2004*, Sydney, p. 317.

Law DJ, Caputo A & Tidball JG (1995). Site and mechanics of failure in normal and dystrophin-deficient skeletal muscle. *Muscle & Nerve* 18, 216-223.

Lovering RM, Michaelson L & Ward CW (2009). Malformed *mdx* myofibers have normal cytoskeletal architecture yet altered EC coupling and stress-induced Ca^{2+} signalling. *American Journal of Physiology Cell Physiology* 297, C571-C580.

Luther PK (2009). The vertebrate muscle Z-disc:sarcomere anchor for structure and signalling. *Journal of Muscle Research and Cell Motility* 30, 171-185.

Lynch GS, Hinkle RT, Chamberlain JS, Brooks SV & Faulkner JA (2001). Force and power output of fast and slow skeletal muscles from *mdx* mice 6-28 months old. *Journal of Physiology* 535, 591-600.

Lynch GS, Faulkner JA & Brooks SV (2008). Force deficits and breakage rates after single lengthening contractions of single fast fibers from unconditioned and conditioned muscles of young and old rats. *American Journal of Physiology Cell Physiology* 295, C249-C256.

MacArthur DG & North KN (2004). A gene for speed? The evolution and function of α-actinin-3. *Bioessays* 26, 786-795.

MacArthur DG, Seto JT, Raftery JM, Quinlan KG, Huttley GA, Hook JW, Lemckert FA, Kee AJ, Edwards MR, Berman Y, Hardeman EC, Gunning PW, Easteal S, Yang N & North KN (2007). Loss of ACTN3 gene function alters mouse muscle metabolism and shows evidence of positive selection in humans. *Nature Genetics* 39, 1261-1265.

MacArthur DG, Seto JT, Chan S, Quinlan KG, Raftery JM, Turner N, Nicholson MD, Kee AJ, Hardeman EC, Gunning PW, Cooney GJ, Head SI, Yang N & North KN (2008). An Actn3 knockout mouse provides mechanistic insights into the association between α-actinin-3 deficiency and human athletic performance. *Human Molecular Genetics* 17, 1076-1086.

Macdonald WA & Stephenson DG (2001). Effects of ADP on sarcoplasmic reticulum function in mechanically skinned skeletal muscle fibres of the rat. *Journal of Physiology* 532, 499-508.

Macdonald WA & Stephenson DG (2006). Effect of ADP on slow-twitch muscle fibres of the rat: implications for muscle fatigue. *Journal of Physiology* 573, 187-198.

Marks DB, Marks AD & Smith CM (1996). *Basic medical biochemistry: a clinical approach*. Williams & Wilkins, Baltimore.

McArdle A, Edwards RH & Jackson MJ (1991). Effects of contractile activity on muscle damage in the dystrophin-deficient *mdx* mouse. *Clinical Science* 80, 367-371.

McCully KK & Faulkner JA (1986). Characteristics of lengthening contractions associated with injury to skeletal muscle fibers. *Journal of Applied Physiology* 61, 293-299.

Millay DP, Goonasekera SA, Sargent MA, Maillet M, Aronow BJ & Molkentin JD (2009). Calcium influx is sufficient to induce muscular dystrophy through a TRPC-dependent mechanism. *Proceedings of the National Academy of Sciences of the United States of America* 106, 19023-19028.

Mills M, Yang N, Weinberger R, Vander Woude DL, Beggs AH, Easteal S & North K (2001). Differential expression of the actin-binding proteins, alpha-actinin-2 and -3, in different species: implications for the evolution of functional redundancy. *Human Molecular Genetics* 10, 1335-1346.

Moens P, Baatsen PH & Marechal G (1993). Increased susceptibility of EDL muscles from mdx mice to damage induced by contractions with stretch. *Journal of Muscle Research & Cell Motility* 14, 446-451.

Moran CN, Yang N, Bailey ME, Tsiokanos A, Jamurtas A, MacArthur DG, North K, Pitsiladis YP & Wilson RH (2007). Association analysis of the ACTN3 R577X polymorphism and complex quantitative body composition and performance phenotypes in adolescent Greeks. *European Journal of Human Genetics* 15, 88-93.

Moss RL, Diffee GM & Greaser ML (1995). Contractile properties of skeletal muscle fibres in relation to myofibrillar protein isoforms. *Reviews of Physiology Biochemistry and Pharmacology* 126, 1-63.

Motulsky HJ & Christopoulos A (2003). *Fitting models to biological data using linear and nonlinear regression. A practical guide to curve fitting*. GraphPad Software Inc., San Diego.

Mueller RF & Young ID (1998). *Emery's Elements of Medical Genetics*. Churchill Livingstone, Edinburgh.

Muntoni F, Torelli S & Ferlini A (2003). Dystrophin and mutations: one gene, several proteins, multiple phenotypes. *Lancet Neurology* 2, 731-740.

Niemi AK & Majamaa K (2005). Mitochondrial DNA and ACTN3 genotypes in Finnish elite endurance and sprint athletes. *European Journal of Human Genetics* 13, 965-969.

North KN, Yang N, Wattanasirichaigoon D, Mills M, Easteal S & Beggs AH (1999). A common nonsense mutation results in α-actinin-3 deficiency in the general population. *Nature Genetics* 21, 353-354.

O'Brien KF & Kunkel LM (2001). Dystrophin and muscular dystrophy: past, present, and future. *Molecular Genetics & Metabolism* 74, 75-88.

Papadimitriou ID, Papadopoulos C, Kouvatsi A & Triantaphyllidis C (2008). The ACTN3 gene in elite Greek track and field athletes. *International Journal of Sports Medicine* 29, 352-355.

Petrof BJ, Shrager JB, Stedman HH, Kelly AM & Sweeney HL (1993). Dystrophin protects the sarcolemma from stresses developed during muscle contraction. *Proceedings of the National Academy of Sciences of the United States of America* 90, 3710-3714.

Petrof BJ (2002). Molecular pathophysiology of myofiber injury in deficiencies of the dystrophin-glycoprotein complex. *American Journal of Physical Medicine & Rehabilitation* 81, S162-S174.

Pette D & Staron RS (1990). Cellular and molecular diversities of mammalian skeletal muscle fibers. *Reviews of Physiology Biochemistry and Pharmacology* 116, 1-76.

Proske U & Morgan DL (2001). Muscle damage from eccentric exercise: mechanism, mechanical signs, adaptation and clinical applications. *Journal of Physiology* 537, 333-345.

Rader EP & Faulkner JA (2006). Recovery from contracton-induced injury is impaired in weight-bearing muscles of old male mice. *Journal of Applied Physiology* 100, 656-661.

Raymackers JM, Debaix H, Colson-Van Schoor M, De Backer F, Tajeddine N, Schwaller B, Gailly P & Gillis JM (2003). Consequence of parvalbumin deficiency in the *mdx* mouse: histological, biochemical and mechanical phenotype of a new double mutant. *Neuromuscular Disorders* 13, 376-387.

Roth SM, Walsh S, Liu D, Metter EJ, Ferrucci L & Hurley BF (2008). The ACTN3 R577X nonsense allele is under-represented in elite-level strength athletes. *European Journal of Human Genetics* 16, 391-394.

Sacco P, Jones DA, Dick JR & Vrbova G (1992). Contractile properties and susceptibility to exercise-induced damage of normal and *mdx* mouse tibialis anterior muscle. *Clinical Science* 82, 227-236.

Schmalbruch H (1984). Regenerated muscle fibers in Duchenne muscular dystrophy: a serial section study. *Neurology* 34, 60-65.

Smith DA & Stephenson DG (2009). The mechanism of spontaneous oscillatory contractions in skeletal muscle. *Biophysical Journal* 96, 3682-3691.

Stephenson DG & Williams DA (1982). Effects of sarcomere length on the force-pCa relation in fast- and slow-twitch skinned muscle fibres from the rat. *Journal of Physiology* 333, 637-653.

Stephenson DG, Lamb GD & Stephenson GMM (1998). Events of the excitation-contraction-relaxation (E-C-R) cycle in fast- and slow-twitch mammalian muscle fibres relevant to muscle fatigue. *Acta Physiologica Scandinavica* 162, 229-245.

Tamaki T & Akatsuka A (1994). Appearance of complex branched fibers following repetitive muscle trauma in normal rat skeletal muscle. *Anatomical Record* 240, 217-224.

Trinh HH & Lamb GD (2006). Matching of sarcoplasmic reticulum and contractile properties in rat fast- and slow-twitch muscle fibres. *Clinical and Experimental Pharmacology and Physiology* 33, 591-600.

Turner PR, Fong PY, Denetclaw WF & Steinhardt RA (1991). Increased calcium influx in dystrophic muscle. *Journal of Cell Biology* 115, 1701-1712.

Tutdibi O, Brinkmeier H, Rudel R & Fohr KJ (1999). Increased calcium entry into dystrophin-deficient muscle fibres of MDX and ADR-MDX mice is reduced by ion channel blockers. *Journal of Physiology* 515, 859-868.

Webster C, Silberstein L, Hays AP & Blau HM (1988). Fast muscles are preferentially affected in Duchenne muscular dystrophy. *Cell* 52, 503-513.

Westerblad H & Lännergren J (1991). Slowing of relaxation during fatigue in single mouse muscle fibres. *Journal of Physiology* 434, 323-336.

Whitehead NP, Yeung EW & Allen DG (2006). Muscle damage in *mdx* (dystrophic) mice: role of calcium and reactive oxygen species. *Clinical and Experimental Pharmacology and Physiology* 33, 657-662.

Williams DA, Head SI, Lynch GS & Stephenson DG (1993). Contractile properties of skinned muscle fibres from young and adult normal and dystrophic (*mdx*) mice. *Journal of Physiology* 460, 51-67.

Yang N, MacArthur DG, Gulbin JP, Hahn AG, Beggs AH, Easteal S & North K (2003). ACTN3 genotype is associated with human elite athletic performance. *American Journal of Human Genetics* 73, 627-631.

Yeung EW, Head SI & Allen DG (2003). Gadolinium reduces short-term stretch-induced muscle damage in isolated *mdx* mouse muscle fibres. *Journal of Physiology* 552, 449-458.

Zanou N, Iwata Y, Schakman O, Lebacq J, Wakabayashi S & Gailly P (2009). Essential role of TRPV2 ion channel in the sensitivity of dystrophic muscle to eccentric contractions. *FEBS Letters* 583, 3600-3604.

Publications

Am J Physiol Cell Physiol 293: C985–C992, 2007.
First published June 13, 2007; doi:10.1152/ajpcell.00128.2007.

Branched fibers in dystrophic *mdx* muscle are associated with a loss of force following lengthening contractions

S. Chan,[1] S. I. Head,[1] and J. W. Morley[1,2]

[1]*School of Medical Sciences, University of New South Wales, and* [2]*School of Medicine, University of Western Sydney, Sydney, Australia*

Submitted 29 March 2007; accepted in final form 11 June 2007

Chan S, Head SI, Morley JW. Branched fibers in dystrophic *mdx* muscle are associated with a loss of force following lengthening contractions. *Am J Physiol Cell Physiol* 293: C985–C992, 2007. First published June 13, 2007; doi:10.1152/ajpcell.00128.2007.—We demonstrated that the susceptibility of skeletal muscle to injury from lengthening contractions in the dystrophin-deficient *mdx* mouse is directly linked with the extent of fiber branching within the muscles and that both parameters increase as the *mdx* animal ages. We subjected isolated extensor digitorum longus muscles to a lengthening contraction protocol of 15% strain and measured the resulting drop in force production (force deficit). We also examined the morphology of individual muscle fibers. In *mdx* mice 1–2 mo of age, 17% of muscle fibers were branched, and the force deficit of 7% was not significantly different from that of age-matched littermate controls. In *mdx* mice 6–7 mo of age, 89% of muscle fibers were branched, and the force deficit of 58% was significantly higher than the 25% force deficit of age-matched littermate controls. These data demonstrated an association between the extent of branching and the greater vulnerability to contraction-induced injury in the older fast-twitch dystrophic muscle. Our findings demonstrate that fiber branching may play a role in the pathogenesis of muscular dystrophy in *mdx* mice, and this could affect the interpretation of previous studies involving lengthening contractions in this animal.

skeletal muscle; *mdx* mouse; lengthening contraction; Duchenne muscular dystrophy

DUCHENNE MUSCULAR DYSTROPHY (DMD) is an X-linked recessive disorder characterized by progressive wasting of skeletal muscle, affecting 1 in 3,500 live male births. It is caused by the absence of dystrophin, a 427-kDa protein that, in normal muscle fibers, is found just internal to the sarcolemma. Controversy still surrounds the function of dystrophin and the mechanisms by which its absence leads to the skeletal muscle degeneration seen in DMD (4, 10). There are several hypotheses as to the role played by dystrophin in skeletal muscle. For simplicity, we have grouped them under two headings: *1*) the structural hypothesis (20) and *2*) the ion channel hypothesis (5).

1) In the structural hypothesis, the absence of dystrophin leaves the membrane weakened and susceptible to tearing during muscle contraction, leading to irreversible fiber damage followed by necrosis. Support for this theory comes from well-established evidence that the fast-twitch muscles of the dystrophin-deficient *mdx* mouse are more easily damaged by lengthening contractions (contractions with stretch) than are normal muscles (see Table 1).

2) In the ion channel hypothesis, the absence of dystrophin is suggested to lead to the pathological function of a sarcolemmal ion channel, and several ion channels have been singled out as promising candidates for the primary cause of the pathology in dystrophin-deficient dystrophies (for review, see Ref. 1). The majority of these studies hypothesize that the end consequence of the proposed channelopathy is an increased intracellular flux of Ca^{2+}, and this increase in intracellular Ca^{2+} concentration results in fiber damage through mediators such as proteases and reactive oxygen species (23). It is important to note that, in the ion channel hypothesis, the absence of dystrophin does not chronically weaken the sarcolemma; rather it disrupts ion channel function.

The etiology of the muscle degeneration in *mdx* mice is complicated by the fact that, as *mdx* muscle ages, the architecture of the dystrophic muscle fibers becomes grossly abnormal (13). These abnormal fibers, termed branched or split fibers, are more prone to damage during contraction, as high shear stresses occur at branch points during intense contractile activity, leading to fiber rupture at these points. Direct evidence demonstrating the increased fragility of branched fibers was presented in Ref. 12, where it was demonstrated that, when individual fibers were stimulated, fiber segments that contained branch points were more liable to rupture than fiber segments without branch points, and when whole muscles were stimulated, branched fibers were preferentially damaged over unbranched fibers within the muscle. The question arises, then, as to whether the increased susceptibility of *mdx* muscles to injury during lengthening contractions is due directly to the absence of dystrophin, or whether the morphological changes (branching) of fibers leads to weakened regions (branch points) that are the site of damage during contraction.

The aim of our study was to address this question by examining *mdx* mice in two age groups: a "younger" group ~1–2 mo old, in which fiber branching was moderate (<20%), and an "older" group ~6–7 mo old, in which fiber branching was more extensive (>80%). We hypothesized that the "older" group would experience a greater loss of force than the "younger" group following a mild protocol of lengthening contractions. By examining the association between the extent of fiber branching and the susceptibility to injury, we attempted to gain some insight into the role of branched fibers in the pathogenesis of muscular dystrophy in the *mdx* mouse.

METHODS

Animals used. The *mdx* mice with littermate controls were obtained from the Animal Resources Centre (Perth, Australia). Female C57BL/10ScSn-DMD (*mdx*) mice were mated with male C57BL/10ScSn

Address for reprint requests and other correspondence: S. I. Head, School of Medical Sciences, Univ. of New South Wales, Sydney 2052, Australia (e-mail: s.head@unsw.edu.au).

The costs of publication of this article were defrayed in part by the payment of page charges. The article must therefore be hereby marked "*advertisement*" in accordance with 18 U.S.C. Section 1734 solely to indicate this fact.

 0363-6143/07 $8.00 Copyright © 2007 the American Physiological Society

Downloaded from ajpcell.physiology.org on March 10, 2008

Table 1. *Force deficits of normal and mdx fast-twitch muscles following lengthening contractions*

Study	Ref. No.	Age of Mice, wk	Strain, %	Muscle	Force Deficits, %	
					Normal	*mdx*
McArdle et al. (1991)	17	5–6	30	EDL	93	94
Sacco et al. (1992)	22	16–26	In situ*	Tibialis anterior	44	48
Head et al. (1992)	13	>45	12	EDL	2	66‡
Moens et al. (1993)	18	~3–70	~8	EDL	13	38‡
Petrof et al. (1993)	20	12–15	10	EDL, diaphragm	29	57‡
Deconinck et al. (1996)	9	16	7	Gastrocnemius	20	64‡
Deconinck et al. (1998)	8	10	8	EDL	10	41‡
Grange et al. (2002)	11	1–2	10	EDL	23	27
Raymackers et al. (2003)	21	12	7	EDL	19	69‡
Consolino and Brooks (2004)	6	20	18†	EDL	15	40‡

Strain is the length by which the muscle is stretched, as a percentage of its original length. Higher force deficits are taken as indicators of a greater degree of muscle damage. *The length of stretch could not be measured in this study, as the muscle was not dissected out. Instead, the muscle was stretched by moving the foot. †A variety of strains was used in this study. Only the results for the middle strain are shown. ‡Significant difference in force deficit between *mdx* and normal.

mice. The offspring of this first mating were then mated together. The male offspring of this second mating comprise a colony of *mdx* mice and littermate controls sharing a common genetic background, and it is this colony that was used in this study. Littermate control mice were distinguished from *mdx* mice on the basis of serum creatine kinase (CK) levels. Mice with CK < 1,000 U/l were classified as controls, while mice with CK > 1,000 U/l were classified as *mdx*. Western blotting for the presence of dystrophin has shown this to be an ultrareliable method for phenotyping the mice in this colony (15). Phenotype was further confirmed when muscle fibers were examined with confocal microscopy; *mdx* fibers have many centrally located nuclei, while almost all nuclei in control fibers are peripherally located.

In all, 13 mice were used for the experiments assessing contractile properties, contraction-induced damage, and fiber morphology. These consisted of six "younger" mice aged 6–8 wk and seven "older" mice aged 27–31 wk. Immediately before experimentation, animals were anesthetized with halothane and killed by cervical dislocation. Use of animals was approved by the University of New South Wales Animal Care and Ethics Committee.

Muscle preparation. The extensor digitorum longus muscle was dissected from the hindlimb and tied by its tendons to a force transducer (World Precision Instruments, Fort 10) at one end and a linear tissue puller (University of New South Wales) at the other, using silk suture (Deknatel 6.0). The muscle was placed in a bath continuously superfused with Krebs solution, with composition as follows (in mM): 4.75 KCl, 118 NaCl, 1.18 KH_2PO_4, 1.18 $MgSO_4$, 24.8 $NaHCO_3$, 2.5 $CaCl_2$, and 10 glucose, with 0.1% fetal calf serum, and continuously bubbled with 95% O_2-5% CO_2 to maintain pH at 7.4. The muscle was stimulated by delivering an electrical current between two parallel platinum electrodes, using an electrical stimulator (A-M Systems). At the start of the experiment, the muscle was set to its optimum length (L_o) by finding the length that produced maximum twitch force. All experiments were conducted at room temperature (~22–24°C).

In total, 23 muscles were used, 11 in the "younger" group (5 controls and 6 *mdx*) and 12 in the "older" group (4 controls and 8 *mdx*).

Lengthening contraction protocol. The lengthening contraction protocol is illustrated in Fig. 1. At time = 0 ms, the muscle was stimulated by supramaximal pulses of 1-ms duration and 100-Hz frequency. At time = 750 ms, after it had attained its maximum isometric force, the muscle was stretched at a speed of 1 mm/s until it was 15% longer than its L_o, held at this length for 2 s, then returned at the same speed to its original position. The electrical stimulus was stopped at time = 5,000 ms. This lengthening contraction was performed three times, at intervals of 5 min. The strain of 15% of muscle length was equivalent to a strain of 33% of fiber length, assuming that fiber length is 45% of muscle length (2).

A mild strain of 15% was chosen because preliminary experiments indicated that this strain did not damage control muscles of younger mice (unpublished data). This would allow us to determine whether muscles from *mdx* mice were more susceptible to damage. An excessively severe strain would substantially damage all muscles, thus obscuring differences in fragility between *mdx* and control muscles. The lengthening contraction protocol was initiated at a similar iso-

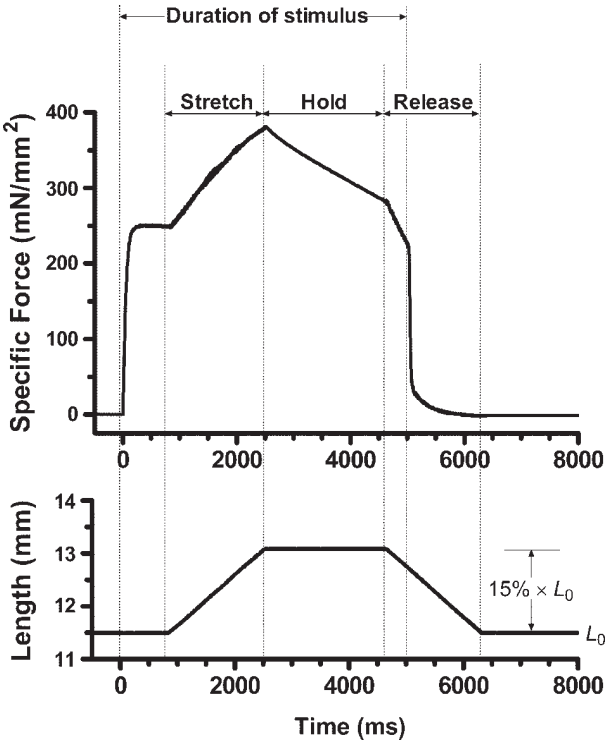

Fig. 1. The lengthening contraction protocol. The diagrams show recordings of force (*top*) and muscle length (*bottom*), obtained during one lengthening contraction in a muscle from an 8-wk-old *mdx* mouse. Electrical stimulation starts at time = 0 ms. At time = 750 ms, the muscle is stretched at 1 mm/s until it is 15% longer than its optimum length (L_o), held at this length for 2 s, then returned at the same rate to its original length. Stimulation is stopped at time = 5,000 ms. Three such contractions were performed, at intervals of 5 min.

Downloaded from ajpcell.physiology.org on March 10, 2008

metric force plateau in all groups tested to ensure a similar absolute force was experienced by all the muscles.

Force measurement. Muscle force was measured using a force-frequency curve, an example of which is shown in Fig. 2. The muscle was stimulated for 500 ms at different frequencies (5, 15, 25, 37.5, 50, 62.5, 75, 87.5, and 100 Hz), and maximum force was recorded at each frequency of stimulation. A curve relating the muscle force P to the stimulation frequency f was then fitted to these data. The curve had the following equation (19):

$$P = P_{min} + \frac{P_{max} - P_{min}}{1 + \left(\frac{K_f}{f}\right)^h}$$

The values of the parameters P_{min}, P_{max}, K_f, and h were outputs of the fitting procedure, and their meaning in relation to the force-frequency curve is illustrated in Fig. 2. P_{min} is the force developed at minimum stimulation frequency; P_{max} is the force developed at maximum stimulation frequency; K_f is the frequency at which the force developed is halfway between P_{min} and P_{max}; and h is known as the Hill coefficient. In this study, the values of r^2 for the fitting procedure were not lower than 99.6%.

Three contractile properties of the muscle were determined from the fitted parameters of the force-frequency curve: the maximum tetanic force (P_{max}), the twitch-to-tetanus ratio (P_{min}/P_{max}), and the half-frequency (K_f).

One force-frequency curve was obtained immediately before the lengthening contraction protocol. Twenty minutes after the final lengthening contraction, the setting of the L_o was repeated, and then a second force-frequency curve was obtained. Muscle damage was assessed functionally, by comparing the above-mentioned contractile properties before and after the contraction protocol. Indicators of damage were the percentage fall in P_{max}, the percentage change in K_f, and the percentage change in P_{min}/P_{max}. The primary indicator of damage was the percentage fall in P_{max}, which will be referred to as the force deficit.

To facilitate comparison between different muscles, forces are expressed as force per cross-sectional area (units mN/mm^2). Cross-sectional area was calculated by dividing the muscle's mass by the product of its L_o and the density of mammalian muscle (1.06 mg/mm^3).

Muscle stiffness. To assess differences in stiffness between muscles, we analyzed the change in force during the ramp phase of the first lengthening contraction in each muscle. Some muscles reached a force that exceeded the capacity of the force transducer during the ramp phase, so we limited our analysis to the first part of the ramp (until the muscle reached 108% of L_o). Stiffness was assessed by dividing the percent change in force over this time by the percent change in length.

Statistical analyses. Analyses were conducted using two-way ANOVA. The null hypothesis was that the effect of dystrophin deficiency is the same in both "younger" and "older" mice; that is, the effect of dystrophin deficiency is independent of age. Posttests, comparing *mdx* with control within each age group, were performed

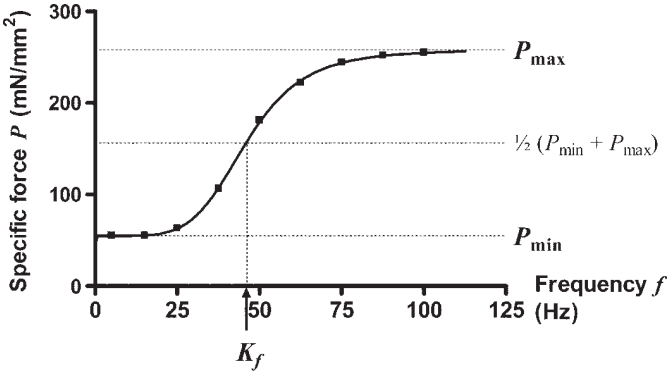

Fig. 2. Representative force-frequency curve from a 6-wk-old control muscle before lengthening contractions. Muscle force was measured at different stimulation frequencies, and a sigmoidal curve was fitted to the data points. The following measurements were then taken from the fitted curve and used to quantify the muscle's contractile properties: P, force; P_{max}, the maximum force; P_{min}, the minimum force; f, stimulation frequency; K_f, the half-frequency.

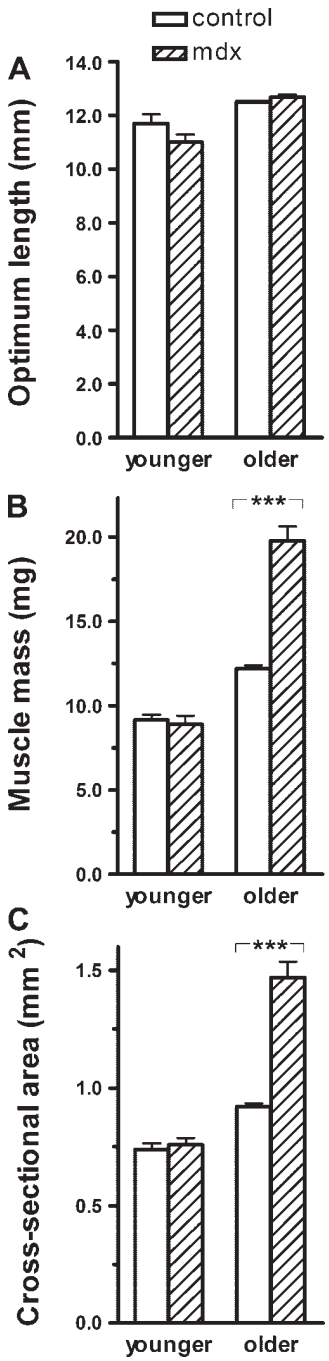

Fig. 3. Length (*A*), mass (*B*), and cross-sectional area (*C*). ***Significant difference between *mdx* and control in that particular age group, $P < 0.001$. $n = 5$ Muscles for younger control; $n = 6$ for younger *mdx*; $n = 4$ for older control; $n = 8$ for older *mdx*.

Downloaded from ajpcell.physiology.org on March 10, 2008

using the Bonferroni correction for multiple comparisons. All tests were conducted at a significance level of 5%. All statistical analyses, plus the fitting of the force-frequency curve, were performed using a standard statistical software package (GraphPad Prism version 4.00 for Windows, GraphPad Software, San Diego, CA). Means are presented as means ± SE.

Muscle fiber morphology. Immediately following experimentation, the muscles were digested to yield individual fibers. The solution used for the digestion was Krebs solution containing 3 mg/ml collagenase Type I (Sigma) and 1 mg/ml trypsin inhibitor (Sigma), continuously bubbled with 95% O_2–5% CO_2 and maintained at 37°C. After ~30 min, the muscles were removed from this solution, rinsed in Krebs solution, and placed in a relaxing solution with the following composition (concentrations in mM): 117 K^+, 36 Na^+, 1 Mg^{2+}, 60 HEPES (*N*-2-hydroxyethylpiperazine-*N*′-2-ethanesulfonic acid), 8 ATP, 50 $EGTA^{2-}$ (ethylene glycol-bis(β-aminoethyl ether)-*N,N,N*′,*N*′-tetraacetic acid), and free Ca^{2+} of 10^{-7} M. The free calcium was determined after titrating the solution with $CaCl_2$ to determine the excess EGTA. The muscle was then gently agitated using pipette suction, releasing some individual fibers from the muscle mass.

Individual fibers were examined either with a light microscope (Olympus BX60) or a laser-scanning confocal microscope (Leica TCS SP). The extent of fiber branching was assessed by counting the number of fibers that were branched and, for those fibers that were branched, counting the number of branches.

RESULTS

Length, mass, and cross-sectional area. Muscles from older mice (~6–7 mo old) were longer than muscles from younger mice (~1–2 mo old), but there were no differences in length between *mdx* and controls in each age group (Fig. 3*A*). In younger mice, *mdx* muscles were similar to control muscles in both mass and cross-sectional area, while in older mice, the mass and cross-sectional area of *mdx* muscles were ~60% higher than those of control muscles (Fig. 3, *B* and *C*). Over the approximate 5-mo period separating the two age groups of mice used in this study, the mass and cross-sectional area of littermate control muscles increased by ~5%/mo, whereas those of *mdx* muscles increased by ~15%/mo. Hence, in our new colony of dystrophin-deficient *mdx* mice with littermate controls, dystrophin deficiency is associated with a higher rate of growth in the physical bulk of muscles. Similar findings were reported for the original colony of *mdx* mice compared with age-matched wild-type controls from a separate colony (16).

Contractile properties before lengthening contractions. The contractile properties of the muscles before lengthening contractions are shown in Fig. 4. Figure 4*A* shows the P_{max} expressed as an absolute force (not corrected for cross-sectional area). The absolute forces of control and *mdx* muscles were similar in each age group. However, when corrected for cross-sectional area, the specific force produced by *mdx* muscles was significantly lower than that for controls in each age group (Fig. 4*B*). In younger mice, the specific force produced by *mdx* muscles was ~15% lower than that for controls, and in older mice ~30% lower than that for controls. In both age groups, the difference was statistically significant. These results show that, as the *mdx* animal ages, the impairment of specific force generation becomes more marked, although the animal is able to compensate for this by muscle hypertrophy, thus maintaining absolute forces at normal levels. The values of specific force obtained here are comparable to those obtained in other studies (for example, in study from Ref. 6: 235 mN/mm^2 for control, 173 mN/mm^2 for *mdx*, in extensor digitorum longus muscles of ~20-wk-old mice).

The twitch-to-tetanus ratios were similar across all of the muscles studied (Fig. 4*C*) and were comparable to the value of ~0.2 normally found in mammalian muscle (14).

Figure 4*D* shows the K_f, which is the stimulation frequency at which the force generated was halfway between the twitch force and the P_{max}. This is an indicator of the muscle's responsiveness to increases in frequency. A higher K_f means that the force-frequency curve has shifted to the right (see Fig. 2), so that the muscle needs higher stimulation frequencies to produce the same amount of force. The K_f of *mdx* muscles was similar to that of controls in each age group. However, older muscles had higher K_f than younger muscles, suggesting that, as the animal grows older, its muscles become less responsive to increases in frequency.

Damage following lengthening contractions. The muscles were subjected to a lengthening contraction protocol of 15% strain. A mild strain was used so that any differences in fragility between normal and dystrophic muscles could be determined. Various contractile properties were measured before and after the contractions, and the changes in these

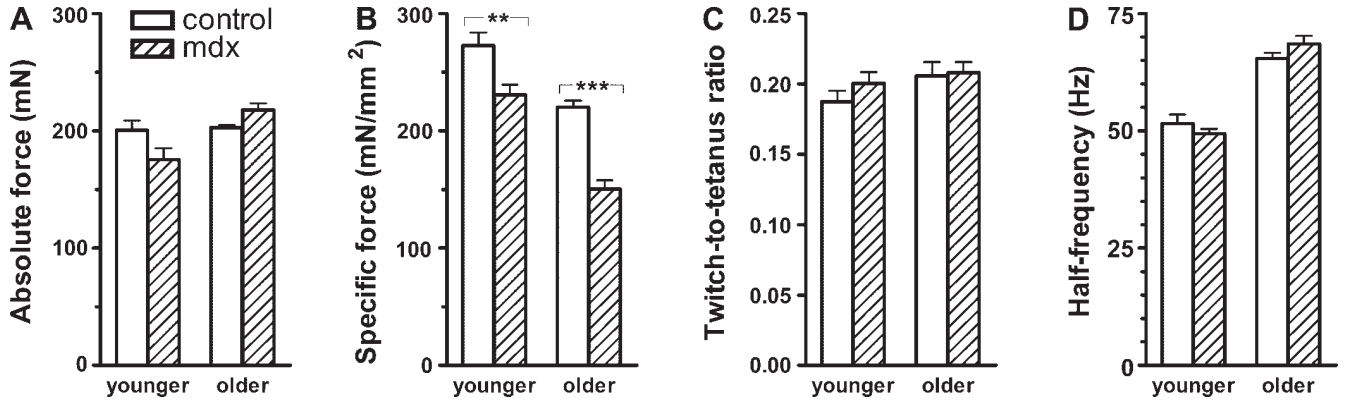

Fig. 4. Contractile properties before lengthening contractions. *A*: maximum tetanic force, expressed as an absolute force (no correction for cross-sectional area). *B*: maximum tetanic force, expressed as a specific force (corrected for cross-sectional area). *C*: twitch-to-tetanus ratio. *D*: the half-frequency. Significant difference between *mdx* and control in that particular age group: ***$P < 0.001$, **$0.001 < P < 0.01$. $n = 5$ Muscles for younger control; $n = 6$ for younger *mdx*; $n = 4$ for older control; $n = 8$ for older *mdx*.

Downloaded from ajpcell.physiology.org on March 10, 2008

properties were used as functional indicators of the extent of damage. The results are shown in Fig. 5.

The force deficit, or the reduction in P_{max} following lengthening contractions, was the primary indicator of muscle damage in this study (Fig. 5*A*). The force deficit is the most reliable and reproducible indicator of damage following lengthening contractions (3). In younger mice, the force deficit for *mdx* muscles (7.3 ± 4.8%, $n = 6$) was not significantly different from the force deficit for control muscles (−1.2 ± 3.5%, $n = 5$), suggesting that dystrophin deficiency did not increase the susceptibility of younger muscles to contraction-induced damage. However, in older mice, the force deficit for *mdx* muscles (58.0 ± 5.0%, $n = 8$) was significantly higher ($P < 0.001$) than the force deficit for controls (24.8 ± 5.3%, $n = 4$), suggesting that dystrophin deficiency did increase the susceptibility of older muscles to contraction-induced injury. Hence the effect of dystrophin deficiency on a muscle's vulnerability to damage was dependent on age, with the effect being more pronounced at older ages.

Our secondary indicators of muscle damage were the change in twitch-to-tetanus ratio and the change in K_f following lengthening contractions. For the twitch-to-tetanus ratio, the change in ratio for older *mdx* muscles was opposite in direction to the change in ratio for all of the other muscles (Fig. 5*B*). However, none of the comparisons made between muscles was statistically significant. For the K_f, the change in older *mdx* muscles was opposite in direction from the changes in all other muscles (Fig. 5*C*). The K_f decreased in older *mdx* muscles, whereas in all other muscles it increased. In this case, the comparison between *mdx* and control in the older age group was statistically significant ($P < 0.001$). These secondary measures of muscle damage suggest that the older *mdx* muscles have been affected differently from all of the other muscles and add further to the suggestion from the force deficit results that older *mdx* muscles are more susceptible to injury.

Muscle fiber morphology. No branched fibers were found among the 151 fibers (63 younger, 88 older) examined from littermate control muscles. The results for *mdx* muscles are shown in Fig. 6. Each of the fibers was categorized according to the number of branch points it contained (none, 1, 2, 3, or 4+). Figure 6*A* shows the proportion of fibers in each category, whereas Fig. 6*B* shows the absolute numbers in each category. Of the 176 *mdx* fibers (106 younger, 70 older) examined, only 17% of the younger *mdx* fibers contained branch points, whereas 89% of the older *mdx* fibers were branched (Fig. 6*A*). Not only did older *mdx* muscles contain more branched fibers than younger *mdx* muscles, they also had more branch points on these fibers. The branched fibers in young *mdx* muscle usually had just one branch point on a fiber, while the branched fibers in older *mdx* muscle usually had multiple branch points on a fiber.

In addition to having more branched fibers and more branches per fiber, the branching patterns in older *mdx* fibers were also more complex than those in younger *mdx* fibers, as is evident from comparing Fig. 7 with Fig. 8. There appeared to be three basic patterns of branching: *1*) a small branch leaving the main fiber, as in Fig. 7*C*; *2*) the main fiber dividing into two similarly sized branches, as in Fig. 8*A*; and *3*) the two branches rejoining into one fiber again, as in Fig. 7*D*. The branches in younger *mdx* fibers are shorter and smaller than in the older *mdx* fibers. In addition, some older *mdx* fibers

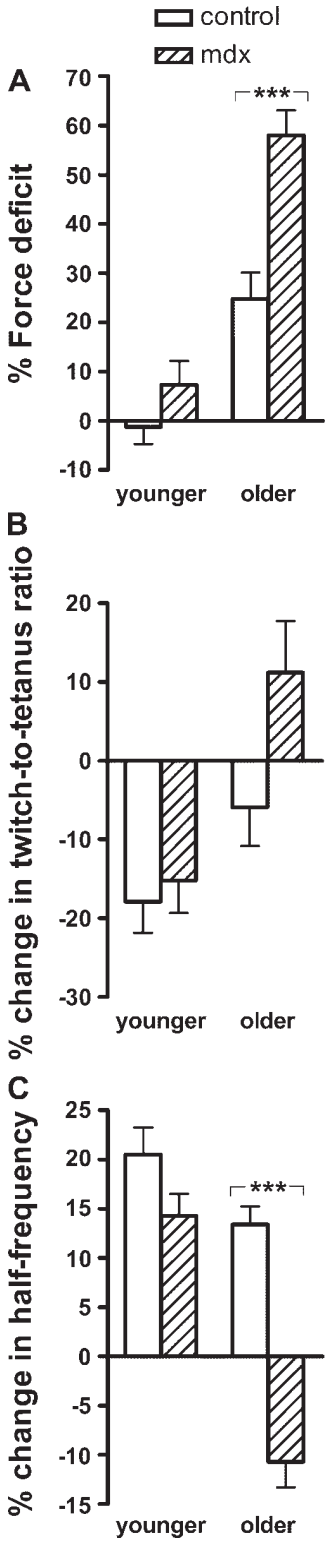

Fig. 5. Damage following lengthening contractions. *A*: force deficit, or the fall in maximum tetanic force. *B*: percentage change in twitch-to-tetanus ratio. *C*: percent change in half-frequency. These results demonstrate a susceptibility of older *mdx* muscles to contraction-induced damage. ***Significant difference between *mdx* and control in that particular age group, $P < 0.001$. $n = 5$ Muscles for younger control; $n = 6$ for younger *mdx*; $n = 4$ for older control; $n = 8$ for older *mdx*.

Downloaded from ajpcell.physiology.org on March 10, 2008

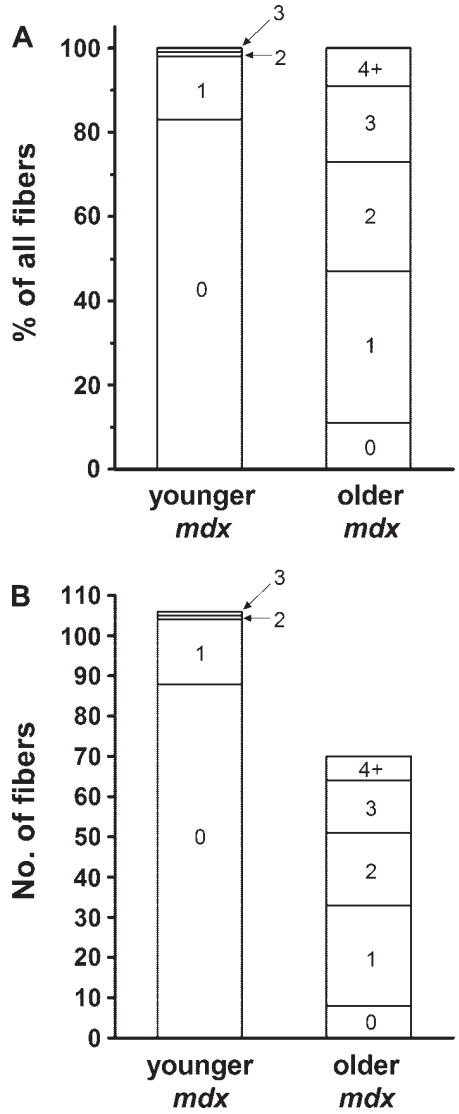

Fig. 6. Fiber branching in younger and older *mdx* muscles. Fibers were categorized according to the number of branch points they displayed (0, 1, 2, 3, or 4+). *A*: proportion of fibers in each category. *B*: absolute number of fibers in each category. Compared with younger *mdx* muscles, older *mdx* muscles had a greater number of branched fibers and a greater number of fibers with multiple branches.

displayed branching so complex that it was difficult to classify them into any of the above patterns.

Muscle stiffness. To ascertain whether the differences between muscles in their susceptibility to damage might be due to differences in the stiffness of the sarcomeres, we analyzed the ramp phase of the lengthening contractions, measuring the change in force as the muscle was stretched from 100 to 108% of its L_o. The results are displayed in Fig. 9, which shows the percent increase in force for each 1% increase in length. No significant differences were found between *mdx* and controls in either age group. However, older muscles showed significantly larger increases in force than younger muscles, in both *mdx* and controls, suggesting that the sarcomeres of older muscles have more stiffness than those of younger muscles.

DISCUSSION

We have demonstrated that a lengthening contraction protocol of 15% strain causes more damage to muscles of *mdx* mice aged 6–7 mo than to muscles of *mdx* mice aged 1–2 mo, relative to age-matched littermate controls. Our results demonstrate that dystrophin deficiency has little effect on the vulnerability of the younger muscles to injury; however, it significantly increases the vulnerability of the older muscles to injury.

Why should dystrophin deficiency have a greater effect on skeletal muscle's vulnerability to damage as age increases? One possible reason, suggested by our fiber morphology results, is that the fiber branching associated with the dystrophic process becomes more extensive as the dystrophic animal ages. It has been demonstrated previously that fibers containing branches are more liable to be damaged during contraction than fibers without branches (12). Compared with younger *mdx* muscles, older *mdx* muscles had more branched fibers, more branch points on each fiber, and greater complexity of branching patterns. These morphological changes mean that the potential number of "weak" branch points is substantially greater in older *mdx* animals, rendering them susceptible to damage by contractions that would not damage either normal (nonbranched) dystrophin-positive skeletal muscle or skeletal

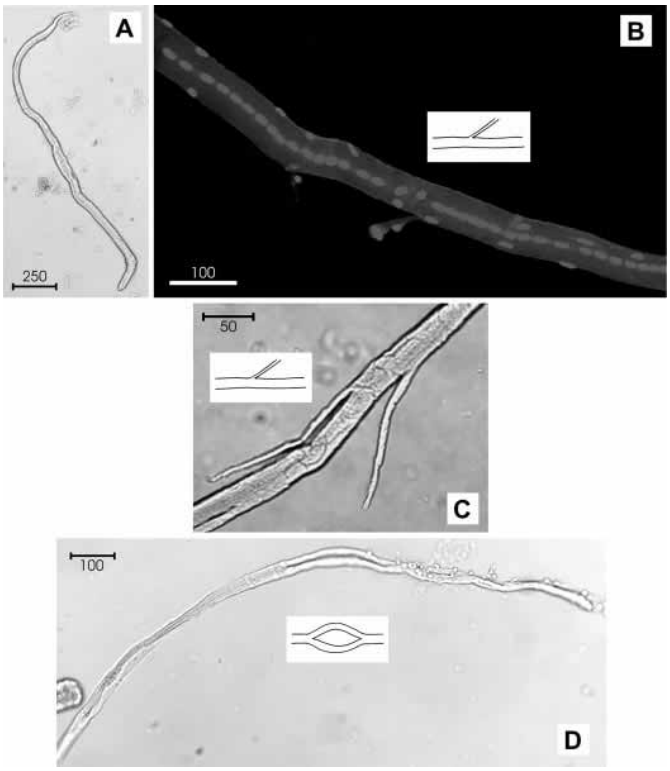

Fig. 7. Low-power images of enzymatically dispersed single-muscle fibers from younger *mdx* mice (1–2 mo of age). *A*: an example of an unbranched extensor digitorum longus fiber. *B*: an image from a confocal laser scanning microscope with the fiber stained with ethidium bromide to label the nuclei, which are predominantly in the center of the fiber; this fiber has one small central branch. *C*: a fiber with two small sprouts coming off the middle and a larger fissure lower left. *D*: a fiber with a split which reconnects. Scale bar measurements are in μm. The *insets* are diagrammatic representations of the main deformity displayed by the fiber.

Downloaded from ajpcell.physiology.org on March 10, 2008

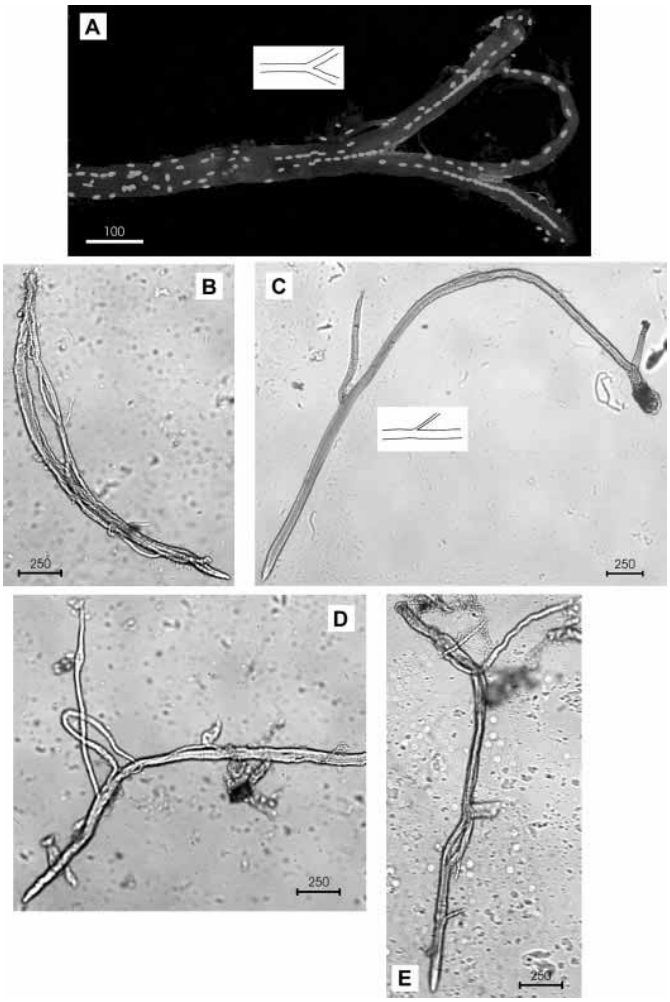

Fig. 8. Low-power images of enzymatically dispersed single-muscle fibers from older *mdx* mice (6–7 mo of age). *A*: an image from a confocal laser scanning microscope with the fiber stained with ethidium bromide to label the nuclei, which are predominantly in the center of the fiber; this fiber has two major and two minor branch points. *B*, *D*, and *E*: fibers with extraordinarily complex patterns of morphological abnormalities. *C*: a fiber which branches into two parts of unequal diameter at two different points. Scale bar measurements are in μm.

muscle from younger (nonbranched) dystrophin-negative *mdx* animals.

The observed association between the degree of damage and the extent of branching has implications for the interpretation of past studies involving lengthening contractions in the *mdx* mouse. The studies in Table 1 that found larger force deficits for *mdx* muscles all used mice that were older than the 6- to 8-wk-old mice of our study. Given that, in our study, 17% of fibers were already branched at 6–8 wk, and 89% were branched by 27–31 wk, the muscles in these other studies may have contained a significant proportion of branched fibers. This means that at least part of the force deficits observed in *mdx* muscle may have been associated with the presence of the branched fibers, rather than the absence of dystrophin.

To remove the potential confounding effect of branched fibers, and to gain a clearer understanding of what is the primary effect of the lack of dystrophin, we can look at muscles in which fiber branching is minimal. One study by Grange et al. (11) used dystrophic mouse pups 9–12 days old. This is much younger than any of the studies listed in Table 1, and hence the effect of fiber branching would be minimized. They found that the extent of membrane damage (as measured by dye uptake) was no different between dystrophic and control animals following lengthening contractions. This suggests that a lack of dystrophin does not in itself weaken the sarcolemma. In contrast to the present study, Yeung et al. (24) used unbranched single fibers from the flexor digitorum brevis muscle and found that unbranched *mdx* fibers had slightly higher force deficits than controls following lengthening contractions. Interestingly, however, this difference was eliminated when specific blockers of stretch-activated ion channels were added to the unbranched single fibers, suggesting that the primary effect of dystrophin deficiency may be the malfunctioning of ion channels rather than a fragile sarcolemma.

Hence, in these studies, it does not appear that dystrophin's primary role is to mechanically strengthen the sarcolemma and that the initiating event in the dystrophic process may not necessarily be mechanical damage during contraction. Popular alternative candidates for the initial step are a pathological calcium homeostasis due to one or more of the following: aberrant ion channel functioning; sarcolemmal ion channel dysfunction, especially with reference to mechanosensitive channels; and reactive oxygen species activity (1, 7, 23).

Interestingly, the aged control muscles were also somewhat damaged by the lengthening contractions. This finding is consistent with those of Brooks and Faulkner (3), who found that aged mice ~24 mo old were more susceptible to contraction-induced damage than younger mice. Our analysis of muscle stiffness provides a possible explanation of this. We found that older muscles had increased stiffness compared with younger muscles. This may mean that older muscles are less compliant and less able to absorb the strain as the muscle is stretched, rendering it more susceptible to damage.

In summary, we have observed that the force deficits in *mdx* muscle following mild lengthening contractions are associated

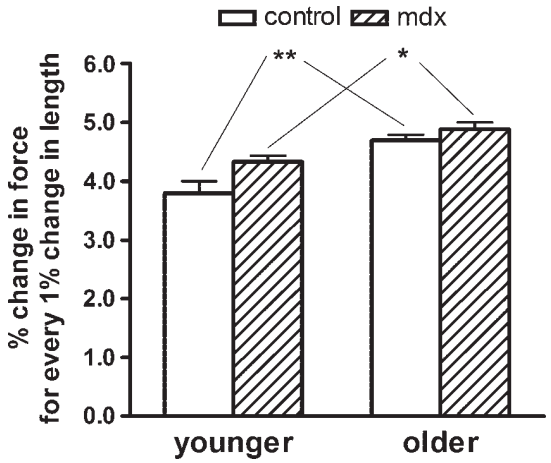

Fig. 9. Muscle stiffness, as measured by the percent change in force for every 1% change in length during the ramp phase of the lengthening contractions. There were no differences between *mdx* and control in either age group, but older muscles showed significantly more stiffness than younger muscles, in both *mdx* and controls. $^{**}0.001 < P < 0.01$; $^{*}0.01 < P < 0.05$. $n = 5$ Muscles for younger control; $n = 6$ for younger *mdx*; $n = 3$ for older control; $n = 8$ for older *mdx*.

Downloaded from ajpcell.physiology.org on March 10, 2008

with the degree of fiber branching. Given this association, it is important to isolate the possible effects of fiber branching from the direct effects of dystrophin deficiency when interpreting the results of similar studies in *mdx* mice. The effect of fiber branching can be removed by using mice that are as young as possible or by using individual fibers that have no branches. In this way, the direct effect of dystrophin deficiency can be more easily seen and provide a clearer understanding of what is the primary initiating event in the pathogenesis of muscular dystrophy.

GRANTS

This work was supported by a grant from the Muscular Dystrophy Association, New South Wales, Australia and Muscular Dystrophy Association, USA.

REFERENCES

1. **Allard B.** Sarcolemmal ion channels in dystrophin-deficient skeletal muscle fibres. *J Muscle Res Cell Motil* 27: 367–373, 2006.
2. **Brooks SV, Faulkner JA.** Contractile properties of skeletal muscles from young, adult and aged mice. *J Physiol* 404: 71–82, 1988.
3. **Brooks SV, Faulkner JA.** The magnitude of the initial injury induced by stretches of maximally activated muscle fibres of mice and rats increases in old age. *J Physiol* 497: 573–580, 1996.
4. **Brown SC, Lucy JA.** Functions of dystrophin. In: *Dystrophin: Gene, Protein, and Cell Biology*, edited by Brown SC and Lucy JA. Cambridge, UK: Cambridge University Press, 1997, chapt. 7, p. 163–200.
5. **Carlson CG.** The dystrophinopathies: an alternative to the structural hypothesis. *Neurobiol Dis* 5: 3–15, 1998.
6. **Consolino CM, Brooks SV.** Susceptibility to sarcomere injury induced by single stretches of maximally activated muscles of mdx mice. *J Appl Physiol* 96: 633–638, 2004.
7. **Deconinck N, Dan B.** Pathophysiology of duchenne muscular dystrophy: current hypotheses. *Pediatr Neurol* 36: 1–7, 2007.
8. **Deconinck N, Rafael JA, Beckers-Bleukx G, Kahn D, Deconinck AE, Davies KE, Gillis JM.** Consequences of the combined deficiency in dystrophin and utrophin on the mechanical properties and myosin composition of some limb and respiratory muscles of the mouse. *Neuromuscul Disord* 8: 362–370, 1998.
9. **Deconinck N, Ragot T, Marechal G, Perricaudet M, Gillis JM.** Functional protection of dystrophic mouse (mdx) muscles after adenovirus-mediated transfer of a dystrophin minigene. *Proc Natl Acad Sci USA* 93: 3570–3574, 1996.
10. **Emery AE.** The muscular dystrophies. *Lancet* 359: 687–695, 2002.
11. **Grange RW, Gainer TG, Marschner KM, Talmadge RJ, Stull JT.** Fast-twitch skeletal muscles of dystrophic mouse pups are resistant to injury from acute mechanical stress. *Am J Physiol Cell Physiol* 283: C1090–C1101, 2002.
12. **Head SI, Stephenson DG, Williams DA.** Properties of enzymatically isolated skeletal fibres from mice with muscular dystrophy. *J Physiol* 422: 351–367, 1990.
13. **Head SI, Williams DA, Stephenson DG.** Abnormalities in structure and function of limb skeletal muscle fibres of dystrophic mdx mice. *Proc Biol Sci* 248: 163–169, 1992.
14. **Keynes RD, Aidley DJ.** *Nerve and Muscle*. Cambridge, UK: Cambridge University Press, 1991.
15. **Kueh SL, Head SI, Morley JW.** A new colony of mdx dystrophic mice with genetically identical littermate controls. *Proceedings of the Australian Health and Medical Research Congress 2004*. Sydney: Australian Health and Medical Research Congress 2004, p. 317.
16. **Lynch GS, Hinkle RT, Chamberlain JS, Brooks SV, Faulkner JA.** Force and power output of fast and slow skeletal muscles from mdx mice 6–28 months old. *J Physiol* 535: 591–600, 2001.
17. **McArdle A, Edwards RH, Jackson MJ.** Effects of contractile activity on muscle damage in the dystrophin-deficient mdx mouse. *Clin Sci (Lond)* 80: 367–371, 1991.
18. **Moens P, Baatsen PH, Marechal G.** Increased susceptibility of EDL muscles from mdx mice to damage induced by contractions with stretch. *J Muscle Res Cell Motil* 14: 446–451, 1993.
19. **Motulsky HJ, Christopoulos A.** *Fitting Models to Biological Data Using Linear and Nonlinear Regression. A Practical Guide to Curve Fitting*. San Diego, CA: GraphPad Software, 2003.
20. **Petrof BJ, Shrager JB, Stedman HH, Kelly AM, Sweeney HL.** Dystrophin protects the sarcolemma from stresses developed during muscle contraction. *Proc Natl Acad Sci USA* 90: 3710–3714, 1993.
21. **Raymackers JM, Debaix H, Colson-Van Schoor M, De Backer F, Tajeddine N, Schwaller B, Gailly P, Gillis JM.** Consequence of parvalbumin deficiency in the mdx mouse: histological, biochemical and mechanical phenotype of a new double mutant. *Neuromuscul Disord* 13: 376–387, 2003.
22. **Sacco P, Jones DA, Dick JR, Vrbova G.** Contractile properties and susceptibility to exercise-induced damage of normal and mdx mouse tibialis anterior muscle. *Clin Sci (Lond)* 82: 227–236, 1992.
23. **Whitehead NP, Yeung EW, Allen DG.** Muscle damage in mdx (dystrophic) mice: role of calcium and reactive oxygen species. *Clin Exp Pharmacol Physiol* 33: 657–662, 2006.
24. **Yeung EW, Head SI, Allen DG.** Gadolinium reduces short-term stretch-induced muscle damage in isolated mdx mouse muscle fibres. *J Physiol* 552: 449–458, 2003.

Downloaded from ajpcell.physiology.org on March 10, 2008

Am J Physiol Cell Physiol 295: C897–C904, 2008.
First published July 23, 2008; doi:10.1152/ajpcell.00179.2008.

A gene for speed: contractile properties of isolated whole EDL muscle from an α-actinin-3 knockout mouse

S. Chan,[1] J. T. Seto,[2,3] D. G. MacArthur,[2,3] N. Yang,[2,3] K. N. North,[2,3] and S. I. Head[1]

[1]*School of Medical Sciences, University of New South Wales, Sydney;* [2]*Institute for Neuromuscular Research, The Children's Hospital at Westmead, Sydney; and* [3]*Discipline of Paediatrics and Child Health, Faculty of Medicine, University of Sydney, Sydney, New South Wales, Australia*

Submitted 31 March 2008; accepted in final form 21 July 2008

Chan S, Seto JT, MacArthur DG, Yang N, North KN, Head SI. A gene for speed: contractile properties of isolated whole EDL muscle from an α-actinin-3 knockout mouse. *Am J Physiol Cell Physiol* 295: C897–C904, 2008. First published July 23, 2008; doi:10.1152/ajpcell.00179.2008.—The actin-binding protein α-actinin-3 is one of the two isoforms of α-actinin that are found in the Z-discs of skeletal muscle. α-Actinin-3 is exclusively expressed in fast glycolytic muscle fibers. Homozygosity for a common polymorphism in the ACTN3 gene results in complete deficiency of α-actinin-3 in about 1 billion individuals worldwide. Recent genetic studies suggest that the absence of α-actinin-3 is detrimental to sprint and power performance in elite athletes and in the general population. In contrast, α-actinin-3 deficiency appears to be beneficial for endurance athletes. To determine the effect of α-actinin-3 deficiency on the contractile properties of skeletal muscle, we studied isolated extensor digitorum longus (fast-twitch) muscles from a specially developed α-actinin-3 knockout (KO) mouse. α-Actinin-3-deficient muscles showed similar levels of damage to wild-type (WT) muscles following lengthening contractions of 20% strain, suggesting that the presence or absence of α-actinin-3 does not significantly influence the mechanical stability of the sarcomere in the mouse. α-Actinin-3 deficiency does not result in any change in myosin heavy chain expression. However, compared with α-actinin-3-positive muscles, α-actinin-3-deficient muscles displayed longer twitch half-relaxation times, better recovery from fatigue, smaller cross-sectional areas, and lower twitch-to-tetanus ratios. We conclude that α-actinin-3 deficiency results in fast-twitch, glycolytic fibers developing slower-twitch, more oxidative properties. These changes in the contractile properties of fast-twitch skeletal muscle from α-actinin-3-deficient individuals would be detrimental to optimal sprint and power performance, but beneficial for endurance performance.

extensor digitorum longus

THE α-ACTININS ARE A GROUP of actin-binding proteins. In skeletal muscle, they are found in the Z-disc, where they cross-link the thin actin filaments of adjacent sarcomeres. The two isoforms found in the Z-disc are α-actinin-2 and α-actinin-3. α-Actinin-2 is the predominant isoform found in oxidative muscle fibers, whereas α-actinin-3 is restricted mainly to fast glycolytic fibers (8).

It is estimated that around 1 billion individuals worldwide completely lack α-actinin-3, due to homozygosity for a common polymorphism in the α-actinin-3 gene (10). α-Actinin-3 deficiency is not associated with any disease phenotype, suggesting that its absence may largely be compensated for by the closely related protein, α-actinin-2 (11). However, the genomic region surrounding the polymorphism shows low levels of genetic variation and recombination in individuals of certain populations, consistent with strong, recent positive selection (10). This suggests that α-actinin-3 deficiency does have an important effect on skeletal muscle, and that muscles lacking α-actinin-3 must be different in some way from muscles that have the protein.

A study of athletes at the Australian Institute of Sport (17) found that those engaged in sprint or power activities had a lower incidence of α-actinin-3 deficiency than the general population (6% compared with 18%). In fact, among Olympic sprint athletes, there were no cases of α-actinin-3 deficiency. Endurance athletes, in contrast, tended to have a higher incidence of α-actinin-3 deficiency, although this trend was only statistically significant in females. The reduced incidence of α-actinin-3 deficiency among elite sprint and power athletes has since been observed in other independent studies (13–15). α-Actinin-3 deficiency has also been associated with reduced muscle strength (5) and poorer sprinting performance (12) in nonathletes. These data strongly suggest that a lack of α-actinin-3 affects skeletal muscle in a way that is detrimental to sprint and power performance but beneficial for endurance activities.

Studies on a specially generated α-actinin-3 knockout mouse (10) lend support to these findings in humans. In an endurance test in which mice were run on a motorized treadmill, knockouts were found to run 33% further than wild types before exhaustion (10), supporting the finding of a higher incidence of α-actinin-3 deficiency in female endurance athletes. Knockouts also had reduced grip strength, lower muscle weights, and smaller fast fiber diameters than wild types (9), supporting the finding that α-actinin-3-deficient individuals are underrepresented in strength and power activities.

There are various hypotheses as to why α-actinin-3 deficiency might adversely affect power performance and benefit endurance performance. One hypothesis is that α-actinin-3 serves to stabilize the sarcomere when muscles are exercised to maximal or near-maximal capacity, as in sprinting. In its absence, the sarcomere may be weakened and more likely to be damaged during extreme athletic activity. Such a role is suggested by the protein's location in the Z-disc and its actin-binding properties.

Another hypothesis is that α-actinin-3 influences fiber-type differentiation toward a fast-twitch, glycolytic profile that is beneficial for sprint performance, while its absence would lead

Address for reprint requests and other correspondence: S. I. Head, School of Medical Sciences, Univ. of New South Wales, Sydney, 2052 NSW, Australia (e-mail: s.head@unsw.edu.au).

The costs of publication of this article were defrayed in part by the payment of page charges. The article must therefore be hereby marked "*advertisement*" in accordance with 18 U.S.C. Section 1734 solely to indicate this fact.

 0363-6143/08 $8.00 Copyright © 2008 the American Physiological Society

Downloaded from ajpcell.physiology.org on April 23, 2009

to differentiation toward a slower oxidative profile that is beneficial for endurance performance. Such a role is suggested by the restricted distribution of the protein, which is confined to fast glycolytic fibers, and by molecular studies that indicate that the sarcomeric α-actinins interact with signaling proteins involved in fiber-type differentiation and with metabolic enzymes involved in glycogenolysis (8). Under this hypothesis, one might expect that fast glycolytic fibers would adopt slower, more oxidative properties when α-actinin-3 is absent. Indeed, the activity of key oxidative enzymes in the α-actinin-3 knockout mouse is significantly higher than in wild-type controls, although there is no change in fiber types as defined by myosin heavy chain composition (9, 10).

In the present study we examined some physiological properties of isolated, whole α-actinin-3-deficient muscles from the α-actinin-3 knockout mouse to gain greater insight into the likely functions of this protein. For comparison, we used littermate wild-type controls that were homozygous for the α-actinin-3 gene. We chose to analyze the extensor digitorum longus (EDL) muscle from the hindlimb, because α-actinin-3 is found predominantly in fast glycolytic fibers (8), and the mouse EDL muscle contains a high proportion of these fibers. Thus any consequences of α-actinin-3 deficiency will be most apparent in this muscle.

To see whether α-actinin-3 plays a mechanical role in stabilizing the sarcomere, we measured the muscle damage resulting from eccentric contractions of 20% strain and also examined the morphology of individual fibers for evidence of repetitive muscle injury. To see whether α-actinin-3 influences fiber-type differentiation and metabolism, we measured some basic contractile properties and also examined the responses of the muscles to a fatigue protocol.

METHODS

Animals used. The use of animals was approved by the University of New South Wales Animal Care and Ethics Committee. Twelve knockout mice and 12 wild-type mice aged 8 to 10 wk, plus 1 knockout and 1 wild-type aged ~6 mo, were used. All mice were males.

Muscle preparation. All animals were anesthetized with halothane and killed by cervical dislocation. The EDL muscle was dissected from the hindlimb and tied by its tendons to a force transducer (Fort 10, World Precision Instruments) at one end and a linear tissue puller (University of New South Wales) at the other, using silk suture (Deknatel 6.0). The EDL muscle was placed in a bath continuously superfused with Krebs solution, with composition (in mM) 4.75 KCl, 118 NaCl, 1.18 KH_2PO_4, 1.18 $MgSO_4$, 24.8 $NaHCO_3$, 2.5 $CaCl_2$, and 10 glucose, with 0.1% fetal calf serum; it was continuously bubbled with 95% O_2-5% CO_2 to maintain pH at 7.4. The muscle was stimulated by delivering a supramaximal current between two parallel platinum electrodes, using an electrical stimulator (A-M Systems). At the start of the experiment, the muscle was set to the optimum length L_O that produced maximum twitch force. All experiments were conducted at room temperature (~22°C to 24°C).

Force-frequency curve. A force-frequency curve was then obtained by delivering 500-ms stimuli of different frequencies (2, 15, 25, 37.5, 50, 75, 100, 125, and 150 Hz) and measuring the force produced at each frequency of stimulation. A 30-s rest was allowed between each frequency. A curve relating the muscle force P to the stimulation frequency f was fitted to these data. The curve had the following equation:

$$P = P_{min} + \frac{P_{max} - P_{min}}{1 + \left(\frac{K_f}{f}\right)^h}$$

The values of r^2 for the fitting procedure were never lower than 99.3%. From the fitted parameters of the curve, the following contractile properties were obtained: maximum force (P_{max}), half-frequency (K_f), Hill coefficient (h) and twitch-to-tetanus ratio (P_{min}/P_{max}).

Eccentric contractions. The muscle was then subjected to a series of eccentric (lengthening) contractions. At time = 0 ms, the muscle was stimulated by supramaximal pulses of 1-ms duration and 125-Hz frequency. At time = 250 ms, after it had attained its maximum isometric force, the muscle was stretched at a speed of 0.2 L_O/s until it was 20% longer than its optimum length, was held at this length for 0.5 s, and was then returned at the same speed to its original position. The electrical stimulus was stopped at time = 2,000 ms. This eccentric contraction was performed 5 times, at intervals of 2 min. After a 15-min recovery period, the optimum length was reset and a second force-frequency curve was obtained.

Muscle mass. Finally, the muscle was removed from the bath. The tendons were trimmed and the muscle was lightly blotted on filter paper and then weighed. An estimate of the cross-sectional area was obtained by dividing the muscle's mass by the product of its optimum length and the density of mammalian muscle (1.06 mg/mm^3) (3).

Muscle stiffness. To estimate muscle stiffness, we divided the change in muscle force (as a percentage of isometric force) by the change in muscle length (as a percentage of optimum length) during the first eccentric contraction. We only measured up to the point where the muscle reached 109% of optimum length; beyond this length, many muscles developed forces that exceeded the measurement capacity of the force transducer.

Fatigue. In a separate set of experiments using different muscles from those used for eccentric contractions, muscles were examined for their responses to a fatiguing protocol. Muscles were set up as described above. A force-frequency curve was obtained as described above, except that the duration of stimulation at each frequency was only 250 ms. After 5 min, the fatigue protocol was started. The muscle was given a 1-s, 100-Hz tetanus every 2 s over a period of 30 s. The muscle was then allowed to recover for a period of 30 min, during which force recovery was monitored with a brief (250 ms) 100-Hz tetanus every 5 min. Additional force-frequency curves were obtained 90 s after the end of the fatigue protocol and 1 min after the final recovery tetanus.

The 30-min recovery period was chosen because of time constraints. At this time, recovery in the muscles ranged from 74% to 92% of prefatigue force. The experiment would have been too prolonged if the muscle had been left to recover to 100%; in any case, it is unlikely that complete recovery would have occurred because of the possible development of an anoxic core during the very vigorous stimulation protocol.

Muscle fiber morphology. Individual fiber morphology was examined in the EDL muscles of one wild-type and one knockout mouse aged ~6 mo. Animals were anesthetized with halothane and killed by cervical dislocation. The EDL muscle was dissected from the hindlimb. Following dissection, the muscles were digested to yield individual fibers. The solution used for the digestion was Krebs solution containing 3 mg/ml collagenase Type I (Sigma) and 1 mg/ml trypsin inhibitor (Sigma), continuously bubbled with 95% O_2-5% CO_2 and maintained at 37°C. After about 30 min, the muscles were removed from this solution, rinsed in Krebs solution, and placed in a relaxing solution with the following composition (concentrations in mM): 117 K^+, 36 Na^+, 1 Mg^{2+}, 60 HEPES, 8 ATP, 50 $EGTA^{2-}$, and free Ca^{2+} of 10^{-7} M. The muscle was gently agitated with pipette suction, releasing some individual fibers from the muscle mass.

Downloaded from ajpcell.physiology.org on April 23, 2009

Individual fibers were examined either with a light microscope (Olympus BX60) or a laser-scanning confocal microscope (Leica TCS SP).

Statistical analyses. Data are presented as means ± SE. For the contractile properties and eccentric contraction data, two-tailed *t*-tests were used. For the fatigue data, the Mann-Whitney *U*-test was used because of smaller sample sizes. All tests were conducted at a significance level of 5%. All statistical tests and curve fitting were performed using a standard statistical software package (GraphPad Prism version 4.00 for Windows, GraphPad Software, San Diego, CA).

RESULTS

Sample sizes and ages. The results presented below for general physical properties, maximum forces, force-frequency characteristics, twitch characteristics, and eccentric contractions were all obtained from one experimental group consisting of 8 wild-type muscles and 10 knockout muscles. Each muscle was taken from a different mouse. Animals were male mice aged 8 to 10 wk.

The fiber morphology was performed on EDL muscles from one wild-type and one knockout mouse, both males aged about 6 mo.

The fatigue experiments were performed on six wild-type muscles and eight knockout muscles. Each muscle was taken from a different mouse. Animals were male mice aged 8 to 10 wk.

General physical properties. The general physical properties of wild-type and knockout muscles are shown in Table 1. While their optimum lengths were virtually identical to those of wild-type muscles, α-actinin-3-deficient muscles were 9% lighter than α-actinin-3-positive muscles, with a corresponding 9% reduction in cross-sectional area.

Maximum forces generated by muscles. Table 1 shows the forces generated by the muscles when stimulated at maximum frequency. There were no statistically significant differences between wild types and knockouts in either absolute force (without correcting for cross-sectional area) or specific force (after correcting for cross-sectional area).

To see whether there were any differences at submaximal levels of stimulation, we analyzed the forces produced at 100 Hz (about 67% of maximum frequency) by the cohort of muscles used in the fatigue experiments (described in *Fatigue* below). The 100-Hz absolute forces of knockouts were 10.9% lower than wild types ($P = 0.008$, by Mann-Whitney test), but there was no difference in 100-Hz specific forces.

Table 1. *Properties of wild-type and α-actinin-3 knockout muscles*

	Wild Type	Knockout	*P* Value
General physical properties			
Optimum length, mm	11.9±0.1	11.9±0.2	
Mass, mg	9.7±0.4	8.8±0.2	0.035
Cross-sectional area, mm^2	0.77±0.02	0.70±0.01	0.015
Maximum forces			
Absolute force, mN	202±5.4	189±5.5	
Specific force, mN/mm^2	262±5.5	271±7.8	
Force-frequency characteristics			
Half-frequency, Hz	56.4±0.5	55.0±1.1	
Hill coefficient	5.0±0.1	5.5±0.2	0.048
Twitch-to-tetanus ratio, %	20.1±0.5	18.3±0.5	0.027

Values are means ± SE. *P* values are shown where there is a significant difference between wild types and knockouts.

Force-frequency characteristics. Table 1 shows various contractile properties derived from the force-frequency curves of individual muscles. The half-frequency is the stimulation frequency at which the muscle develops a force which is halfway between its minimum and maximum forces. The Hill coefficient is a measure of the slope of the curve. The half-frequency and Hill coefficient indicate the sensitivity of the contractile proteins to calcium. The lower the half-frequency and the higher the Hill coefficient, the greater the sensitivity. The twitch-to-tetanus ratio measures the minimum force as a proportion of the maximum force.

The half-frequency in wild-type muscles was not significantly different from the half-frequency in knockouts. The Hill coefficient was significantly higher in knockouts than in wild types. The twitch-to-tetanus ratio in knockouts was significantly lower than the ratio in wild types.

The effects of these differences on the shape of the force-frequency curve are shown in Fig. 1, in which individual force-frequency data for wild types and knockouts have been aggregated into single curves. At low frequencies, the curve for knockouts is depressed slightly compared with wild types, reflecting the lower twitch-to-tetanus ratio in knockouts. Over middle frequencies, where the curves are rising steeply, the curve for knockouts has a slightly steeper slope than the curve for wild types, reflecting the higher Hill coefficient in knockouts.

Eccentric contractions. The muscles were subjected to eccentric contractions of 20% strain to determine whether there were any differences between wild types and knockouts in their susceptibility to eccentric damage. Figure 2 shows results from these experiments. Before the contraction protocol, a force-frequency curve was obtained. This precontraction curve is the solid line shown in Fig. 2*A* for wild types and in Fig. 2*B* for knockouts. The muscle was then subjected to the eccentric contraction protocol. Force tracings obtained during the five contractions in an individual wild-type muscle are shown in Fig. 2*C*, and force tracings for one knockout muscle are shown in Fig. 2*D*. Following the eccentric contractions, the muscle was allowed to recover for 15 min and its optimum length was reset. Then a second force-frequency curve was obtained, shown by the dashed line in Fig. 2*A* for wild types and in Fig. 2*B* for knockouts.

By comparing the "before" and "after" curves, it can be seen that muscle damage is reflected in three changes to the force-frequency relationship: *1*) a fall in maximum force; *2*) a rightward shift of the curve, meaning that the half-frequency has increased; and *3*) a reduction in the steepness of the curve, meaning that the Hill coefficient has decreased. The rightward shift and reduced steepness of the force-frequency curve is commonly observed following eccentric contractions and could indicate some damage to the excitation-contraction coupling mechanism.

The extent of each of these three changes was used to assess the degree of muscle damage in wild types and knockouts, and the results are shown in Fig. 3. Fig. 3*A* shows the force deficit, or the percentage fall in maximum force. This was 1.6 ± 2.0% in wild types and 2.6 ± 1.5% in knockouts. Fig. 3*B* shows the percentage increase in half-frequency, or the extent of the rightward shift of the curve. This was 15.2 ± 0.6% in wild

Downloaded from ajpcell.physiology.org on April 23, 2009

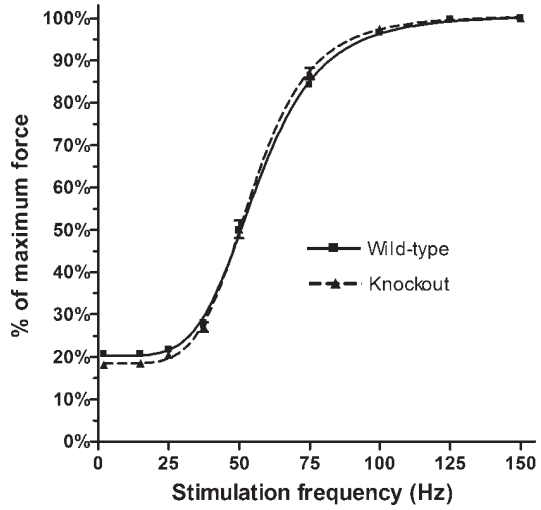

Fig. 1. Aggregated force-frequency curves. Force-frequency data from individual muscles were aggregated to produce a single curve for wild types (WT; solid line) and a single curve for knockouts (KO; dashed line). Compared with the curve for WT, the curve for KO is slightly depressed at low frequencies, reflecting the lower twitch-to-tetanus ratio, and rises more steeply, reflecting the higher Hill coefficient. (n = 8 muscles for WT; n = 10 muscles for KO.)

types and 12.9 ± 1.1% in knockouts. Fig. 3*C* shows the percentage decrease in the Hill coefficient, or the extent of the reduction in the curve's steepness. This was 10.1 ± 1.5% in wild types and 12.4 ± 1.4% in knockouts. There were no statistically significant differences between wild types and knockouts in any of these measures.

Muscle stiffness. The stiffness of wild-type and knockout muscles was compared by measuring the percentage change in muscle force as the muscle was stretched from 100% to 109% of its optimum length during the first eccentric contraction. A stiffer muscle would be expected to exhibit a greater change in force for a given change in length. Figure 4 shows the change in muscle force (expressed as a percentage of isometric force) for every 1% increase in muscle length. There were no significant differences between wild types and knockouts, suggesting that the stiffness of both groups of muscles was similar.

Fiber morphology. A feature of repetitive muscle damage is the development of muscle fibers which are branched, or split (16). Branched fibers are found in processes involving continuous degeneration and regeneration of muscle, such as in the X-linked recessive condition of Duchenne muscular dystrophy. In mice with an equivalent condition, muscles contain a large proportion of branched fibers, and these fibers have centrally located nuclei, another feature of regenerating muscle (6).

A muscle which was particularly susceptible to eccentric injury might be expected to develop a large number of branched fibers over time. We thus examined the individual fiber morphology from muscles of older mice (~6 mo old) to see whether there was any fiber branching indicative of repetitive muscle damage.

Individual fibers from the EDL muscles of one wild-type and one knockout mouse were examined by laser-scanning confocal microscopy. Examples of fibers are shown in Fig. 5. Almost all fibers were normal, with no branches and with peripherally located nuclei, as shown in Fig. 5*A*. Branching was detected in a very small number of knockout fibers, such as the one shown in Fig. 5*B*. All the branched fibers had peripherally located nuclei. Hence any morphological evidence of fiber damage was minimal and was not sufficient to suggest that knockouts were any more susceptible than wild types to eccentric muscle injury.

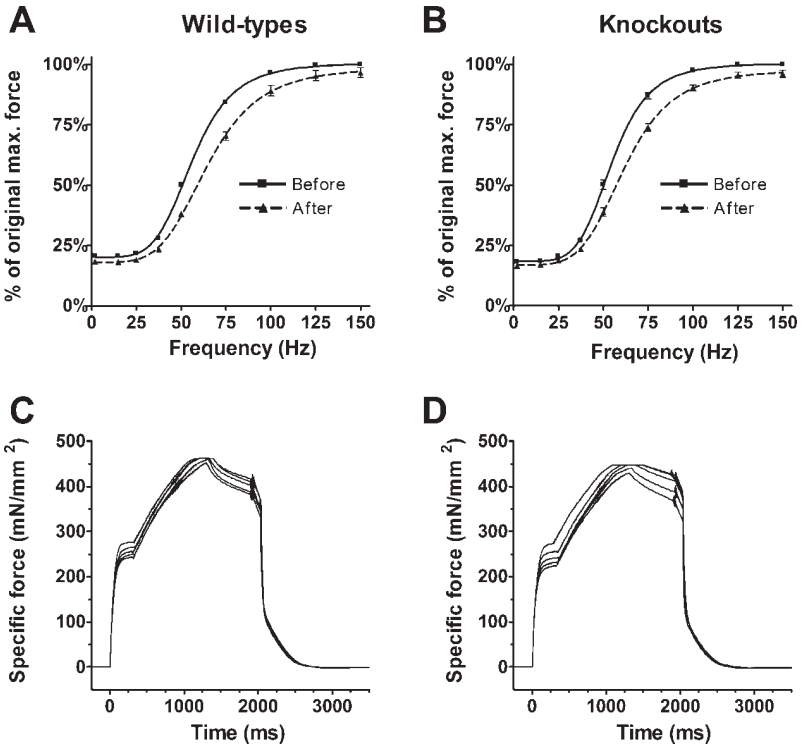

Fig. 2. Eccentric contractions. *A* and *B*: force-frequency curves obtained before (solid line) and after (dashed line) the eccentric contraction protocol. *A*: aggregated data for WT. *B*: aggregated data for KO (n = 8 muscles for WT; n = 10 muscles for KO). The eccentric contractions have caused a fall in maximum force, a rightward shift of the force-frequency curve, and a reduction in steepness of the curve. Also shown are the force tracings obtained during the 5 eccentric contractions in one particular WT muscle (*C*) and one particular KO muscle (*D*). The force tracing for each contraction is slightly lower than that of the preceding contraction.

Downloaded from ajpcell.physiology.org on April 23, 2009

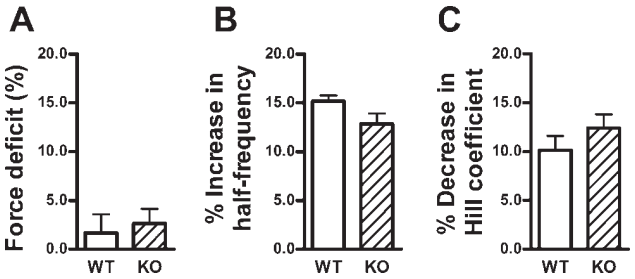

Fig. 3. Measures of damage from eccentric contractions. Three measures were used to assess the extent of damage from eccentric contractions: the force deficit (*A*), which is the percentage fall in maximum force; the percentage increase in the half-frequency (*B*), which measures the extent of rightward shift of the force-frequency curve; and the percentage decrease in the Hill coefficient (*C*), which measures the reduction in steepness of the force-frequency curve. There were no statistically significant differences between WT and KO muscles in any of these measures. (n = 8 muscles for WT; n = 10 muscles for KO.)

Fatigue. Muscles were subjected to a fatigue protocol in which they were given a 1-s, 100-Hz tetanus every 2 s over a period of 30 s. The muscles were then allowed to recover for a period of 30 min, during which force recovery was monitored with a brief 100-Hz tetanus every 5 min.

Figure 6 shows the results obtained from six wild-type muscles and eight knockout muscles. The descending part of the curve shows the decline in 100-Hz force with each successive tetanus during the 30-s fatigue protocol. By the end of this fatigue protocol, 100-Hz force had declined to 45.1 ± 1.3% of original in wild types and to 42.9 ± 4.5% of original in knockouts. These values were not significantly different (Mann-Whitney test). The ascending part of the curve shows the recovery in 100-Hz force over the 30 min following the fatigue protocol. By the end of this period, knockouts had recovered to 86.1 ± 1.1% of their original force, but wild types recovered to only 78.4 ± 1.9% of original. These values were significantly different (P = 0.013, by Mann-Whitney test), indicating that recovery of 100-Hz force following fatigue was better in knockouts than in wild types. The difference in 30-min recovery has previously been presented by MacArthur et al. (9), but the full data are included here so as to show the time course of the changes in force during fatigue and recovery.

In addition to measurements of 100-Hz force, force-frequency (FF) curves were also obtained for each muscle at various stages of the experiment. The times at which they were obtained are indicated by the shaded regions in Fig. 6. The first curve (FF1) was obtained just before the start of the fatigue protocol, the second (FF2) was obtained shortly after the end of the fatigue protocol, and the third (FF3) was obtained at the end of the 30-min recovery period.

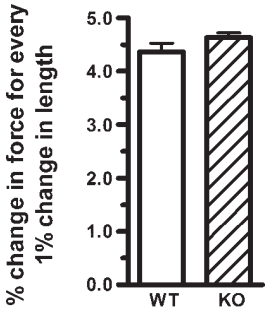

Fig. 4. Muscle stiffness. The graph shows the change in force (expressed as a percentage of isometric force) for every 1% increase in muscle length during the first eccentric contraction. This was used as an indicator of muscle stiffness. There were no significant differences in stiffness between WT and KO muscles. (n = 8 muscles for WT; n = 10 muscles for KO.)

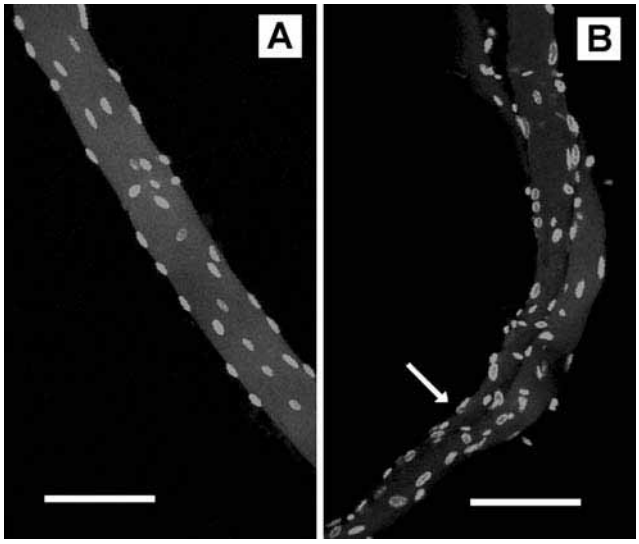

Fig. 5. Fiber morphology. Individual muscle fibers from ~6-mo-old animals were examined by confocal microscopy. All fibers from the WT mouse and almost all of the fibers from the KO mouse had an appearance similar to *A*, which shows a portion of a fiber with no branches and with peripherally located nuclei. A very small number of fibers from the KO mouse were split, and an example is shown in *B*. The arrow indicates the site where the single fiber divides into two separate branches. The nuclei, however, are still peripherally located. (Scale bars represent 100 μm.)

These force-frequency curves are shown in Fig. 7, *A* and *B*. Here, data from individual muscles have been aggregated and forces expressed as a percentage of the prefatigue maximum to facilitate comparison. Wild-type muscles are shown in Fig. 7*A* and knockouts are shown in Fig. 7*B*. The fatiguing protocol produced a rightward shift of the force-frequency curve, as is evident from the rightward displacement of FF2 compared with FF1 in both wild types and knockouts. Right-shifting of the force-frequency curve is commonly found after fatigue and may indicate some impairment of the excitation-contraction coupling mechanism. The magnitude of the rightward shift can be quantified as the percentage increase in half-frequency between FF1 and FF2. This percentage increase is shown in Fig. 7*C*. There was a 33.7 ± 2.8% increase in half-frequency for wild types and a 23.3 ± 4.0% increase for knockouts, but this difference was not statistically significant (Mann-Whitney test).

After 30-min recovery, the force-frequency curve shifts back slightly to the left, as can be seen by comparing FF3 with FF2 in Fig. 7, *A* and *B*. However, FF3 is still noticeably displaced to the right of FF1. The magnitude of this displacement is shown in Fig. 7*D*. In wild types, the half-frequency for FF3 is still 32.2 ± 1.8% higher than the half-frequency for FF1, while in knockouts the increase is only 19.7 ± 1.3%. Here, the difference between wild types and knockouts is significant (P = 0.048, by Mann-Whitney test), suggesting that, after the 30-min recovery period, the extent of right-shifting of the force-frequency curve is more

Downloaded from ajpcell.physiology.org on April 23, 2009

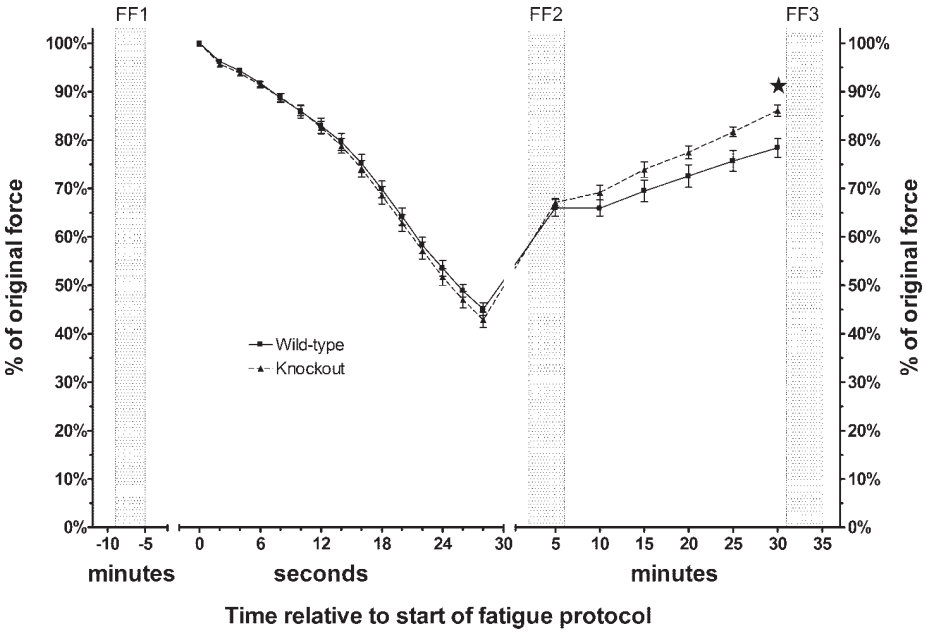

Fig. 6. Changes in 100-Hz force during fatigue and recovery. Muscles were subjected to a fatigue protocol consisting of a 1-s, 100-Hz tetanus every 2 s for 30 s. The descending part of the curve shows the decline in 100-Hz force over the duration of the fatigue protocol. Muscles were then allowed to recover for a period of 30 min. The ascending part of the curve shows the recovery in 100-Hz force during the recovery period (n = 6 muscles for WT; n = 8 muscles for KO). ★, Significant difference in force between WT and KO at 30 min (P = 0.013). Shaded regions represent 4-min time intervals during which force-frequency (FF) curves were obtained for each muscle. The three curves (FF1, FF2, and FF3) are shown in Fig. 7.

pronounced in wild types than in knockouts, and hence the knockout muscles have recovered better than the wild-type muscles.

By comparing FF3 with FF1 in Fig. 7, *A* and *B*, it can be seen that after 30 min, the force at very low and very high frequencies is very close to prefatigue levels; it is only over the middle frequencies that force remains significantly depressed. This is illustrated in Fig. 8, where the force at each frequency following 30-min recovery is expressed as a percentage of the force generated at that frequency before the muscle was fatigued. At very low and very high frequencies, the postrecovery force is ~90% of the prefatigue force. However, over middle frequencies, this percentage is considerably lower. Another feature of the graph is that, at very high and very low frequencies, the percentages for both wild types and knockouts are similar, but over intermediate frequencies, wild types have not recovered to the same degree as knockouts. At 37.5, 50, 75, and 100 Hz, the recovery in wild types is significantly less than in knockouts (2-way ANOVA with Bonferroni posttests). As maximum force was usually reached at ~150 Hz, these frequencies represent a range that is ~25% to 67% of maximum stimulation frequency.

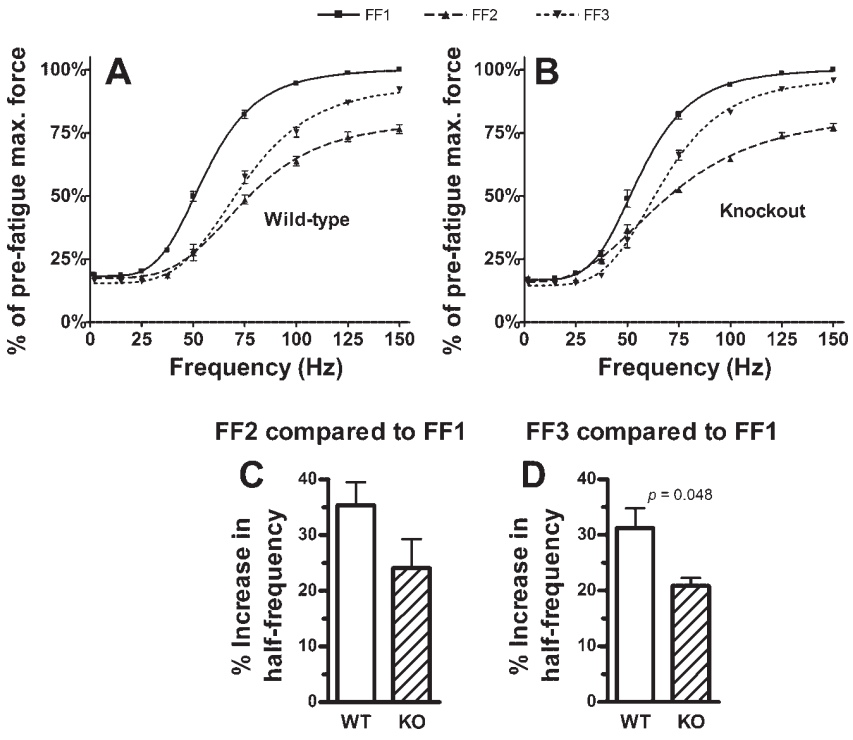

Fig. 7. Force-frequency characteristics at various stages of fatigue experiments. *A* and *B*: changes in the shape of the force-frequency curve over time for WT (*A*) and KO (*B*). FF1 (solid line) is the prefatigue curve. FF2 (dashed line) is the curve shortly after the fatigue protocol has ended. It is right-shifted compared with FF1. FF3 (dotted line) is the curve at the end of the 30-min recovery period. It has moved back slightly toward the prefatigue curve but is still noticeably right-shifted compared with FF1. The fatigue-induced rightward shift of the force-frequency curve is reflected in increased half-frequencies for FF2 and FF3 compared with FF1. *C* and *D*: percentage increase in half-frequency indicates the extent of the shift and is shown for FF2 (*C*) and FF3 (*D*). In both of these cases, WT had larger increases in half-frequency than KO, but this was only statistically significant in the case of FF3. (n = 6 muscles for WT; n = 8 muscles for KO. P value is shown where there is a significant difference between WT and KO.)

Downloaded from ajpcell.physiology.org on April 23, 2009

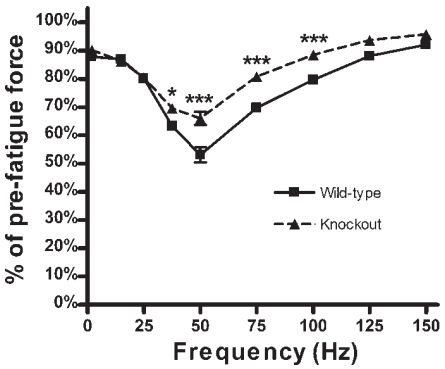

Fig. 8. Postrecovery force as a percentage of prefatigue force. Each data point shows the force developed at a particular frequency following 30-min recovery, expressed as a percentage of the force generated at that frequency before the fatigue protocol. At very low and very high frequencies, the postrecovery force is ~90% of the prefatigue force. However, over middle frequencies, force was still considerably lower than prefatigue levels. Also, at frequencies of 37.5, 50, 75, and 100 Hz, the loss of force was significantly greater in WT than in KO. (n = 6 muscles for WT, n = 8 muscles for KO. *$P < 0.05$ and ***$P < 0.001$, significant differences between WT and KO using 2-way ANOVA with Bonferroni posttests.)

DISCUSSION

Our current knowledge about the functions of α-actinin-3 is still in an early stage. We do know that its expression is confined largely to fast glycolytic muscle fibers and that its presence is somehow beneficial for power and sprint athletes at the elite level. One of the proposed roles for this protein is as a mechanical stabilizer of the sarcomere, while another possible function may be as an influencer of signaling and metabolic pathways, enabling a muscle fiber to differentiate toward a fast-twitch, glycolytic profile. The present study and the one by MacArthur et al. (9) represent the first investigations of the physiological properties of isolated skeletal muscle in the α-actinin-3 knockout mouse and provide some data against which to evaluate these hypotheses about the protein's functions.

Our findings in the eccentric contraction studies do not appear to support the hypothesis that α-actinin-3 mechanically strengthens the sarcomere during extreme muscle activity. Following an eccentric contraction protocol with a large (20%) strain, knockout muscles did not show any more damage than wild-type muscles in any of the measures of damage. Moreover, morphological analysis of muscle fibers of older mice did not reveal any major evidence of repetitive injury in knockout muscles, apart from a very small number of split fibers.

One complicating factor in interpreting these results is the size of the muscle fibers. Fast glycolytic fibers in knockout mice have reduced fiber diameters compared with wild types (9), so there would be less shear stress on the fast fibers in knockouts, thus protecting them from eccentric damage (7). Hence it is still possible that sarcomeres are inherently weaker when they lack α-actinin-3, but this is masked by the protective effect of smaller fiber diameter.

Our measurements of muscle stiffness concur with our eccentric contraction studies because no difference was found in muscle stiffness between wild types and knockouts, suggesting that α-actinin-3 deficiency did not affect the strength or stiffness of the muscle as a whole.

Besides their interactions with actin, the sarcomeric α-actinins are also known to interact with cell-signaling proteins that are involved in fiber type differentiation and with enzymes involved in metabolic pathways. This raises the possibility that one role of α-actinin-3 could be to influence fiber type differentiation toward a fast-twitch, glycolytic profile. While there is no evidence of a shift in myosin heavy chain composition from IIB to other isoforms in α-actinin-3-deficient muscle, there is evidence that α-actinin-3-deficient fibers have higher levels of oxidative enzymes than would be expected in a fast glycolytic fiber (10). Enzyme assays reveal that the activity of key enzymes involved in oxidative metabolism, such as citrate synthase, succinate dehydrogenase, and cytochrome-*c* oxidase, is significantly higher in knockouts than in wild types, while the anaerobic pathway enzyme, lactate dehydrogenase, has significantly lower activity in knockouts (9). Thus it may also be hypothesized that α-actinin-3 somehow helps fast glycolytic fibers to use more anaerobic pathways, and in its absence these fibers resort to more oxidative pathways.

In the present study, we found that some features of the knockout muscle that were consistent with the hypothesis that α-actinin-3-deficient fibers are more oxidative than normal. These features were smaller cross-sectional areas, lower twitch-to-tetanus ratios, and better recovery from fatigue.

We found that α-actinin-3-deficient muscles had a 9% smaller cross-sectional area than α-actinin-3-positive muscles. This is consistent with the fact that the diameter of fast glycolytic fibers is smaller in knockouts than in wild types (9) and supports the hypothesis that these fibers take on more oxidative characteristics when α-actinin-3 is absent, because oxidative fibers have smaller diameters than fast glycolytic fibers.

Slow-twitch motor units tend to have lower twitch-to-tetanus ratios than fast-twitch motor units (4). Our finding that knockout muscles had lower twitch-to-tetanus ratios than wild-type muscles is therefore consistent with the α-actinin-3-deficient fast glycolytic fibers changing to a more slow-twitch, oxidative profile.

Knockout muscles also recovered better from fatigue than wild-type muscles. At the end of the 30-min recovery period, knockouts had recovered significantly more of their original 100-Hz force than wild types, and the rightward shift of the force-frequency curve, thought to represent impairment of excitation-contraction coupling due to fatigue, was much less pronounced in knockouts than in wild types. The difference in recovery between wild types and knockouts was most apparent at stimulation frequencies that were between 25% and 67% of maximum. At these frequencies, knockouts were able to develop a much higher percentage of their prefatigue force than wild types. The improved recovery from fatigue in knockouts is consistent with the notion that α-actinin-3-deficient fibers may change toward the properties of more oxidative fiber types, which are more fatigue-resistant than glycolytic fibers. This also lends support to earlier findings that knockout mice can run 33% further than wild types before exhaustion when subjected to treadmill running (9), and may be one factor behind the increased incidence of α-actinin-3 deficiency in endurance athletes (17).

Downloaded from ajpcell.physiology.org on April 23, 2009

Although wild types and knockouts showed differences in their rates of recovery from fatigue, it can be seen from Fig. 6 that there were no differences in their rates of force decline during the 30 s of fatiguing stimulation. One explanation for this may be the accumulation of extracellular K^+ that occurs when muscles are subjected, as they were in the present study, to intense, repeated stimulation in vitro (1). Although only small amounts of K^+ leave the muscle fiber during each action potential, repeated action potentials can significantly increase the $[K^+]$ inside the lumen of the t-tubules, which comprise only 1% of the total fiber volume but 80% of the total membrane surface area. The increased extracellular $[K^+]$ and reduced intracellular $[K^+]$ result in membrane depolarization and a reduction of membrane excitability (1).

It is possible that this impaired excitability is the predominant factor underlying the reduction in force during the fatigue protocol in our study. This may have masked any differences in metabolic efficiency between wild types and knockouts during the fatiguing stimulation, so that their forces declined at similar rates. However, $[K^+]$ and membrane potential rapidly return to normal once stimulation is stopped (1), so the differences we observed between wild types and knockouts during recovery are likely to be due to metabolic factors, and these differences are consistent with α-actinin-3 deficient fibers developing more oxidative properties, enabling knockout muscles to recover more quickly from fatigue.

There is one further piece of evidence suggesting that the contractile properties of α-actinin-3-deficient fibers may change toward those of a slower-twitch, more oxidative fiber type. This is the 2.6-ms increase in the twitch half-relaxation time of knockout muscles compared with wild types, as we reported previously in experiments on the same set of muscles (9). Such a change is consistent with the observation that elite sprinters have a very low incidence of α-actinin-3 deficiency. Lack of this protein would significantly prolong the time taken for muscles to relax and would thus be detrimental to activities requiring repeated rapid contractions, such as sprinting (2).

To summarize, the present study has provided an overview of some basic contractile properties of the EDL muscle in a new knockout mouse, together with data on its responses to eccentric contractions and fatiguing stimulation. While these data do not appear to support the hypothesis that α-actinin-3 provides mechanical protection to the muscle fiber during strenuous physical activity, some results are consistent with the hypothesis that α-actinin-3 plays an important role in the differentiation of the fiber toward a fast-twitch, glycolytic profile, and that in its absence the fiber may tend toward a slower-twitch, more oxidative profile. The present study demonstrates that α-actinin-3 deficiency does have important effects on physiological function in muscle, and since α-actinin-3 deficiency is common in humans, it will be important to determine the effects of such deficiency in situations such as ageing and congenital muscle disease.

GRANTS

This project was funded in part by a grant (301590) from the Australian National Health and Medical Research Council. D. G. MacArthur and J. T. Seto were supported by Australian Postgraduate Awards.

REFERENCES

1. **Allen DG, Lamb GD, Westerblad H.** Skeletal muscle fatigue: cellular mechanisms. *Physiol Rev* 88: 287–332, 2008.
2. **Allen DG, Lannergren J, Westerblad H.** Muscle cell function during prolonged activity: cellular mechanisms of fatigue. *Exp Physiol* 80: 497–527, 1995.
3. **Brooks SV, Zerba E, Faulkner JA.** Injury to muscle fibres after single stretches of passive and maximally stimulated muscles in mice. *J Physiol* 488: 459–469, 1995.
4. **Celichowski J, Grottel K.** Twitch/tetanus ratio and its relation to other properties of motor units. *Neuroreport* 5: 201–204, 1993.
5. **Clarkson PM, Devaney JM, Gordish-Dressman H, Thompson PD, Hubal MJ, Urso M, Price TB, Angelopoulos TJ, Gordon PM, Moyna NM, Pescatello LS, Visich PS, Zoeller RF, Seip RL, Hoffman EP.** ACTN3 genotype is associated with increases in muscle strength in response to resistance training in women. *J Appl Physiol* 99: 154–163, 2005.
6. **Head SI, Williams DA, Stephenson DG.** Abnormalities in structure and function of limb skeletal muscle fibres of dystrophic *mdx* mice. *Proc Biol Sci* 248: 163–169, 1992.
7. **Karpati G, Carpenter S, Prescott S.** Small-caliber skeletal muscle fibers do not suffer necrosis in *mdx* mouse dystrophy. *Muscle Nerve* 11: 795–803, 1988.
8. **MacArthur DG, North KN.** A gene for speed? The evolution and function of alpha-actinin-3. *Bioessays* 26: 786–795, 2004.
9. **MacArthur DG, Seto JT, Chan S, Quinlan KG, Raftery JM, Turner N, Nicholson MD, Kee AJ, Hardeman EC, Gunning PW, Cooney GJ, Head SI, Yang N, North KN.** An Actn3 knockout mouse provides mechanistic insights into the association between alpha-actinin-3 deficiency and human athletic performance. *Hum Mol Genet* 17: 1076–1086, 2008.
10. **MacArthur DG, Seto JT, Raftery JM, Quinlan KG, Huttley GA, Hook JW, Lemckert FA, Kee AJ, Edwards MR, Berman Y, Hardeman EC, Gunning PW, Easteal S, Yang N, North KN.** Loss of ACTN3 gene function alters mouse muscle metabolism and shows evidence of positive selection in humans. *Nat Genet* 39: 1261–1265, 2007.
11. **Mills M, Yang N, Weinberger R, Vander Woude DL, Beggs AH, Easteal S, North K.** Differential expression of the actin-binding proteins, alpha-actinin-2 and -3, in different species: implications for the evolution of functional redundancy. *Hum Mol Genet* 10: 1335–1346, 2001.
12. **Moran CN, Yang N, Bailey ME, Tsiokanos A, Jamurtas A, MacArthur DG, North K, Pitsiladis YP, Wilson RH.** Association analysis of the ACTN3 R577X polymorphism and complex quantitative body composition and performance phenotypes in adolescent Greeks. *Eur J Hum Genet* 15: 88–93, 2007.
13. **Niemi AK, Majamaa K.** Mitochondrial DNA and ACTN3 genotypes in Finnish elite endurance and sprint athletes. *Eur J Hum Genet* 13: 965–969, 2005.
14. **Papadimitriou ID, Papadopoulos C, Kouvatsi A, Triantaphyllidis C.** The ACTN3 gene in elite Greek track and field athletes. *Int J Sports Med* 29: 352–355, 2008.
15. **Roth SM, Walsh S, Liu D, Metter EJ, Ferrucci L, Hurley BF.** The ACTN3 R577X nonsense allele is under-represented in elite-level strength athletes. *Eur J Hum Genet* 16: 391–394, 2008.
16. **Tamaki T, Akatsuka A.** Appearance of complex branched fibers following repetitive muscle trauma in normal rat skeletal muscle. *Anat Rec* 240: 217–224, 1994.
17. **Yang N, MacArthur DG, Gulbin JP, Hahn AG, Beggs AH, Easteal S, North K.** ACTN3 genotype is associated with human elite athletic performance. *Am J Hum Genet* 73: 627–631, 2003.

Downloaded from ajpcell.physiology.org on April 23, 2009